教育部補助大專校院延攬國際頂尖人才執行成果簡介

請依下列標題提供中英文版本，影音、照片及檔案若無，可免填。*為必填。

*標題	Directional asymmetry in gonad length indicates moray eels (Teleostei, Anguilliformes, Muraenidae) are “right-gonadal. 鰻類生殖腺之左右不對稱性。
*計畫成果簡述	We examined close to 3000 individuals of moray eels, and found the general occurrence of the asymmetry in the gonad length. Some of possible evolutionary origins were examined and ruled out. This study is published in a SCI journal. 我們檢驗了將近三千隻鰻類及外群之生殖腺外觀，發現其長度普遍有左右不對稱的現象，並探討此不對稱可能之演化涵義。 此研究已發表致 SCI 國際期刊 ” Scientific Report” 。
*成果說明	This study examines the directional asymmetry in the gonad length of 20 species of moray eels (Muraenidae) and two outgroup species with 2959 individuals. We tested three hypotheses: (1) moray eel species did not exhibit directional asymmetry in the gonad length; (2) the directional asymmetry pattern was the same for all selected species; (3) the directional asymmetry was not related to the major habitat types, depth and size classes, and taxonomic closeness of the species. Moray eels were generally “right-gonadal”, the right gonad length being constantly and significantly longer than the left one in all studied Muraenidae species. The degree of asymmetry varied among species and was not significantly related to taxonomic closeness. The habitat types, depth, and size classes had intermingled effects on observed asymmetry without a clear correspondence. The directional asymmetry in the gonad length is a unique and widely occurring phenomenon in the Family Muraenidae, which was likely a by-product in the evolutionary history without significant disadvantage in survival.

	本研究分析了二十種種鯨類，以及兩種非鯨類作為對照之外群，總共將近三千隻個體。同時檢驗了三種假說:(1)鯨類普遍都有生殖腺長度不對稱性，(2)鯨類生殖腺在檢驗過之種類都有相同程度之不對稱性，以及(3)此不對稱性和演化親緣程度、主要棲息地、體型大小等因素無關。結果發現，檢驗的鯨種類都出現生殖腺長度之不對稱性，同時非鯨類的並無此不對稱性。此不對稱性程度有很大的種間差異，同時並無檢測到與演化親緣程度、主要棲息地、體型大小等顯著的相關性。目前推測，此不對稱性可能是演化上的偶然，同時並無明顯在存活上之劣勢。	
成果影音	成果影音標題	
	Youtube 網址	
	說明	
成果照片 (請另行提供圖檔)	成果照片	
	照片說明	
成果檔案 (請另行提供檔案)	檔案名稱	3. 執行成果簡介(可公開資訊)_1.pdf

*標題	Compartmentation of trace metals in *Cymodocea nodosa* from a heavily polluted area (Central Gulf of Gabes; Southern Mediterranean Sea): Potential use of the seagrass as an environmental monitoring and bioremediation tool 地中海重度污染加伯斯海灣的海草微量金屬區隔化: 海草做為潛在環境監測及生物移除工具之研究
*計畫成果簡述	We examined the contaminants in the seagrass in the central Gulf of Gabes, Mediterranean. We found that the seagrasses can remove the pollutants in the soil for able to trap the pollutants in root and transfer them to the leaves. This study is published in a SCI journal. "Regional Studies in Marine Science" 我們檢驗在地中海重度污染的加伯斯灣海草的重金屬含量。海草能夠將汙染物捕捉進根部，進而將其轉移至葉片。因此海草有可能作為一潛在之生物移除工具。此研究已發表致 SCI 國際期刊 " Regional Studies in Marine Science" 。
*成果說明	This study was conducted to better understand the adaptative strategies of *Cymodocea nodosa* occurring in the heavily polluted environment of central Gulf of Gabes (SE Tunisia). Cd, Cu, Pb and Zn concentrations were assessed in the seagrass roots, rhizomes, and leaves, and in the surrounding seawater and sediments. Sediments were found to be the main source of contaminants bioaccumulated in *C. nodosa*. Bioaccumulation patterns differed significantly with metals and plant organs. While Cd, Cu and Zn were found to accumulate in leaves, Pb concentrates mainly in roots. In the heavily polluted environment of the Gulf of Gabes, *C. nodosa* seems to have developed two different adaptative strategies: metal trapping in roots and metal transfer from permanent (roots) to temporary (leaves) organs. These mechanisms allow the seagrass to remove the excess of metals. These properties show the potential use of C. nodosa not only as bioindicator but also as an effective bioremediation. 本研究分析在重度污染地中海加伯斯灣所採集海水、沉積

	物、及海草樣本不同組織內之重金素含量。沉積物為海草內汙染物主要來源，不同組織累積不同的元素，葉主要累積鎘、銅及鋅，而根部主要累積鉛。同時海草會將重金屬捕捉至根部，之後再將其轉移至葉。這機制也顯示海草可以將沉積物的汙染物移除，也暗示海草能當過污染的指標生物，也可以當生物修復之可能方案之一。	
成果影音	成果影音標題	
	Youtube 網址	
	說明	
成果照片 (請另行提供圖檔)	成果照片	
	照片說明	
成果檔案 (請另行提供檔案)	檔案名稱	3. 執行成果簡介(可公開資訊)_2.pdf

*標題	Stomach Content Analysis for Juvenile Great Hammerhead Sharks *Sphyrna mokarran* (Rüppell, 1837) from the Arabian Gulf 沙烏地阿拉伯灣錘頭雙髻鮫雉魚的胃內含物分析。
*計畫成果簡述	We examined the stomach contents in the great hammerhead sharks caught from the Arabian Gulf. Fish, the bartail flathead, was the most important prey. Juvenile great hammerhead sharks are a specialized predator at the top of the food web. This study is published in a SCI journal. "Fishes" 我們檢驗在沙烏地阿拉伯灣漁業所捕捉到錘頭雙髻鮫雉魚的胃內含物，結果發現魚類，特別是印度牛尾魚，是最重要的餌料生物。阿拉伯灣錘頭雙髻鮫雉魚是有選擇性、位在海洋食物網的最頂端的捕食者。此研究已發表致 SCI 國際期刊 "Fishes" 。
*成果說明	The stomach contents of 30 male and 43 female (age < 3 years) juvenile great hammerhead sharks (*Sphyrna mokarran*) obtained from commercial fisheries operating in Saudi Arabian waters of the Arabian Gulf were analyzed for the first time. After exclusion of parasites and abiotics, a total of 31 prey items, including the remains of cephalopods, fish, crustaceans, and bivalve mollusks, were identified in the stomachs of 59 great hammerheads. Based on the index of relative importance, teleosts were their main prey, and *Platycephalus indicus* (Linnaeus, 1758) was the most important prey at the species level. Significant age-related dietary differences were noted, indicating that the prey of the hammerheads aged 0–3 years shifted from Platycephalidae to Myliobatidae. Levin' s niche overlap index was low (0.05–0.21), indicating that <3-year-old juvenile great hammerheads are specialized predators. The estimated trophic level was 4.40–5.01 (mean ± SD, 4.66 ± 0.45), indicating that the great hammerhead is a tertiary consumer. 本研究分析沙烏地阿拉伯灣所捕捉到之錘頭雙髻鮫雉魚的胃內容物。魚類，特別是印度牛尾魚是最主要的餌料。同時我

	們觀察到有成長性的食性轉換，從牛尾魚類轉移鳶鰾類。錘頭雙髻鮫雉魚平均食性位階為4.66，代表他們是海洋食物網的頂層捕食者。	
成果影音	成果影音標題	
	Youtube 網址	
	說明	
成果照片 (請另行提供圖檔)	成果照片	
	照片說明	
成果檔案 (請另行提供檔案)	檔案名稱	3. 執行成果簡介(可公開資訊)_3.pdf

*標題	Elasmobranchs of the western Arabian Gulf: Diversity, status, and implications for conservation. 西部阿拉伯灣之軟骨魚現況'、多樣性及保育。	
*計畫成果簡述	We examined the sharks and batoids collected from the trawl surveys in the western Arabian Gulf from 2013 to 2016. We revealed the hotspots of the sharks and batoids, and examined biodiversity properties and conservation statuses. 我們利用拖網調查，以及漁港調查檢驗阿拉伯灣軟骨魚類之多樣性與保育狀況。 此研究已發表致 SCI 國際期刊。" Regional Studies in Marine Science"	
*成果說明	This paper presents information on elasmobranch diversity in the Saudi waters of the Arabian Gulf based on fishery-independent and dependent surveys. A total of 369 individual sharks and batoids were collected from 228 trawl stations surveyed between 2013 and 2016. *Gymnura poecilura* and *Carcharhinus dussumieri* were the most dominant batoid and shark species, respectively. The catch per unit area indicated the waters around Jana Island as a hotspot of elasmobranchs. A total of 135 surveys at the landing sites and fish markets from 2016 to 2020 showed that 88% of elasmobranchs (out of 4,055 individuals recorded) were caught by gill nets. Sharks were the most abundant (> 80 %). Of the 47 species recorded, six species were Critically Endangered regionally, six Endangered, and seven species Vulnerable according to the IUCN Red List of Threatened Species, necessitating proper management and conservation measures. 本研究利用兩種採樣方法，研究沙烏地阿拉伯灣軟骨魚類多樣性及其保育狀況。拖網研究採集到369隻軟骨魚個體，同時將其在阿拉伯灣之分布熱點描繪出。漁港採樣共觀測到四千隻以上之個體，鯊類最為常見，主要的捕撈網具為刺網。記錄到47種，依照 IUCN 紅皮書分類，6種是區域極度瀕危、6種瀕危、以及七種是收到威脅之種類，也因此沙烏地阿拉伯灣地區軟骨魚類需要適時的保護措施。	
成果影音	成果影音標題	

	Youtube 網址	
	說明	
成果照片 (請另行提供圖檔)	成果照片	
	照片說明	
成果檔案 (請另行提供檔案)	檔案名稱	3. 執行成果簡介(可公開資訊)_4.pdf

scientific reports

Check for updates

OPEN

Directional asymmetry in gonad length indicates moray eels (Teleostei, Anguilliformes, Muraenidae) are "right-gonadal"

Yu-Jia Lin[1] & Hong-Ming Chen[2,3]✉

Directional asymmetry indicates a unidirectional deviation from perfect bilateral symmetry, which was rarely examined in the inner organs of the teleost (Teleostei) compared to external traits. This study examines the directional asymmetry in the gonad length of 20 species of moray eels (Muraenidae) and two outgroup species with 2959 individuals. We tested three hypotheses: (1) moray eel species did not exhibit directional asymmetry in the gonad length; (2) the directional asymmetry pattern was the same for all selected species; (3) the directional asymmetry was not related to the major habitat types, depth and size classes, and taxonomic closeness of the species. Moray eels were generally "right-gonadal", the right gonad length being constantly and significantly longer than the left one in all studied Muraenidae species. The degree of asymmetry varied among species and was not significantly related to taxonomic closeness. The habitat types, depth, and size classes had intermingled effects on observed asymmetry without a clear correspondence. The directional asymmetry in the gonad length is a unique and widely occurring phenomenon in the Family Muraenidae, which was likely a by-product in the evolutionary history without significant disadvantage in survival.

Bilateral symmetry, the most common form of symmetry in the animal kingdom, involves reflection across an axis of symmetry (usually along the left–right axis)[1]. The deviation from perfect bilateral symmetry is called asymmetry and directional asymmetry indicates that such deviation is biased in one direction[2,3]. Directional asymmetry is commonly found in nature and taxonomically widespread[1,4]. Directional asymmetry can be an adaptation to selection[5], a consequence due to stresses in the environments[6], or simply an evolutionary by-product arising from mutations from pleiotropic genes[7,8].

In teleosts (Teleostei), the asymmetry in the inner organs has received far less attention compared to external morphological traits[8,9], with an exception for the otolith[10]. Some cases were reported of directional asymmetry in gonad sizes, such as the albacore *Thunnus alalunga*[11], the pollan *Coregonus autumnalis*[12], the ayu *Plecoglossus altivelis*[13], and the whitefish *Coregonus* sp.[14] and *Coregonus lavaretus*[15]. The limitation of these studies included limited sample sizes, small size ranges, and only single species analysis. Systematic studies with large sample sizes, wide size ranges, and multiple congeneric species examined simultaneously are still lacking.

Belonging to Anguilliformes, an elongated and eel-like Order with at least 16 families, the moray eels (Family: Muraenidae) is a large family with about 16 genera and 224 species[16]. In recent years, the taxonomy of moray eels has advanced greatly and scientists keep discovering new species in this family around the world[17–22]. Moray eels could reach 12 years old[23] and three groups of sexuality were found: gonochoristic, protogynous hermaphrodite, and simultaneous hermaphrodite[24]. Moray eels are important components of coral reef ecosystems as top predators, feeding on fish and other large invertebrates[25]. Being carnivorous, and especially piscivorous, they play significant roles in regulating the abundance of numerous preys[26], affecting the dynamics of coral reef-fish assemblages[27], and controlling alien fish species such as the lionfish[28,29]. They are found to be able to communicate and coordinate with other fish species in hunting[30].

Examination of the biology of the moray eels in Taiwan has continued for decades and we have accumulated a considerable amount of valuable data to examine the directional asymmetry of gonads with large sample sizes and numerous species examined simultaneously in a systematic manner. The major objective of this study is to examine the directional asymmetry in the gonad length of selected moray eel and outgroup species. Specifically,

[1]Institute of Marine Ecology and Conservation, National Sun Yat-Sen University, Kaohsiung, Taiwan. [2]Department of Aquaculture, National Taiwan Ocean University, Keelung, Taiwan. [3]Center of Excellence for the Oceans, National Taiwan Ocean University, Keelung, Taiwan. ✉email: hmchen@mail.ntou.edu.tw

we are going to test the following hypothesis: (1) some moray eel species did not exhibit directional asymmetry in the gonad length; (2) the degree of directional asymmetry was the same for all examined species; (3) the degree of directional asymmetry was not related to the major habitat types, depth and size classes, and taxonomic closeness. We further propose hypotheses that (1) observed directional asymmetry in the gonad length did not affect reproduction success and (2) it is a neutral by-product of evolutionary history, rather than exogenous environmental factors without significant adaptive advantages.

Results

A total of 22 species with 2,959 individuals and sufficient samples were selected for modeling directional asymmetry in gonad lengths. Among them 20 species from 5 genera belong to Muraenidae and two species, longfin snake-eel *Pisodonophis cancrivorus* (Ophichthidae) and shortbelly eel *Dysomma anguillare* (Synaphobranchidae) were included as the outgroup. The total lengths and weights by sex and species were summarized in Supplement material 1.

The gonad length ratios were the highest in reticulated moray eel *Gymnothorax minor* (previously *Gymnothorax reticularis*) with a mean (± SD) of 3.45 ± 1.41 and 7.70 ± 4.73 for females and males, respectively (Fig. 1, Table 1). The natural log-transformed ratios were significantly larger than 0 (equivalent to a ratio larger than 1) in the studied Muraenidae species (all ps < 0.004), indicating the existence of directional asymmetry in gonad length. The Akaike Information Criterion (AIC) values for model selection are shown in Supplement material 2. For a majority (13 out of 20) of Muraenidae species, the males had stronger degrees of directional asymmetry in the gonad length than the females, as indicated by their effects (i.e., $\ln(GLR_M - GLR_F)$) being significantly larger than 0 (all ps < 0.004, Table 1). The log-transformed gonad length ratios of two outgroup species were either close to zero (logged ratio = 0.051, p = 0.029 in *Pisodonophis cancrivorus*) or statistically zero (logged ratio = − 0.016, p = 0.474 in *Dysomma anguillare*, Table 1). The outgroup species had insignificant differences in gonad length ratio between sexes.

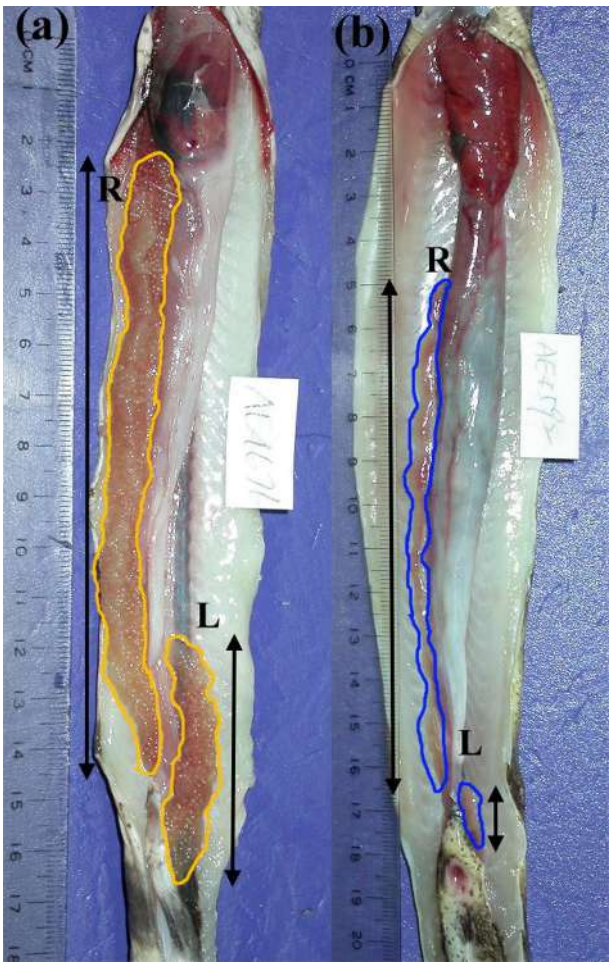

Figure 1. (**a**) A female *Gymnothorax minor*, collection ID: TOU-AE-4676 and (**b**) a male collection ID: TOU-AE-4592, showing the measurement of gonad length at both sides. The ovary is enclosed in orange and testis in blue. The left side (L) and right side (R) are defined when the fish is head up and belly down, and therefore, left–right direction appears opposite when the belly is up as shown this figure. Scale bar = 1 mm. (Photo credit: Huang, L.Y.)

Species	GLR_F	GLR_M	$\ln(GLR_F)$	$\ln(GLR_M - GLR_F)$
G. minor	3.45 ± 1.41	7.70 ± 4.73	1.187 (< 0.001)	0.720 (< 0.001)
G. chilospilus	1.45 ± 0.28	1.57 ± 0.44	0.409 (< 0.001)	0
G. eurostus	1.21 ± 0.19	1.47 ± 0.46	0.176 (< 0.001)	0.167 (< 0.001)
G. shaoi	1.65 ± 0.34	2.30 ± 0.47	0.482 (< 0.001)	0.331 (< 0.001)
G. prionodon	1.98 ± 0.43	2.45 ± 0.80	0.666 (< 0.001)	0.188 (< 0.001)
G. fimbriatus	1.25 ± 0.21	1.46 ± 0.46	0.208 (< 0.001)	0.129 (0.002)
G. flavimarginatus	1.62 ± 0.36	2.32 ± 0.58	0.458 (< 0.001)	0.353 (< 0.001)
G. hepaticus	1.25 ± 0.19	1.42 ± 0.21	0.211 (< 0.001)	0.127 (0.001)
G. kidako	1.85 ± 0.45	2.49 ± 0.76	0.572 (< 0.001)	0.294 (< 0.001)
G. pseudothyrsoideus	1.34 ± 0.25	1.66 ± 0.31	0.273 (< 0.001)	0.211 (< 0.001)
G. thyrsoideus	1.42 ± 0.23	1.49 ± 0.27	0.363 (< 0.001)	0
G. rueppelliae	1.51 ± 0.30	1.95 ± 0.54	0.392 (< 0.001)	0.240 (0.001)
G. neglectus	1.99 ± 0.37	2.60 ± 2.59	0.723 (< 0.001)	0
G. margaritophorus	1.73 ± 0.47	2.42 ± 1.15	0.698 (< 0.001)	0
G. pictus	1.48 ± 0.14	1.42 ± 0.19	0.372 (< 0.001)	0
E. polyzona	1.11 ± 0.34	1.27 ± 0.89	0.114 (< 0.001)	0
E. nebulosa	1.75 ± 0.38	1.85 ± 0.40	0.565 (< 0.001)	0
U. macrocephalus	1.13 ± 0.19	1.44 ± 0.52	0.110 (0.078)	0.207 (0.004)
U. micropterus	1.26 ± 0.18	1.57 ± 0.35	0.220 (< 0.001)	0.206 (0.001)
S. sathete	1.88 ± 0.52	1.59 ± 0.35	0.604 (< 0.001)	-0.162 (0.004)
P. cancrivorus	1.06 ± 0.20	1.10 ± 0.10	0.051 (0.029)	0
D. anguillare	1.00 ± 0.10	0.96 ± 0.17	-0.016 (0.474)	0

Table 1. Observed ratio of the right gonad length divided by the left (GLR), by species and sex (subscript F = female and set as the baseline and M = male), and estimated parameters (in natural logarithm, *p*-values in parenthesis) for the baseline gonad length ratio (GLR_F), and the sexual difference (GLR_M–GLR_F). Abbreviation for genera: *G. Gymnothorax*, *E. Echidna*, *U. Uropterygius*, *P. Pisodonophis*, *S. Strophidon* and *D. Dysomma.*

The studied species of Muraenidae had diverse relationships between the gonad length difference and both total length and sex (See Materials and Methods for details and Supplement material 3 for the demonstrating diagrams and Supplement 4 for AIC values of the candidate models for model selection). For example, the gonad length differences in *Gymnothorax minor* were significantly affected by the total length and sex (Supplement material 4). Moreover, the differences of *G. minor* females increased with total length faster than those of males (Table 2). This means that the degrees of directional asymmetry in the gonad length of *G. minor* became stronger as the size increased, particularly in females. On the other hand, the gonad length differences in *Gymnothorax thyrsoideus* were not affected by the total length and sex (Supplement material 4), with a difference significantly larger than zero ($p < 0001$, Table 2). Similar to the gonad length ratio, the gonad length differences of the two outgroup species were not affected significantly by the total length and sex. The gonad length differences of the two outgroup species were also either close to zero (0.644, $p = 0.046$ in *Pisodonophis cancrivorus*) or statistically zero (− 0.169, $p = 0.544$ in *Dysomma anguillare*, Table 2).

The directional asymmetry in the gonad length for 22 selected species was visualized by the biplot of principal component analysis (PCA), with the first two PCA axes explaining 85.6% of the total variation (Fig. 2). The first PCA axis is contributed mainly by the logged gonad length ratio and the slope of the relationship between the gonad length difference to the total length. In contrast, the second PCA axis is mostly the intercept (purple arrows in Fig. 3). Generally, the studied species were scattered randomly in the biplot, but two species stood out, *G. minor* (number 1) and yellow-edged moray *Gymnothorax flavimarginatus* (number 8). Two outgroup species (numbers in green) were also distributed close to the species in Muraenidae (numbers in blue).

Generally, the hierarchical cluster grouping of the directional asymmetry coefficients did not exhibit a strong and visible relationship to the habitat types, depth, and size classes, because these classes exhibited an intermingled pattern without a strong correspondence (Fig. 3). The taxonomic closeness, represented by the taxonomic distance based on the COI marker or the taxonomic distinctness index, did not play a significant role in this asymmetry as indicated by the Mantel test (9999 permutations, $p = 0.625$ and 0.535, respectively).

Discussion

In this study, we examined nearly 3000 individuals from 22 eel species and found a directional asymmetry in the gonad lengths of the moray eel species (Muraenidae). The length of their gonads on the right side was significantly longer than that on the left side, leading to the rejection of our first hypothesis, no directional asymmetry. This was likely a unique and widely-occurring phenomenon in moray eels, because this phenomenon was observed in all 20 muraenids examined, but not in two outgroup species, *Pisodonophis cancrivorus* (Ophichthidae) and *Dysomma anguillare* (Synaphobranchidae). Moreover, rather than a consistent pattern, the species examined exhibited considerable variation in the degree of directional asymmetry in the gonad length (Tables 1, 2; Fig. 2),

Species	A_F	B_F	A_M–A_F	B_M–B_F
G. minor	− 1.570 (0.006)	0.250 (< 0.001)	1.859(0.032)	− 0.063 (0.001)
G. chilospilus	3.462 (< 0.001)	0.100 (< 0.001)	− 3.069 (< 0.001)	0
G. eurostus	0.223 (0.875)	0.041 (0.031)	0.805 (0.006)	0
G. shaoi	− 1.422 (0.097)	0.150 (< 0.001)	0.787 (0.004)	0
G. prionodon	− 0.661 (0.252)	0.140 (< 0.001)	0	0
G. fimbriatus	0.995 (0.210)	0.030 (0.042)	0	0.019 (0.008)
G. flavimarginatus	− 2.298 (< 0.001)	0.097 (< 0.001)	0.826 (0.013)	0
G. hepaticus	3.249 (0.093)	0.043 (0.216)	− 6.074 (0.024)	0.135 (0.005)
G. kidako	− 0.022 (0.981)	0.122 (< 0.001)	0	0
G. pseudothyrsoideus	3.821 (< 0.001)	0	0	0
G. thyrsoideus	3.297 (< 0.001)	0	0	0
G. rueppelliae	− 1.976 (0.118)	0.130 (< 0.001)	0	0
G. neglectus	− 0.539 (0.636)	0.158 (< 0.001)	0	− 0.041 (< 0.001)
G. margaritophorus	− 2.170 (0.204)	0.155 (< 0.001)	0	0
G. pictus	− 1.118 (0.208)	0.114 (< 0.001)	0	− 0.048 (< 0.001)
E. polyzona	1.143 (< 0.001)	0	0	0
E. nebulosa	0.526 (0.758)	0.108 (0.004)	0	0
U. macrocephalus	1.067 (< 0.001)	0	0	0
U. micropterus	− 1.040 (0.096)	0.106 (< 0.001)	0	0
S. sathete	8.077 (< 0.001)	0.033 (0.078)	− 6.784 (< 0.001)	0
P. cancrivorus	0.644 (0.046)	0	0	0
D. anguillare	− 0.169 (0.544)	0	0	0

Table 2. Parameter estimates (A is the intercept and B is the slope) and corresponding *p*-values (in parentheses) for the best model representing the relationship between gonad length difference (GLD, right–left) and total length, and sex (subscript F and M for females and males, respectively).

thus leading to the rejection of the second hypothesis, the same degree of directional asymmetry for all examined species. This variation in the degree of asymmetry was not affected by the major habitat types, depth, and size classes (Fig. 3). Therefore, the third hypothesis, no effects from the habitat types, depth, and size classes on the directional asymmetry, was retained.

Natural variation can lead to the asymmetry in the gonad morphology[15]. The asymmetry in the gonad morphology was considered as an abnormal phenomenon[14] because it occurred in a minority (0 to 10% in 15) of the specimens. However, this study shows a different case that most of the moray eel specimens exhibit this directional asymmetry in the gonad length (Supplement material 5 for the scatter plots). Therefore, directional asymmetry in the gonad length might be the norm of the moray eel species examined and the possibility of natural variation can be ruled out.

Asymmetry in the gonad length (or weight) was occasionally observed in the teleost with one side being longer or heavier than the other one, and often related to somatic size and sex[11–13]. Asymmetry in gonad size was observed in 95% of the albacore (*Thunnus alalunga*) specimens examined of both sexes, with the right gonad larger than the left in 72% of the specimens and increased with increasing fork length[11]. Both sexes of the pollan (*Coregonus autumnalis*) showed directional asymmetry in gonad weight, with the left more prominent than the right in 70% of the specimens[12]. The frequency and degree of asymmetry are size-independent in males but became progressively more marked in females of > 120 g in weight. The gonad at the left side of the ayu, *Plecoglossus altivelis* was consistently longer and heavier than on the right side[13]. This asymmetry also became more pronounced with increasing age, especially in females.

Observed directional asymmetry in the gonad length may lead to some functional differences[31]. For example, the shorter side might contribute fewer gametes[32]. As the mature stages advanced, fully matured females might encounter a balance issue in the left–right direction in the spawning season because the egg sizes become larger and heavier, especially in *Gymnothorax minor* which showed the most extreme asymmetry. However, the directional asymmetry had, if there is any, only limited adaptive disadvantage in survival because these moray eels have persisted. Since the gonads are located in the abdominal cavity, the asymmetry would lead to little external morphological difference and therefore, the selection resulting from the morphological difference can hardly work. Fully matured gonads were found on both sides for most of the moray species examined[33,34] and therefore, the smaller contribution from the shorter side can be compensated by the longer side[35].

We hypothesize that observed directional asymmetry in moray eels is a by-product of evolutionary history[8,36], rather than an adaptation for better survival[37], or a consequence of environmental stresses[6]. First, all morays exhibited this asymmetry, while two outgroup species from different families did not, suggesting this asymmetry likely to be a by-product of the evolution of Muraenidae, which involves many unique morphological adaptations, such as highly modified gill arches that the fourth arc can be projected anteriorly[38]. Second, as argued earlier, the directional asymmetry might lead to little adaptive disadvantage in survival. Third, as represented by the

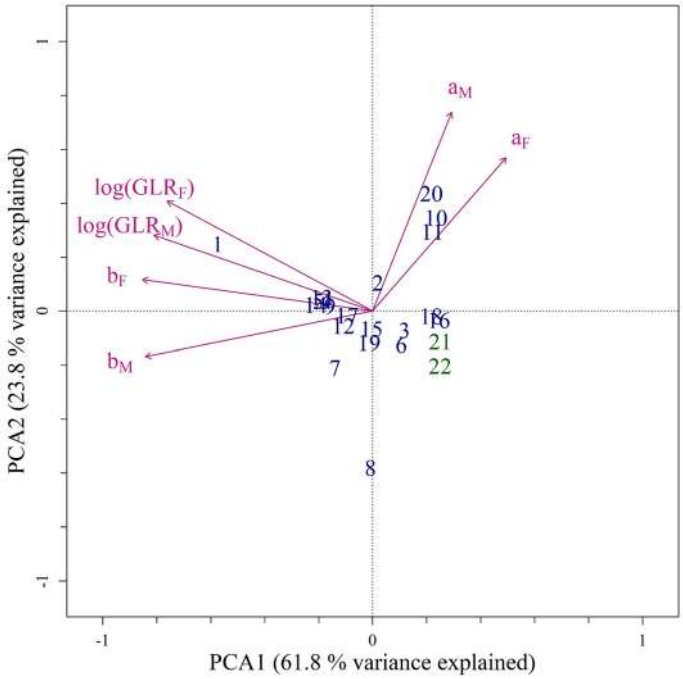

Figure 2. Biplot of the correlation-based principal component analysis on the standardized coefficients representing the directional symmetry in gonad length (log(GLR) is the natural log ratio of the gonad length, (**a**) and (**b**) is the intercept and slope of the relationship between the gonad length difference and the total length, respectively. Subscript F and M indicate females and males, respectively). The arrows indicate the correlation of variables to the first and second principal component axis (PCA1, 61.8%of total variance explained and PCA2, 23.8%of total variance explained). Numbers indicate the taxa examined (1: *G. minor*, 2: *G. chilospilus*, 3: *G. eurostus*, 4: *G. shaoi*, 5: *G. prionodon*, 6: *G. fimbriatus*, 7: *G. hepaticus*, 8: *G. flavimarginatus*, 9: *G. kidako*, 10: *G. pseudothyrsoideus*, 11: *G. thyrsoideus*, 12: *G. rueppelliae*, 13: *G. neglectus*, 14: *G. margaritophorus*, 15: *G. pictus*, 16: *E. polyzona*, 17: *E. nebulosa*, 18: *U. macrocephalus*, 19: *U. micropterus*, 20: *S. sathete*, 21: *P. cancrivorus,* and 22: *D. anguillare*). Numbers in blue belong to the Family Muraenidae and numbers in green represent the outgroup.

mosaic patterns in Fig. 3, the degree of asymmetry was not related to major habitat types and depth classes. This suggested that environmental factors had played insignificant roles in shaping observed directional asymmetry.

This study provides new puzzle pieces for the full picture of the directional asymmetry in gonad size observed in other vertebrates, particularly in birds[39–41]. Witschi[41] hypothesized that the asymmetry in the oviducts of female birds might have evolved as an adaptation to the aviatic life for reduced body weight and enhanced air dynamics. This is probably not the major factor in the marine environment where the density of water allows organisms to attain neutral buoyancy[42]. The packaging hypothesis states that asymmetry in gonads might reflect space constraints within the body cavity[35], which is also not sufficient to explain the observed asymmetry in the moray eels because their elongated body provides enough room in the abdomen for the gonads for both sides (Fig. 1). Sexual selection[37,43] or a by-product of the development of the secondary jaw[5,38] are two possible explanations for observed asymmetry in the moray eels, which can be tested in future studies.

Materials and methods

Collection of specimens. The moray eels used in this study were collected from eastern and northeastern Taiwan from 2003 to 2008 by various methods. Using bottom long-lines operating over eastern Taiwanese rocky coasts, most specimens were collected by collaborating fishermen. Some specimens were collected from the by-catch of trawlers operating over the northeastern Taiwan coast. Specimens were also collected from nearshore tidal pools by hook-and-line or anesthesia (clove oil). The specimens were transported back to the laboratory and frozen at − 20 °C.

After defrosting, total lengths (to 0.1 cm) and weights (to 0.1 g) of the specimens were measured. Then both sides of the gonads were removed after dissection. The left and right sides are defined when the fish head up and belly down (Fig. 1). The length of the gonad was measured to the nearest 0.1 mm and the weight was measured to the nearest 0.01 g. The sexes were determined by macroscopical examination of the gonads and later double-checked by microscopical examination[33,34]. We observed that both gonad length and weight exhibit left–right asymmetry. We use the gonad length, not the gonad weight, to represent the left–right asymmetry for being more robust to variation in sampling months.

Information about the major habitats, observed maximum length, and maximum depth of the studied taxon was obtained from FishBase[25]. The observed maximum length value from FishBase was replaced by the maximum

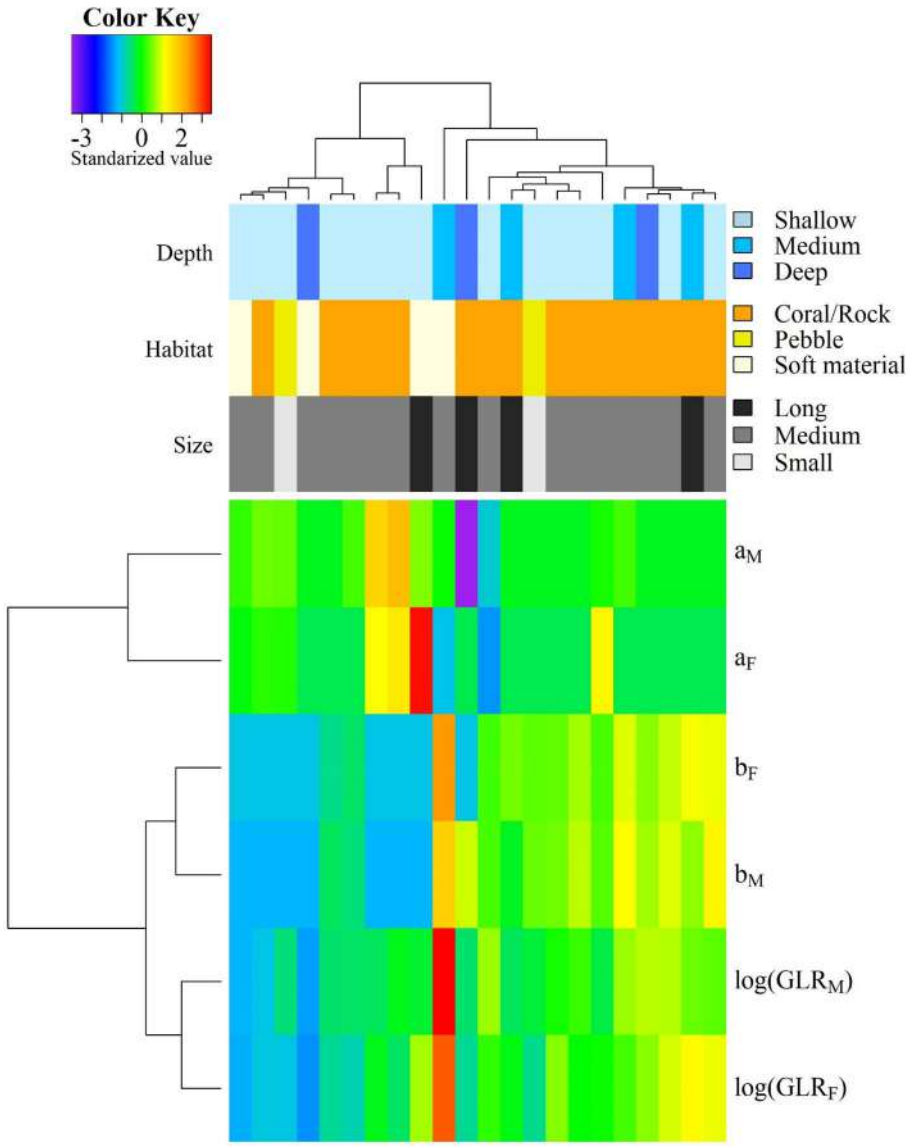

Figure 3. Heat-map of the standardized directional symmetry coefficients and habitat types (coral/rocky reefs, peddle beach, and seabed of soft materials), and maximum observed depth (shallow ≤ 50 m, medium: 50–100 m, and deep: > 100 m) and size categories (small: < 50 cm, medium (50–100 cm) and long (> 100 cm).

observed length in our database if the latter was larger than that in the FishBase. The major habitats were categorized into three types: coral/rocky reef, pebble beach, and seabed of soft materials. The maximum observed lengths were categorized into three size classes: small (< 50 cm), medium (50–100 cm), and long (> 100 cm), and the maximum observed depths into three categories: shallow (≤ 50 m), medium (50–100 m), and deep (> 100 m).

Representing the directional asymmetry, quantifying the degree of directional asymmetry, and testing the effects of total length and sex. Two indicators represent the directional asymmetry in the gonad length of the species examined. The first is the ratio of the gonad length of two sides (right divided by left) and the second is the gonad length difference (right minus left).

Ratios are commonly used as a measure without strong effects on the total length[12,44]. Ratios deviating from 1 indicate the existence of directional asymmetry in the gonad length; the larger the deviation the stronger the degree of directional asymmetry. The gonad length ratio was log-transformed and the effect of sex on the gonad length ratio was tested by a linear regression model with the Gaussian likelihood function. Two models were constructed: null model: the ratio was not affected by the sex, and an alternative model where the ratio was affected by the sex. Akaike information criterion (AIC) values for both models were calculated and used for model comparison. However, according to Burnham and Anderson[45], a difference in AIC value (δAIC, the AIC value between the AIC value from a candidate model and the lowest AIC value) < 2.0 between the two models indicates an insignificant difference. Therefore, we selected the best model according to the following criteria:

(1) the lowest AIC value with a δAIC value > 2.0, (2) if δAIC value < 2.0, then we select the one with the fewest parameters following the parsimony principle. The significance level (α) was set at ≤ 0.05. All the computation was completed in *R* (version 4.1.3)[46]

It is also common to use the difference in a given trait between the two sides to represent the directional asymmetry[2,3]. Moreover, the gonad length ratio is still not completely independent of the total length (Supplement material 4), while the gonad length difference can explicitly model the linear effect of total length on gonad length[2]. Therefore, multiple linear regression was applied to test the effects of total length and sex. Five models were constructed, as visualized in Supplement material 6: Null model: the gonad length difference was a constant (intercept-only model). In this model, a directional asymmetry exists if the intercept > 0. Model 1: the gonad length difference increased with the total length without differences between sexes. Model 2: the gonad length difference increased with total length, and the difference in intercepts represented the difference between sexes. Model 3: the gonad length difference increased with total length, and the difference in slopes represented the difference between sexes. Model 4: the gonad length difference increased with total length, and the difference in intercepts and slopes represented the difference between sexes. The best model was selected by the criteria previously described.

Taxonomic distances between species. Two approaches were applied to represent the taxonomic closeness among selected species. The first approach was to calculate a taxonomic distance based on the mitochondrial cytochrome oxidase subunit I (COI) sequence as done in Lin et al.[47]. The COI sequences were obtained from GenBank (www.ncbi.nlm.nih.gov/genbank/) where sequences for 20 species were available. One to six sequences were downloaded for each species and the sequences of specimens from Taiwan were preferred (see Supplement material 7 for detailed records of downloaded COI sequences). Multiple sequence alignment was applied to the raw COI sequences from GenBank using the ClustalW algorithm in the *R* package *msa*[48]. The Kimura two-parameter (K2P) distances between the specimens were calculated using the *R* package *ape*[49]. Then the average distances between the 20 species were calculated using *R* package *vegan*[50] and used as one measure of the taxonomic closeness.

The second approach is to use the taxonomic distinctness index, the average path length through a standard Linnaean tree[51] as a measure of taxonomic closeness. A Linnaean taxonomic tree (Family, Genus, and Species) of these 20 species whose COI sequences are available in Genbank was constructed and the averaged taxonomic distinctness index among species was calculated using the *R* package *vegan*.

Multivariate analysis. Correlation-based principal component analysis was applied to visualize the coefficients representing the directional symmetry in gonad length (i.e., the gonad length ratios, and the intercepts and slopes of the linear relationship between the gonad length difference and total length). These coefficients were standardized with a mean of zero and a standard deviation of 1. We applied cluster analysis based on the Euclidean distance of standardized coefficients representing the directional symmetry in gonad length with Ward's algorithm[52]. The heatmap was produced to simultaneously reveal the hierarchical cluster structures over the coefficients and the species with different categories (i.e., habitat types, depth, and size classes). Mantel test with 9999 permutations[53] was applied to test the non-parametric correlation (Kendall's τ) between the distance matrix of directional asymmetry coefficients and distance matrices representing the taxonomic closeness using *R* package *vegan*.

Data availability

The datasets analyzed during the current study are available from the corresponding author on reasonable request.

Received: 20 October 2022; Accepted: 31 January 2023
Published online: 20 February 2023

References

1. Graham, J. H., Raz, S., Hel-Or, H. & Nevo, E. Fluctuating asymmetry: Methods, theory, and applications. *Symmetry* **2**(2), 466–540 (2010).
2. Graham, J. H., Emlen, J. M., Freeman, D. C., Leamy, L. J. & Kieser, J. A. Directional asymmetry and the measurement of developmental instability. *Biol. J. Lin. Soc.* **64**(1), 1–16 (1998).
3. Dongen, V., Lensm, L. & Molenberghs, G. Mixture analysis of asymmetry: Modelling directional asymmetry, antisymmetry and heterogeneity in fluctuating asymmetry. *Ecol. Lett.* **2**(6), 387–396 (1999).
4. Palmer, A. R. Symmetry breaking and the evolution of development. *Science* **306**(5697), 828–833 (2004).
5. Møller, A. P. Directional selection on directional asymmetry: Testes size and secondary sexual characters in birds. *Proc. R. Soc. Lond. Ser. B Biol. Sci.* **258**(1352), 147–151 (1994).
6. Allenbach, D. M. Fluctuating asymmetry and exogenous stress in fishes: A review. *Rev. Fish Biol. Fish.* **21**(3), 355–376 (2011).
7. Werner, Y. L., Rothenstein, D. & Sivan, N. Directional asymmetry in reptiles (Sauria: Gekkonidae: Ptyodactylus) and its possible evolutionary role, with implications for biometrical methodology. *J. Zool.* **225**(4), 647–658 (1991).
8. Loehr, J. *et al.* Asymmetry in threespine stickleback lateral plates. *J. Zool.* **289**(4), 279–284 (2013).
9. Bell, M. A., Khalef, V. & Travis, M. P. Directional asymmetry of pelvic vestiges in threespine stickleback. *J. Exp. Zool. B Mol. Dev. Evol.* **308**(2), 189–199 (2007).
10. Somarakis, S., Kostikas, I. & Tsimenides, N. Fluctuating asymmetry in the otoliths of larval fish as an indicator of condition: Conceptual and methodological aspects. *J. Fish Biol.* **51**, 30–38 (1997).
11. Ratty, F. J., Laurs, R. M. & Kelly, R. M. Gonad morphology, histology, and spermatogenesis in South Pacific albacore tuna *Thunnus alalunga* (Scombridae). *Fish. Bull.* **88**, 207–216 (1989).
12. Harrod, C. & Griffiths, D. Parasitism, space constraints, and gonad asymmetry in the pollan (*Coregonus autumnalis*). *Can. J. Fish. Aquat. Sci.* **62**(12), 2796–2801 (2005).

13. Park, I. S., Zhang, C. I., Kim, Y. J. & Bang, I. C. Directional asymmetry of gonadal development in Ayu (*Plecoglossus altivelis*). *Fish. Aquat. Sci.* **8**(4), 207–212 (2005).
14. Bernet, D., Wahli, T., Kueng, C. & Segner, H. Frequent and unexplained gonadal abnormalities in whitefish (central alpine *Coregonus* sp.) from an alpine oligotrophic lake in Switzerland. *Dis. Aquat. Org.* **61**(1–2), 137–148 (2004).
15. Bittner, D. *et al.* How normal is abnormal? Discrimination between deformations and natural variation in gonad morphology of European whitefish *Coregonus lavaretus*. *J. Fish Biol.* **74**(7), 1594–1614 (2009).
16. Fricke, R., Eschmeyer, W. N. & R. van der Laan (eds) 2022. Eschmeyer's Catalog of Fishes: Genera, Species, References. (http://researcharchive.calacademy.org/research/ichthyology/catalog/fishcatmain.asp). Electronic version Accessed 31 12 2022).
17. Chen, H. M., Shao, K. T. & Chen, C. T. A review of the muraenid eels (Family Muraenidae) from Taiwan with descriptions of twelve new records. *Zool. Stud.* **33**(1), 44–64 (1994).
18. Chen, H. M., Loh, K. H. & Shao, K. T. A new species of moray eel, *Gymnothorax taiwanensis* (Anguilliformes: Muraenidae) from eastern Taiwan. *Raffles Bull. Zool.* **19**, 131–134 (2008).
19. Loh, K. H., Shao, K. T. & Chen, H. M. *Gymnothorax melanosomatus*, a new moray eel (Teleostei: Anguilliformes: Muraenidae) from southeastern Taiwan. *Zootaxa* **3134**(1), 43–52 (2011).
20. Loh, K. H., Shao, K. T., Ho, H. C., Lim, P. E. & Chen, H. M. A new species of moray eel (Anguilliformes: Muraenidae) from Taiwan, with comments on related elongate unpatterned species. *Zootaxa* **4060**(1), 30–40 (2015).
21. Huang, W. C., Mohapatra, A., Thu, P. T., Chen, H. M. & Liao, T. Y. A review of the genus *Strophidon* (Anguilliformes: Muraenidae), with description of a new species. *J. Fish Biol.* **97**(5), 1462–1480 (2020).
22. Huang, W. C., Smith, D. G., Loh, K. H. & Liao, T. Y. Two New Moray Eels of Genera *Diaphenchelys* and *Gymnothorax* (Anguilliformes: Muraenidae) from Taiwan and the Philippines. *Zool. Stud.* **60**, e24 (2021).
23. Matić-Skoko, S. *et al.* Mediterranean moray eel *Muraena helena* (Pisces: Muraenidae): biological indices for life history. *Aquat. Biol.* **13**(3), 275–284 (2011).
24. Fishelson, L. Comparative gonad morphology and sexuality of the Muraenidae (Pisces, Teleostei). *Copeia* **1992**, 197–209 (1992).
25. Froese, R. & D. Pauly. Editors. 2022.FishBase. World Wide Web electronic publication. www.fishbase.org. Accessed March 2022.
26. Almany, G. R. Differential effects of habitat complexity, predators and competitors on abundance of juvenile and adult coral reef fishes. *Oecologia* **141**(1), 105–113 (2004).
27. Hixon, M. A. & Beets, J. P. Predation, prey refuges, and the structure of coral-reef fish assemblages. *Ecol. Monogr.* **63**(1), 77–101 (1993).
28. Muñoz, R. C. Evidence of natural predation on invasive lionfish, Pterois s, by the spotted moray eel, *Gymnothorax moringa*. *Bull. Marine Sci.* **93**(3), 789–790 (2017).
29. Bos, A. R., Sanad, A. M. & Elsayed, K. *Gymnothorax* spp. (Muraenidae) as natural predators of the lionfish *Pterois miles* in its native biogeographical range. *Environ. Biol. Fish.* **100**(6), 745–748 (2017).
30. Bshary, R., Hohner, A., Ait-el-Djoudi, K. & Fricke, H. Interspecific communicative and coordinated hunting between groupers and giant moray eels in the Red Sea. *PLoS Biol.* **4**(12), e431 (2006).
31. Hedrick, B. P., Antalek-Schrag, P., Conith, A. J., Natanson, L. J. & Brennan, P. L. Variability and asymmetry in the shape of the spiny dogfish vagina revealed by 2D and 3D geometric morphometrics. *J. Zool.* **308**(1), 16–27 (2019).
32. Winters, G. H. Fecundity of the left and right ovaries of Grand Bank capelin (*Mallotus villosus*). *J. Fish. Board Can.* **28**(7), 1029–1033 (1971).
33. Huang, L.Y. Reproductive biology of *Gymnothorax reticularis* from the waters off northeastern Taiwan. Master Thesis, Department of Aquaculture, College of Life Sciences, National Taiwan Ocean University, Keelung, Taiwan (2008).
34. Loh, K.H. Molecular phylogeny and reproductive biology of moray eels (Muraenidae) around Taiwan. Ph.D. Thesis, Department of Aquaculture, College of Life Sciences, National Taiwan Ocean University, Keelung, Taiwan (2009).
35. Calhim, S. & Birkhead, T. R. Intraspecific variation in testis asymmetry in birds: evidence for naturally occurring compensation. *Proc. R. Soc. B Biol. Sci.* **276**(1665), 2279–2284 (2009).
36. Palmer, A. R. What determines direction of asymmetry: Genes, environment or chance?. *Philos. Trans. R. Soc. B Biol. Sci.* **371**(1710), 20150417 (2016).
37. Calhim, S. & Montgomerie, R. Testis asymmetry in birds: The influences of sexual and natural selection. *J. Avian Biol.* **46**(2), 175–185 (2015).
38. Johnson, G. D. Revisions of anatomical descriptions of the pharyngeal jaw apparatus in moray eels of the family Muraenidae (Teleostei: Anguilliformes). *Copeia* **107**(2), 341–357 (2019).
39. Blackburn, D. G. Structure, function, and evolution of the oviducts of squamate reptiles, with special reference to viviparity and placentation. *J. Exp. Zool.* **282**(4–5), 560–617 (1998).
40. Guioli, S. *et al.* Gonadal asymmetry and sex determination in birds. *Sex. Dev.* **8**(5), 227–242 (2014).
41. Witschi, E. Origin of asymmetry in the reproductive system of birds. *Am. J. Anat.* **56**(1), 119–141 (1935).
42. Ramirez-Llodra, E. *et al.* Deep, diverse and definitely different: Unique attributes of the world's largest ecosystem. *Biogeosciences* **7**(9), 2851–2899 (2010).
43. Calhim, S., Pruett-Jones, S., Webster, M. S. & Rowe, M. Asymmetries in reproductive anatomy: insights from promiscuous songbirds. *Biol. J. Lin. Soc.* **128**(3), 569–582 (2019).
44. Quillet, E., Labbe, L. & Queau, I. Asymmetry in sexual development of gonads in intersex rainbow trout. *J. Fish Biol.* **64**(4), 1147–1151 (2004).
45. Burnham, K. P. & Anderson, D. R. *Model Selection and Multimodel Inference: A Practical Information-Theoretic Approach* 2nd edn. (Springer, 2002).
46. R Core Team. R: A language and environment for statistical computing. R Foundation for Statistical Computing, Vienna, Austria. https://www.R-project.org/ (2022).
47. Lin, Y. J., Qurban, M. A., Shen, K. N. & Chao, N. L. Delimitation of Tiger-tooth croaker Otolithes species (Teleostei: Sciaenidae) from the Western Arabian Gulf using an integrative approach, with a description of *Otolithes arabicus* sp. nov. *Zool. Stud.* **58**, 10 (2019).
48. Bodenhofer, U., Bonatesta, E., Horejs-Kainrath, C. & Hochreiter, S. msa: An R package for multiple sequence alignment. *Bioinformatics* **31**(24), 3997–9999 (2015).
49. Paradis, E. & Schliep, K. ape 5.0: An environment for modern phylogenetics and evolutionary analyses in R. *Bioinformatics* **35**, 526–528 (2019).
50. Oksanen, J., Blanchet, F. G., Friendly, M., Kindt, R., Legendre, P., McGlinn, D., Minchin, P. R., O'Hara, R. B., Simpson, G. L., Solymos, P., Stevens, M. H. H., Szoecs E. & Wagner, H. vegan: Community Ecology Package. R package version 2.5–7. https://CRAN.R-project.org/package=vegan (2020).
51. Clarke, K. R. & Warwick, R. M. A taxonomic distinctness index and its statistical properties. *J. Appl. Ecol.* **35**(4), 523–531 (1998).
52. Murtagh, F. & Legendre, P. Ward's hierarchical agglomerative clustering method: which algorithms implement Ward's criterion?. *J. Classif.* **31**(3), 274–295 (2014).
53. Legendre, P. & Legendre, L. *Numerical Ecology* (Elsevier, 2012).

Acknowledgements
We would like to thank cooperative fishermen for collecting samples and providing information about the habitats of the specimens in the field. The team members in H.M. Chen's laboratory for dissecting and measuring the specimens. Brian M Jessop for reviewing the early draft and correcting the English use.

Author contributions
Y.J.L conceived the ideas, conducted the analysis, and drafted the manuscript. H.M.C chaired the data collection, discussed and rereviewed the manuscript. Both authors gave final approval for publication.

Competing interests
The authors declare no competing interests.

Additional information
Supplementary Information The online version contains supplementary material available at https://doi.org/10.1038/s41598-023-29218-3.

Correspondence and requests for materials should be addressed to H.-M.C.

Reprints and permissions information is available at www.nature.com/reprints.

Publisher's note Springer Nature remains neutral with regard to jurisdictional claims in published maps and institutional affiliations.

Regional Studies in Marine Science 65 (2023) 103056

Contents lists available at ScienceDirect

Regional Studies in Marine Science

journal homepage: www.elsevier.com/locate/rsma

Compartmentation of trace metals in *Cymodocea nodosa* from a heavily polluted area (Central Gulf of Gabes; Southern Mediterranean Sea): Potential use of the seagrass as environmental monitoring and bioremediation tool

Radhouan Belgacem El Zrelli [a,*], Lamia Yacoubi [b], Sylvie Castet [c], Michel Grégoire [c], Yu-Jia Lin [d], Faouzi Attia [e], Korhan Ayranci [f], Zaher Abdel Baki [g], Pierre Courjault-Radé [c], Lotfi Jilani Rabaoui [b,h]

[a] SADEF Agronomy & Environment, 30 Rue de la Station, 68700 Aspach-Le-Bas, France
[b] University of Tunis El Manar, Faculty of Science of Tunis, Laboratory of Biodiversity and Parasitology of Aquatic Ecosystems (LR18ES05), 2092 Tunis, Tunisia
[c] Géosciences Environnement Toulouse (GET), Université de Toulouse, UMR 5563 CNRS/UPS/IRD/CNES, 14 Avenue Edouard Belin, 31400 Toulouse, France
[d] National Taiwan University, Institute of Oceanography, Taipei 10617, Taiwan
[e] Manaseer Group, Life Science Direction, Amman 11110, Jordan
[f] College of Petroleum Engineering & Geosciences, King Fahd University of Petroleum & Minerals, Dhahran, 31261, Saudi Arabia
[g] College of Engineering and Technology, American University of the Middle East, Kuwait
[h] National Center for Wildlife, Riyadh, Saudi Arabia

ARTICLE INFO

Article history:
Received 7 February 2023
Received in revised form 8 June 2023
Accepted 12 June 2023
Available online xxxx

Keywords:
Cymodocea nodosa
Gulf of Gabes
Phosphogypsum
Trace metals
Bioaccumulation

ABSTRACT

This study was conducted to better understand the adaptative strategies of *Cymodocea nodosa* occurring in the heavily polluted environment of central Gulf of Gabes (SE Tunisia). Cd, Cu, Pb and Zn concentrations were assessed in the seagrass roots, rhizomes, and leaves, and in the surrounding seawater and sediments. Sediments were found to be the main source of contaminants bioaccumulated in *C. nodosa*. Bioaccumulation patterns differed significantly with metals and plant organs. While Cd, Cu and Zn were found to accumulate in leaves, Pb concentrates mainly in roots. In the heavily polluted environment of the Gulf of Gabes, *C. nodosa* seems to have developed two different adaptative strategies: metal trapping in roots and metal transfer from permanent (roots) to temporary (leaves) organs. These mechanisms allow the seagrass to remove the excess of metals. These properties show the potential use of *C. nodosa* not only as bioindicator but also as an effective bioremediation tool.

1. Introduction

Coastal habitats are continuously affected by various contaminants originating from urban, agricultural, and industrial sources (Gao and Chen, 2012; Pérez-López et al., 2016; Rabaoui et al., 2020; Solaun et al., 2021; Cunha et al., 2022). Consequently, many pollutants, in particular trace metals, reached critical levels in sediments, seawater, and biota (MEA, 2005; Halpern et al., 2008; Rabaoui et al., 2014; Sánchez-Quiles et al., 2017; Luo et al., 2022). Due to persistence of trace metals in natural environments, their tendency to accumulate in living organisms, and their toxicity (Yu et al., 2008; Gao and Chen, 2012), metals pose serious risks for marine biodiversity, habitats, and humans (Rainbow, 2007; Liu et al., 2011; Rabaoui et al., 2015; El Kateb et al., 2016; El Zrelli et al., 2018a). In the marine environment, metals tend to accumulate at the sediment-water interface and bio-magnify through food webs, leading to several disorders and diseases in marine organisms, but also in humans through seafood consumption (Barwick and Maher, 2003; Roberts et al., 2008; Solaun et al., 2021; Garcia-Vazquez et al., 2021; Liu et al., 2022; Cunha et al., 2022).

Many marine organisms were reported as informative bioindicators which can reflect the status of metallic pollution in marine environments (Zorba et al., 1992; Campanella et al., 2001; Conti and Cecchetti, 2003; Rabaoui et al., 2017; Richir and Gobert, 2016; El Zrelli, 2017; Hu et al., 2019; Bonanno et al., 2020). Because of their longevity and ability to integrate several environmental aspects, seagrasses are considered as excellent bioindicators which can inform not only on the current pollution status, but

* Corresponding author.
E-mail address: radhouan.elzrelli@gmail.com (R.B. El Zrelli).

https://doi.org/10.1016/j.rsma.2023.103056
2352-4855/

also on the historical changes of pollution in the marine environments (Reizopoulou and Nicolaidou, 2004; Llagostera et al., 2011; Orlando-Bonaca et al., 2015; El Zrelli et al., 2017; Hu et al., 2019; Rabaoui et al., 2020). Seagrasses were reported to have a high capacity to accumulate metals, due to their direct interaction with seawater and sediments through their roots and leaves (Romero et al., 2006). In fact, marine plants represent the major primary producers in marine environments, and they can bioaccumulate large quantities of metals through nutrient recycling (Kaldy, 2006). The usefulness of seagrasses as important tools to monitor trace metals has been reported in several studies conducted in many regions around the globe (El Zrelli et al., 2017; Bonanno and Borg, 2018; Hu et al., 2019; Rabaoui et al., 2020; Menicagli et al., 2022).

The Sea Straw or little Neptune Grass, *Cymodocea nodosa* (Ucria) Ascherson (1870) is a marine angiosperm species widely distributed along the Mediterranean and North Atlantic coasts (Reyes and Sansón, 1994; Green and Short, 2003; OSPAR Commission, 2010; Menicagli et al., 2022). *C. nodosa* is known by its large annual root growth facilitating therefore its colonization potential in various aquatic environments from very shallow waters up to 40 m depths (Reizopoulou and Nicolaidou, 2004). Although several studies using *C. nodosa* to monitor trace elements (Al, As, B, Ba, Ca, Cd, Cu, Co, Cr, Fe, K, Na, Ni, Mg, Mo, Mn, Pb, Se, Sr, Tl, U, V, and Zn) were conducted in the northern Mediterranean coasts (Catsiki and Panayotidis, 1993; Malea and Haritonidis, 1999; Llagostera et al., 2011; Malea and Kevrekidis, 2013; Bonanno and Di Martino, 2016; Bonanno and Borg, 2018), studies using this seagrass species to monitor metal pollution along the Southern Mediterranean coasts are not available. Within this context, the Gulf of Gabes (south-eastern Tunisia) is known to be one of the heavily polluted regions in Southern Mediterranean Sea (Darmoul et al., 1980; Darmoul and Vitiello, 1980; Darmoul, 1988; Rabaoui et al., 2014, 2015, 2017; El Zrelli et al., 2015, 2021; El Zrelli, 2017) which hosts seagrass species including *C. nodosa*. Therefore, studying bioaccumulation patterns of heavy metals in *C. nodosa* from the Gulf of Gabes provides crucial insights into defining the adaptative strategies that this plant might has developed as a response to high pollutant levels and to better understand how the plant can get rid of the excess of pollutants in its tissues. The present study aims (*i*) to investigate the relationships of trace metal contents in different organs of *C. nodosa* with those of seawater and sediments, (*ii*) to examine the compartmentation (roots, rhizomes, leaves) of trace metals in *C. nodosa*, and (*iii*) to determine the bioaccumulation patterns and adaptive strategies of the seagrass plant in heavily polluted environments such as in the Gulf of Gabes.

2. Materials and methods

2.1. Study area and sampling

This study was conducted in the central part of the Gulf of Gabes, one of the heavily polluted marine areas in the Mediterranean Basin (Darmoul, 1988; Rabaoui et al., 2014; El Kateb et al., 2016; El Zrelli et al., 2019a,c). The major pollution source in the area is represented by the coastal phosphate industry of Gabes city, named the Tunisian Chemical Group (GCT), which dumps huge quantities of phosphogypsum (PG) wastes directly in the marine environment (El Zrelli et al., 2018b). It is estimated that ~10.5 10^6t of untreated humid PG are discharged annually by the GCT into the Gulf of Gabes (more than 500 10^6t of untreated wet PG since 1972), with severe consequences on seagrass meadows and marine biota (Darmoul et al., 1980; Darmoul, 1988; El Kateb et al., 2016; Rabaoui et al., 2015; El Zrelli et al., 2017, 2020, 2023a).

Table 1
Locations (GPS coordinates; dd format) of the six sampling sites, in the central coastal area of the Gabes Gulf (south-eastern Tunisia).

Sampling site	Distance to the GCT industrial discharge wastes	Coordinates
OS	11.07 km	33.8499722 10.1940389
LM	14.23 km	33.8307444 10.2185417
BJ	17.27 km	33.8136278 10.2447611
KK	20.38 km	33.7965750 10.2711250
KT	23.45 km	33.7783139 10.2953694
LI	26.47 km	33.7575806 10.3278361

C. nodosa samples were collected from six sampling sites (from north to south: OS, LM, BJ, KK, KT, LI), along a 2.5 km transect defined in parallel to the shoreline (Fig. 1 & Table 1), and in the southern direction of marine PG dispersion (El Zrelli et al., 2018a, 2019b). The sampling sites are 3 km equidistant. The closest site to PG discharge canal (i.e., OS) which is located ~11 km away from this discharge is the site where the first appearance of *C. nodosa* seagrass was recorded in high densities (Table 1). A total of 60 *C. nodosa* samples were collected, with the rate of 10 samples per site. In parallel to seagrass sampling, 3 surface sediment samples (500 g each) and 3 seawater samples (500 mL each) were collected from each site. Surface sediment samples were taken from the upper 10 cm layer, from a quadrat area, using a 100 cm^2 area Van Veen Grab sampler. As described in Bonanno and Raccuia (2018), seawater samples were collected at the height of *C. nodosa* seagrass canopy. From each station, three sub-samples were collected and mixed altogether to have one single sample (composite sample) representative of each station. Collected *C. nodosa*, sediment and seawater samples were immediately stored in sterilized and airtight polyethylene bags (seagrass and sediment samples) and glass jars and transported to the laboratory in ice chests and stored at 4 °C.

2.2. Laboratory analysis of samples collected

C. nodosa plant samples were rinsed with seawater and separated into their roots, rhizomes, and leaves, after being rinsed with ultrapure water (Milli-Q®) to remove epiphytic organisms and fine sediment particles. The samples of different seagrass organs were left to dry at 60 °C for 24 h. The dried samples were thereafter manually grounded, weighted, and digested following the protocol described by Tovar-Sánchez et al. (2010).

The sediment samples collected from each site were mixed to make composite samples which were thereafter dried, sieved (Ø < 2 mm), and homogenized. From each composite sediment sample, a 0.5 g subsample was digested using a mixed solution of HNO_3-H_2O_2-HCl, prior to chemical analysis following the protocol of USA EPA method 3050B (USEPA, 1999). Collected seawater samples were filtered through a 0.22 μm diameter filter, acidified with ultrapure 10% HNO_3, and kept at 4°C until further chemical analysis.

The concentrations of cadmium (Cd), copper (Cu), lead (Pb) and zinc (Zn) were analyzed in all samples collected (i.e., different organs of *C. nodosa*, sediment, and seawater) by inductively coupled plasma optical emission spectroscopy (ICP-OES, ULTIMA Expert Horiba Scientific). The accuracy of measurements was checked using three standard reference materials: BCR 060 (developed by the Institute for Reference Materials and Measurements; Lagarosiphon major for aquatic plants), GeoPT10 (CH-1) (developed by the Institute of Rock and Mineral Analysis of Beijing for coastal sediments), and XSPEXF-2812 (from SPEX CertiPrep® for seawater analyses). The analytical results of the quality control samples indicated good agreement between the

Fig. 1. Location of the six sampling sites along the Central Gulf of Gabes. The map also shows the location of the main industrial wastes (phosphogypsum wastes) discharge from the coastal industrial complex of Gabes (represented mainly by the *Groupe Chimique Tunisien*, GCT).

certified and measured values of the used reference materials, with recoveries within ±10% for all studied trace metals (seagrass: 98.63% (Pb) - 105.96% (Cu), sediments: 96.26% (Cd) - 108.04% (Zn) and seawater: 93.65% (Cd) - 105.42% (Cu); Table S1).

2.3. Data analysis of the trace metal concentrations

Trace metal concentrations analyzed in the different *C. nodosa* organs, sediments, and seawater were compared using boxplots, combining the results of all sampling stations. In addition, a principal component analysis (PCA) was applied to summarize the multivariate elemental concentration data. The elemental concentrations were standardized before running PCA to remove the effect of different magnitudes among elements. Then the correlation matrix was used to run PCA. The first two principal component axes (PCA axes) were used to visualize the variation of elemental composition of the different plant organs and compartments (seawater and sediments). PCA was conducted using statistical software R (ver 4.2.1, R Core Team, 2022).

2.4. Calculation of environmental and ecological indices using geochemical data of marine sediments

The environmental status of marine sediments was assessed using four known pollution indices: the Contamination factor (C_f), Contamination degree (C_d), Pollution Load Index (PLI), and Geoaccumulation Index (I_{geo}) (Table 2). These indices help to interpret the geochemical data of surface sediment samples collected from Central Gulf of Gabes. Four additional indices were also calculated in surface sediment samples to assess the ecological status of the study area. These ecological indices include the Potential ecological risk (Eri), Potential Ecological Risk Index (PERI), Mean ERM Quotient (M-ERM-Q) and Hazard Quotient (HQ) (Table 2). For these indices, the northern Metouia locality (Fig. S1) was selected as a reference site, because it is located away from of the industrial complex of Gabes (main source of metallic pollution in the study area), and hence its surface sediments are not considered to be affected by metallic enrichment caused by this latter complex (El Zrelli et al., 2015). The average concentrations of Cd, Cu, Pb, and Zn in the sediments of Metouia (0.11 mg kg^{-1}, 0.59 mg kg^{-1}, 5 mg kg^{-1} 5.4 mg kg^{-1}, respectively) were used as references of the local background values (El Zrelli et al., 2015).

2.5. Trace metal transfer from sediments to C. nodosa

To assess the mobility of the trace metals analyzed from sediments to the different plant tissues, the two following factors were further calculated:

2.5.1. Bio-concentration Factor (BCF)

For each of the four trace metals analyzed, BCF was calculated by dividing the metal concentration in the root ($[C]_{root}$; mg kg^{-1} DW) by its concentrations in sediments ($[C]_{sediments}$; mg kg^{-1} DW) using the following equation:

$$BCF = \frac{[C]_{root}}{[C]_{sediments}} \quad (1)$$

BCF is an indicator of plant's ability to uptake trace elements from sediments and to accumulate them in their roots (Bonanno and Raccuia, 2018). BCF increases with the increase of the plant bioaccumulation capability and *vice versa* (USEPA, 2007).

2.5.2. Translocation Factors (TF)

This factor was proposed by Deng et al. (2004) to evaluate the inter-organs mobility of trace elements in a plant. TF can be calculated using the following equation:

$$TF = \frac{[C]_{organ1}}{[C]_{organ2}} \quad (2)$$

where $[C]_{organ}$ is the concentration of the trace element tested in roots, rhizomes or leaves of *C. nodosa* (mg kg^{-1} DW). According to Deng et al. (2004), TF values and plant translocation capability increase proportionally.

3. Results and discussion

Table 3 represents the concentrations of four trace metals analyzed in different organs of *C. nodosa*, as well as in sediments and seawater. All trace metals studied herein were detected in all *C. nodosa* organs, as well as in sediment and seawater samples, except for Cd which was found only in KK, TT, and LI sampling sites, and Zn which was detected only in KT (Table 3). The boxplot analysis showed significant variations between the average trace metal concentrations analyzed in all sites between *C. nodosa* organs and the seawater and sediment compartments (Fig. 2). The presence of trace metals in all analyzed samples could be

Table 2
Indexes and methods used in the environmental and ecological risk assessments of the surface sediments of Central Gulf of Gabes.

Indexes	Formulae/description	Variables	Scales and Interpretation	References
Contamination factor (C_f)	$C_f = Cs/C_b$	• C_s: trace element concentration in the sample • C_b: trace element background concentration	• $C_f < 1$: low factor • $1 \leq C_f < 3$: moderate factor • $3 \leq C_f < 6$: considerable factor • $C_f \geq 6$: very high factor	Håkanson (1980)
Contamination degree (C_d)	$C_d = \sum C_f$	C_f : Contamination factor	• $C_d < 8$: low sediment contamination • $8 \leq C_d < 16$: moderate sediment contamination • $16 \leq C_d < 32$: considerable sediment contamination • $C_d \geq 32$: very high sediment contamination	Håkanson (1980)
Pollution Load Index (PLI)	$PLI = (C_{f1} \times C_{f2} \times_{...} C_{fn})^{1/n}$	• C_f: contamination factor • n: number of trace elements analyzed	• PLI $\leq$ 1: non-polluted • PLI > 1: polluted	Tomlinson et al. (1980)
Geoaccumulation index (I_{geo})	$I_{geo} = \log_2 (C_s/1.5\ C_b)$	• C_s: trace element concentration in the sample • C_b: trace element background concentration • 1.5: background matrix correction factor	• $I_{geo} \leq 0$: uncontaminated • $0 < I_{geo} \leq 1$: uncontaminated to moderately contaminated • $1 < I_{geo} \leq 2$: moderately contaminated • $2 < I_{geo} \leq 3$: moderately to strongly contaminated • $3 < I_{geo} \leq 4$: strongly contaminated • $4 < I_{geo} \leq 5$: strongly to extremely contaminated • $I_{geo} > 5$: extremely contaminated	Müller (1969)
Potential Ecological Risk Index (PERI)	$RI = \sum E^i_r = \sum T^i_r . C^i_f$	• RI: sum of individual potential ecological risk for all trace elements • E^i_r: PERI of an individual trace element • T^i_r: toxic-response factor for a given trace element (As = 10, Cd = 30, Cr = 2, Cu = Pb = 5, Hg = 40 and Zn = 1) • C^i_f: contamination factor	• RI < 150: low ecological risk • 150 $\leq$ RI < 300: moderate ecological risk • 300 $\leq$ RI < 600: considerable ecological risk • RI $\geq$ 600: very high ecological risk	Håkanson (1980)
Mean ERM quotient (M-ERM-Q)	M-ERM-Q = $\sum(C_i/ERM_i)/n$	• C_i: trace element concentration in the sample • ERM_i: Effect Range-Median value • n: number of trace elements analyzed	• M-ERM-Q < 0.1: 9% probability of toxicity • 0.11 $\leq$ M-ERM-Q < 0.5: 21% probability of toxicity • 0.51 $\leq$ M-ERM-Q < 1.5: 49% probability of toxicity • M-ERM-Q > 1.5: 76% probability of toxicity	Long et al. (2000)
Hazard Quotient (HQ)	HQ = SCC/SQG	• SCC: the concentration of metal in sediments • SQG: the sediment quality guidelines. SQG values were determined at ERL levels (Long et al., 1995).	• HQ < 0.1: no adverse effects • 0.1 $\leq$ HQ < 1: potential hazards • 1 $\leq$ HQ < 10: moderate hazards • HQ > 10: high hazards	Wang et al. (2015b) and Feng et al. (2011)
Effect Range-Low (ERL)	Represents the chemical concentration below which adverse effects would be rarely observed.		ERL_{Cd} = 1.2; ERL_{Cu} = 34, ERL_{Pb} = 46.7 and ERL_{Zn} = 150 (mg kg^{-1}; NOAA, 2012)	Long and Morgan (1991)

explained by the heavy pollution level characterizing the central part of Gabes Gulf. In fact, the huge quantities of untreated phosphogypsum discharged from GCT factories of Gabes into the open sea were reported to enrich the marine environment with diverse pollutants including heavy metals (Rabaoui et al., 2014, 2015, 2017; El Zrelli et al., 2015, 2017). In the case of the four trace metals analyzed herein, El Zrelli et al. (2018b) previously reported that the annual industrial flows from GCT untreated PG wastes into the coastal environment of Gabes Gulf may reach up to 93.03 t y^{-1} for Cd, 50.46 t y^{-1} for Cu, 4.73 t y^{-1} for Pb and 720.07 t y^{-1} for Zn.

With respect to sampling sites, the decreasing orders of trace metal concentrations were found to be OS > LM > LI > KK > BJ > KT for Cd, LI > LM > OS > KT > KK > BJ for Cu, OS > LI > LM > KT > KK > BJ for Pb, and OS > KT > LM > LI > KK > BJ for Zn (Table 3). Except for Cu concentrations in LI, the highest concentrations of trace metals were in general recorded in the sampling site of 'OS'. In contrast, the lowest elemental concentrations were found in BJ, except for Cd with which the lowest record was found in KT. The PCA plot made based on the two first principal components (axes 1 and 2), given in Fig. 3, confirmed the boxplot result showing clear separation between the different plant organs and compartment (sediment and seawater). A site-based separation can be observed between the analyzed samples, in particular with *C. nodosa* roots and leaves showing a clear segregation between KT and BJ (least polluted sites) from the rest of sites (Fig. 3).

The results of the eight environmental and ecological indices are given in Tables 4 and 5. While C_f values showed considerable contamination with Cu, in all sampling sites, these latter were all found moderately contaminated by Pb and Zn. In the case of Cd, C_f records showed that all sites are considerably

Table 3
Concentrations of Cd, Cu, Pb, and Zn in organs of *C. nodosa* (leaves, rhizomes, and roots; mg kg^{-1}), and associated sediments (mg kg^{-1}) and waters (μg l^{-1}). Nd*: Not detected.

Trace metals	Plant tissue or materials	Sampling sites					
		OS	LM	BJ	KK	KT	LI
Cd	*Leaves*	2.40 ± 0.17	3.40 ± 0.18	1.42 ± 0.13	2.44 ± 0.12	1.51 ± 0.11	2.77 ± 0.11
	Rhizomes	0.45 ± 0.09	0.36 ± 0.07	0.53 ± 0.08	0.53 ± 0.22	0.36 ± 0.07	0.27 ± 010
	Roots	1.33 ± 0.13	1.24 ± 0.11	3.27 ± 0.15	1.32 ± 0.11	2.24 ± 0.08	1.39 ± 0.35
	Sediment	0.59 ± 0.01	0.54 ± 0.03	0.32 ± 0.01	0.33 ± 0.01	0.17 ± 0.02	0.40 ± 0.01
	Seawater	0.45 ± 0.11	0.35 ± 0.06	0.32 ± 0.10	<0.27	<0.27	<0.27
Cu	*Leaves*	3.95 ± 0.16	3.33 ± 0.22	2.56 ± 0.12	4.22 ± 0.19	2.74 ± 0.18	3.59 ± 0.32
	Rhizomes	0.99 ± 0.11	1.02 ± 0.23	1.23 ± 0.12	1.44 ±.14	0.97 ± 0.18	1.11 ± 0.23
	Roots	3.51 ± 0.19	2.83 ± 0.34	3.14 ± 0.08	2.36 ± 0.19	2.68 ± 0.23	1.82 ± 0.31
	Sediment	2.69 ± 0.13	2.81 ± 0.02	2.49 ± 0.03	2.57 ± 0.07	2.58 ± 0.13	3.08 ± 0.06
	Seawater	3.63 ± 1.22	2.90 ± 0.24	2.94 ± 0.53	2.81 ± 0.04	2.61 ± 0.07	2.84 ± 0.13
Pb	*Leaves*	1.74 ± 0.23	1.56 ± 0.09	1.52 ± 0.12	1.33 ± 0.11	1.15 ± 0.03	1.45 ± 0.33
	Rhizomes	0.26 ± 0.08	0.51 ± 0.15	0.44 ± 0.08	0.36 ± 0.10	0.24 ± 0.05	0.25 ± 0.13
	Roots	3.76 ± 0.26	3.55 ± 0.29	2.81 ± 0.09	2.64 ± 0.29	3.37 ± 0.43	3.98 ± 0.10
	Sediment	5.08 ± 0.04	4.72 ± 0.06	3.90 ± 0.01	3.92 ± 0.10	4.53 ± 0.05	4.87 ± 0.07
	Seawater	0.10 ± 0.01	0.12 ± 0.01	0.16 ± 0.02	0.10 ± 0.03	0.09 ± 0.02	0.16 ± 0.04
Zn	*Leaves*	131.33 ± 8.08	184.33 ± 12.34	163.67 ± 4.93	159.00 ± 17.69	117.67 ± 12.50	135.67 ± 11.15
	Rhizomes	55.00 ± 9.64	71.33 ± 5.51	72.67 ± 14.57	72.00 ± 4.58	62.67 ± 4.16	54.67 ± 7.51
	Roots	31.00 ± 6.24	40.00 ± 4.58	65.67 ± 13.32	47.67 ± 8.50	54.00 ± 11.36	37.33 ± 7.09
	Sediment	12.48 ± 0.09	10.05 ± 0.20	7.54 ± 0.09	7.59 ± 0.12	10.19 ± 0.06	9.96 ± 0.12
	Seawater	2.39 ± 0.28	2.73 ± 0.42	4.13 ± 0.43	2.26 ± 0.38	<1.95	2.57 ± 0.16

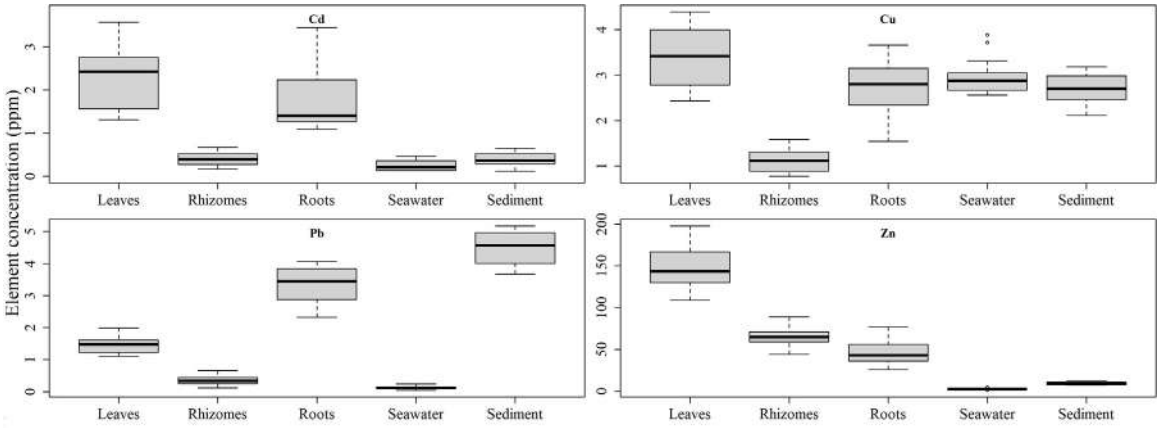

Fig. 2. The boxplots of four trace elements (cadmium: Cd, copper: Cu, lead: Pb, zinc: Zn) analyzed in the three *Cymodocea nodosa* organs (leaves, rhizomes, and roots), seawater, and sediments.

contaminated, except for BJ and KT which showed a moderate contamination with this heavy metal. In addition, C_d and PLI classified all sampling sites as "moderately contaminated" and "polluted", respectively. Moreover, the I_{geo} index showed that apart from sites OS ("extremely contaminated") and KT ("moderately to strongly contaminated"), the other sites were either "strongly to extremely contaminated" (LM and LI), and "strongly contaminated" (BJ and KK) (Table 4). In terms of ecological status assessment, PERI index results indicated that while the sediments of the two sites OS and LM showed a moderate ecological risk, those of the other sites have a low ecological risk (Table 5). The M-ERM-Q showed a 9% probability of toxicity in all sampling sites. In the same sense, HQ index showed that all these sites have potential hazards (Table 5). These results showed that all sampling sites have different levels of metallic pollution and ecological risks. In general, these indices showed that the study area is heavily contaminated with trace metals taken into consideration (see Table 4).

Compared to seawater samples, sediment elemental concentrations were found to be higher from 916 (for Cu) to 36 774 times (for Pb) (Table 3). This can be explained by the fact that trace metal load is mostly bound to sediments (Calmano et al., 1993). In fact, it is known that trace elements have higher affinity to sediments (Gaur et al., 2005; Yu et al., 2008) which can play the role of a sink for these pollutants (Lafabrie et al., 2013). Since *C. nodosa* roots are in direct contact with sediments, they constitute the main system up-taking the contaminants from the marine environment (sediments) into the other organs of the plant. The absorption of seawater pollutants by the plant leaves represents the second pathway of metal transfer from the marine environment to *C. nodosa*, as reported by Bat et al. (2021).

The concentrations of Cd in *C. nodosa* organs ranged from 0.27 (in *C. nodosa* rhizomes from LI) to 3.40 mg kg^{-1} (in *C. nodosa* leaves from LM; Table 3). Those of Pb were found to vary between 0.97 (in *C. nodosa* rhizomes from KT) to 4.22 mg kg^{-1} (leaves from KK). In the case of Cu, the concentrations in seagrass tissues fluctuated from 0.26 (in *C. nodosa* rhizomes from OS) to 3.98 mg kg^{-1} (in *C. nodosa* roots from LI). Regarding Zn, its concentrations oscillated between 31.00 (in *C. nodosa* roots from OS) to 184.33 mg kg^{-1} (in *C. nodosa* leaves from LM).

The average concentrations of Cd, Cu, Pb and Zn in *C. nodosa* were found to be 1.51, 2.42, 1.72, and 86.34 mg kg^{-1}, respectively (Table 3). Taking into consideration all studied *C. nodosa* organs (roots, rhizomes, and leaves), the decreasing order of trace metals concentrations was found to be as follows: *Leaves* > *Roots* > *Rhizomes* for both Cd and Cu, *Roots* > *Leaves* > *Rhizomes* for Pb,

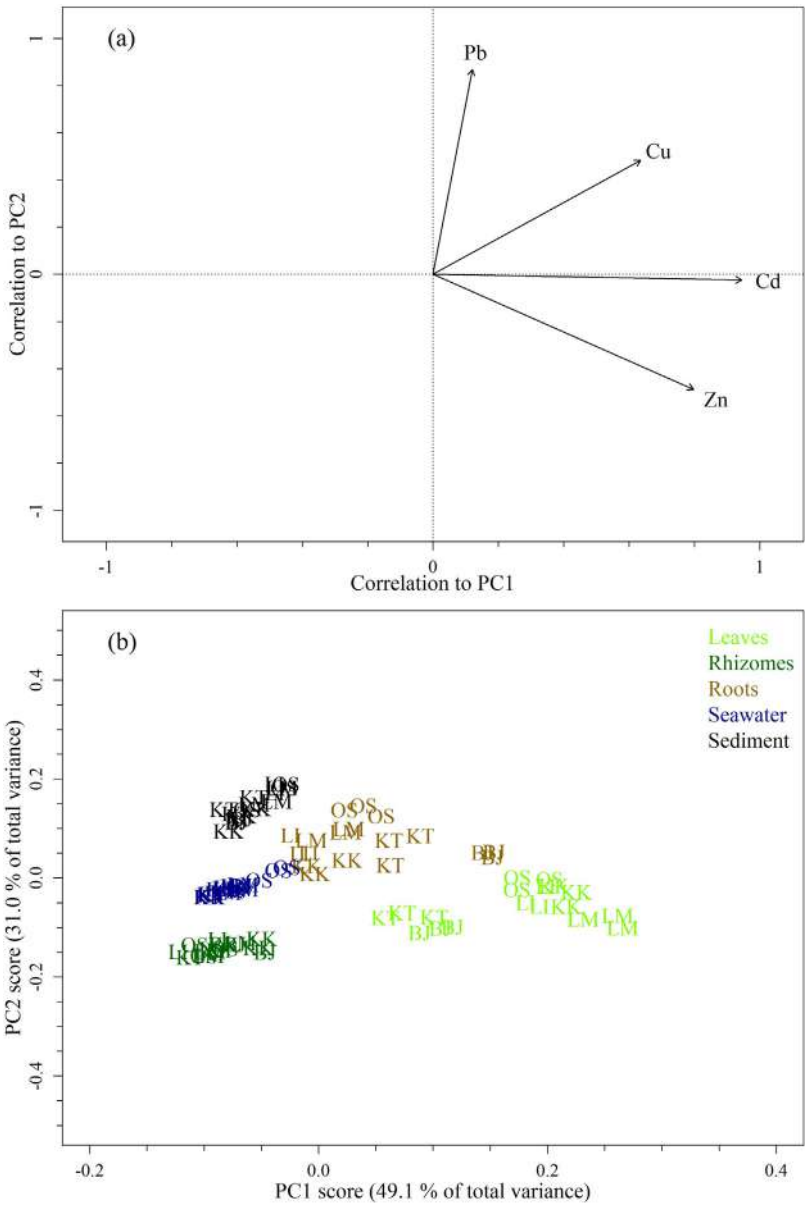

Fig. 3. Principal component analysis plots representing the correlations of the four elements analyzed (cadmium: Cd, copper: Cu, lead: Pb, zinc: Zn) with the first two principal component/axes, PC1 and PC2 (a), and scatter plots of the analyzed *Cymodocea nodosa* samples (leaves = green, rhizomes = dark green, and roots = brown), seawater (blue), and sediments (black) (b). Different letters indicate the different sampling sites (BJ, KK, KT, LI, LM, and OS, as shown in Fig. 1).

Table 4
Values of the contamination factor (C_f), Contamination degree (C_d), Pollution Load Index (PLI) and Geoaccumulation Index (I_{geo}), calculated based on the geochemical sediment data of the central coastal area of the Gabes Gulf, and the classification of sampling sites.

Site	C_f				C_d		PLI		I_{geo}					
	Cd	Cu	Pb	Zn	Value	Classification	Value	Classification	Cd	Cu	Pb	Zn	Total	Classification
OS	5.36	4.56	2.75	2.31	13.25		2.75		−4.53	0.08	4.08	5.49	5.12	Extremely contaminated
LM	4.91	4.76	2.53	1.86	12.48		2.53		−4.66	0.14	3.98	5.18	4.64	Strongly to extremely contaminated
BJ	2.91	4.22	1.91	1.40	9.31	Moderate sediment contamination	1.91	Polluted	−5.41	−0.03	3.70	4.76	3.02	Strongly contaminated
KK	3.00	4.36	1.95	1.41	9.55		1.95		−5.37	0.02	3.71	4.77	3.13	
KT	1.55	4.37	1.84	1.89	8.71		1.84		−6.33	0.02	3.92	5.20	2.81	Moderately to strongly contaminated
LI	3.64	5.22	2.42	1.84	11.68		2.42		−5.09	0.28	4.02	5.16	4.37	Strongly to extremely contaminated

Table 5
Values of the Potential Ecological Risk (Eri), Potential Ecological Risk Index (PERI), Mean ERM Quotient (M-ERM-Q) and Hazard Quotient (HQ), calculated based on the geochemical sediment data of the central coastal area of Gabes Gulf, and the classification of sampling sites.

Site	E_r^i				PERI		M-ERM-Q		HQ	
	Cd	Cu	Pb	Zn	Value	Classification	Value	Classification	Value	Classification
OS	160.91	22.80	5.08	2.31	191.10	Moderate ecological risk	0.03	9% probability of toxicity	0.76	Potential hazards
LM	147.27	23.81	4.72	1.86	177.67		0.03		0.70	
BJ	87.27	21.10	3.90	1.40	113.67	Low ecological risk	0.02		0.47	
KK	90.00	21.78	3.92	1.41	117.11		0.02		0.49	
KT	46.36	21.86	4.53	1.89	74.65		0.02		0.38	
LI	109.09	26.10	4.87	1.84	141.91		0.02		0.59	

Table 6
Mean bio-concentration (BCF) and translocation factors (TF) of Cd, Cu, Pb, and Zn in *Cymodocea nodosa* roots, rhizomes, and leaves.

Trace metals	BCF	TF		
	$C_{roots}/C_{sediments}$	$C_{rhizomes}/C_{roots}$	$C_{leaves}/C_{rhizomes}$	C_{leaves}/C_{roots}
Cd	5.98	0.78	6.09	1.58
Cu	1.02	0.84	3.06	1.32
Pb	0.74	1.24	4.59	0.44
Zn	5.08	1.26	2.30	3.42
Mean	3.18	1.03	4.01	1.69

Leaves > *Rhizomes* > *Roots* for Zn. These results lead to deduce that Cd, Cu, and Zn are mainly accumulated in the leaves, whereas Pb is mostly concentrated in the roots. The different patterns of metal bioaccumulation observed in the three organs of *C. nodosa* are most likely due to the physiological properties of the seagrass. The decreased Pb bioaccumulation in the leaves can be explained by the existence of certain physiological barriers preventing the transport of this metal in the upper organs of the plant. The same physiological mechanism appears to ease the translocation of the other metals (Cd, Cu, and Zn) in these organs, in accordance with the observations made by Kumar et al. (2013). From these findings, it can be deduced that *C. nodosa* rhizomes are most likely the organ playing the role of transferring elements between the roots and leaves. Similar observations were also observed with the seagrass species *C. nodosa* and *Posidonia oceanica* in other Mediterranean areas (Bonanno and Di Martino, 2016; Bonanno and Borg, 2018).

Based on the results of the present work, it can be understood that the seagrass *C. nodosa* has developed two different adaptative strategies to acclimate to the high industrial contamination levels of trace metals in the central part of Gabes Gulf. The first strategy consists in storing some highly concentrated trace metals in the marine surface sediments to the root system of *C. nodosa,* such as Pb. Within this context, Llagostera et al. (2011) considered the bioaccumulation of Pb in *C. nodosa* roots as a response to the high levels of this trace metal in the surrounding environment (sediments), as in the case of our study area. This adaptative strategy was already reported in other aquatic plants such as *Typha angustifolia* and *Phragmites australis* (Aksoy et al., 2005), *Myriophyllum spicatum* (Yabanli et al., 2014) and *Posidonia oceanica* (El Zrelli et al., 2017). A similar mechanism was also observed with some terrestrial plant species including *Lathyrus sativus L.* (Brunet et al., 2008), *Zea mays* (Gupta et al., 2009) and *Hirschfeldia incana* (Auguy et al., 2013).

The second strategy consists in translocating the transfer of some highly concentrated contaminants such as Cd, Cu, and Zn, from the lower parts (roots: '*permanent organs*') to the upper parts of the plants (leaves: '*temporary organs*'). In terms of pollutant removal, this adaptative strategy appears to be more effective because it allows the seagrass species to eliminate an important quantity of bio-accumulated toxic metals through the leaf fall and regeneration. The fall of *C. nodosa* leaves is a commonly observed phenomenon in the central part of the Gulf of Gabes. The strategy of toxic trace metal elimination through the fall of temporary organs (leaves) has already been observed with *C. nodosa* in other Mediterranean regions such as Thermaikos Gulf in Greece (Malea and Haritonidis, 1999) and Sicily (Bonanno and Di Martino, 2016). The latter authors attributed the high turnover rate of *C. nodosa* leaves to its removal strategy against the high concentrations of toxic elements in the marine environment. According to Cancemi et al. (2002), the lifespan of *C. nodosa* leaves ranges between 2 and 6 months.

Fig. 4 represents the spatial variations in the concentration percentages of Cd, Cu, Pb, and Zn, among the three studied organs of *C. nodosa*. The values ranged from 6.02% (in *C. nodosa* rhizomes from LI) to 67.98% (in *C. nodosa* leaves from LM) for Cd, from 11.69% (in *C. nodosa* rhizomes from OS) to 55.04% (in *C. nodosa* leaves from LI) for Cu, from 4.40 (in *C. nodosa* rhizomes from Li) to 70.92% (in *C. nodosa* roots from KT) for Pb, and from 13.53% (in *C. nodosa* roots from LM) to 62.34% (in *C. nodosa* leaves from LM) for Zn. The concentration percentages of both Pb and Zn showed similar patterns among the six sampling sites, with more than 50% of their contents in roots and leaves, respectively. The variations of Cd and Cu among *C. nodosa* organs followed a similar pattern to that of Zn in all sampling stations, except for BJ and KT where Cu and/or Cd showed different trends. The highest *C. nodosa* root concentrations of Cd and Cu in BJ and that of Cd in KT confirm that the roots act as an accumulation organ for these contaminants (Fig. 4). Moreover, it was found that *C. nodosa* rhizomes constitute the least-accumulating organ of toxic metals for all sampling stations and studied elements (Fig. 4). Similar findings were reported in previously reported studies (Martínez-Crego et al., 2008; Llagostera et al., 2011; Malea and Kevrekidis, 2013; Bonanno and Di Martino, 2016). Some of these latter studies reported that seagrass rhizomes act as contaminant translocating organs, between the roots and leaves (Bonanno and Di Martino, 2016; Bonanno and Borg, 2018).

The spatial variations in trace metals' concentrations, shown in Fig. 4, are most likely due to the variability in physicochemical and granulometric characteristics among the sampling sites. In fact, it is known that some environmental factors such as pH, salinity, temperature, soil texture, clay, and organic matter contents may affect the solubility of trace metals (and other contaminants) in marine environments, and hence their availability in submersed plants (Greger, 2004; Fritioff et al., 2005; Lafabrie et al., 2013). In addition, the variations in trace metal bioaccumulation patterns among the different organs of *C. nodosa* indicated, in general, that while leaves accumulate Cd, Cu, and Zn, while roots concentrate Pb (Fig. 4). Within this context, Llagostera et al. (2011) attributed this inter-organ variations to several phenomena including the inter-organ difference of uptake kinetics and passive absorption properties, as well as the inter-element variability of their internal redistribution by different transport mechanisms (passive or active). Therefore, the bioaccumulation of contaminants by *C. nodosa* depends mainly on the environmental factors, accumulated elements, and accumulating organs. Similar observations were also reported in Sicily by Bonanno and Di Martino (2016).

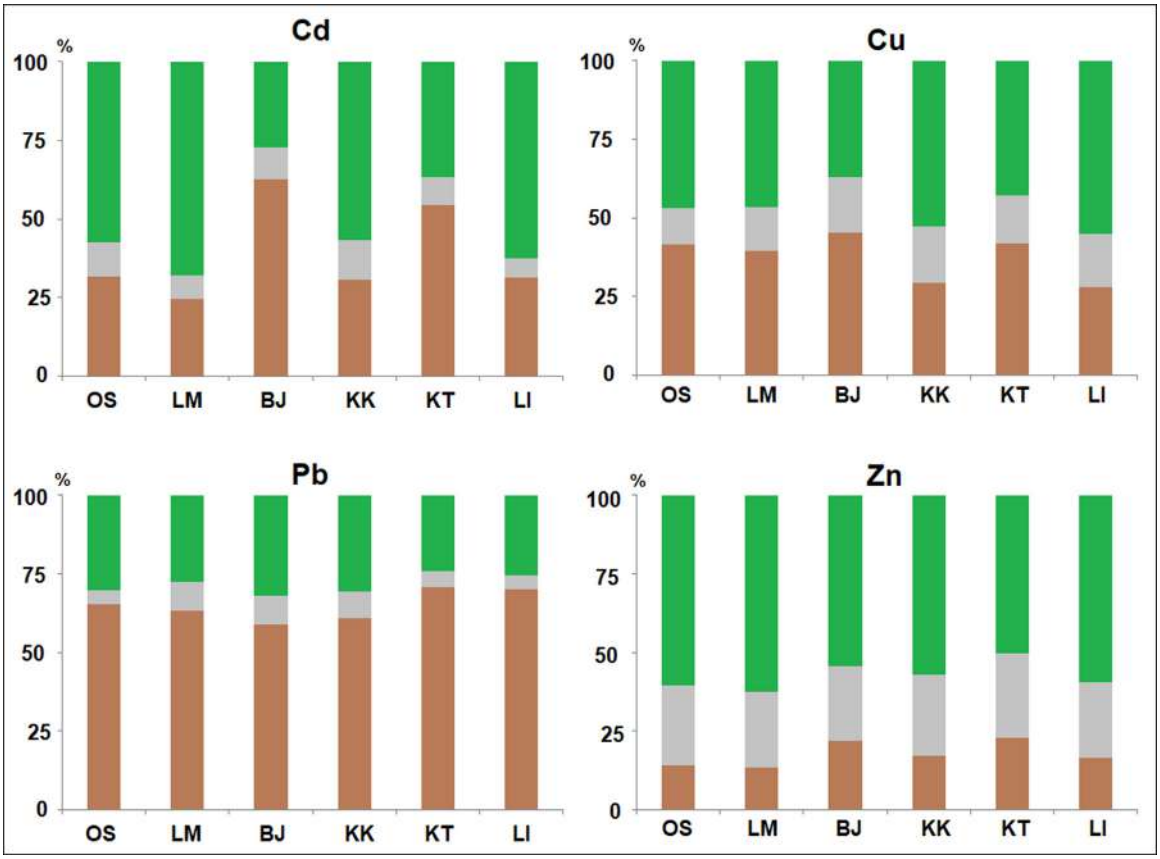

Fig. 4. Spatial variations of cumulative concentration percentages of cadmium (Cd), copper (Cu), lead (Pb), and zinc (Zn), assessed in the roots (brown color), rhizomes (gray color) and leaves (green color) of *Cymodocea nodosa*.

Table 7 compares the concentrations of trace metals recorded during this study (in sediment, seawater, and *C. nodosa* organs) with those recorded in other Mediterranean regions. Compared to *P. oceanica* from the same study area (Gulf of Gabes), *C. nodosa* was found to accumulate more metals. *C. nodosa*'s ability to acclimatize to high levels of industrial pollutants can explain the continued occurrence of this plant in the Gulf of Gabes. This ability to acclimatize seems to be less developed with *P. oceanica* which has known a considerable and continuous decline from the Gulf of Gabes (Darmoul et al., 1980; Darmoul and Vitiello, 1980; Darmoul, 1988; Zaouali, 1993; El Zrelli et al., 2017, 2020, 2023b). The *C. nodosa*'s ability to bioaccumulate trace metals was found to be higher in the Gulf of Gabes, compared to other Mediterranean regions such as Sicily (Bonanno and Di Martino, 2016). In contrast, this metal bioaccumulation ability was found lower than that described with the same species from Thermaikos Gulf in Greece (Malea and Haritonidis, 1999) (Table 7). These differences in the plant ability to accumulate metals seems to be dependent on various factors including the physiological properties of the species studied (e.g., uptake kinetics inter-organ difference, absorption properties…etc.; Llagostera et al., 2011), marine environmental conditions (temperature, salinity, … etc.; Fritioff et al., 2005) and analyzed elements (levels, bioavailability…etc.; Greger, 2004).

In the central part of the Gulf of Gabes, a major loss of *Posidonia oceanica* seagrass meadows (∼96%) have occurred in the Gulf of Gabes, during the past 4 decades (El Zrelli et al., 2017, 2020). This has certainly led to the fact that the herbivorous species occurring in the region are mainly feeding on *C. nodosa* seagrass. Since most of trace metals were found to accumulate in the edible parts of *C. nodosa* in the central part of Gabes Gulf, these persistent and toxic pollutants can be incorporated in the trophic chain of local marine ecosystems, through the consumption of the seagrass leaves by herbivorous species, as pointed out by Bustamante et al. (1998) and Lahaye et al. (2005). Therefore, the biomagnification of these toxic metals may pose serious threats to marine organisms and to local inhabitants. Within this context, previous studies reported that the high levels of industrial pollution in the central part of Gabes Gulf may be behind the skeletal malformations and high mortality rates observed with some marine species, as well as the high frequency of various human diseases (e.g., cancers, birth defects, infertility, abortion, impotence, cardiovascular diseases, premature deaths, high cancer mortality, etc.) observed with local inhabitants (Rabaoui et al., 2017; El Zrelli et al., 2018b, 2019b,c). Thus, *C. nodosa* can be considered as the main trophic link which considerably contaminates the various edible and non-edible fish and shellfish species with trace metals, through its ability of trace metal bioaccumulation, allowing and facilitating their transfer from the polluted marine environment to humans.

From an environmental bioremediation point of view, the high potential of trace metal bioaccumulation observed in the leaves of *C. nodosa* may be used as an excellent bioremediation tool to decontaminate or detoxify contaminated marine environments such as the Gulf of Gabes. In fact, compared to the known conventional techniques of marine sediment decontamination (e.g., ion exchange/chelation, electrolytic recovery, chemical precipitation; Kumar et al., 2013), phytoremediation techniques, such as using the little Neptune grass seems to be an effective, cheap, and sustainable alternative. Unfortunately, similarly to *P. oceanica* seagrass, *C. nodosa* is in a continuous decline in the Gulf of Gabes (Darmoul, 1988; Zaouali, 1993; El Zrelli et al., 2017). If continued, this decline will certainly lead to accentuating the heavily polluted status of the Gulf of Gabes.

Table 7
Mean concentrations of Cd, Cu, Pb and Zn in *C. nodosa* organs (leaves, rhizomes and roots; mg kg^{-1}), sediments (mg kg^{-1}) and water (μg l^{-1}) reported by various studies.

Plant tissues/ Compartments	Cd	Cu	Pb	Zn	Species	Location	Reference
Leaves	2.32 ± 0.12	3.40 ± 0.17	1.46 ± 0.07	148.61 ± 7.43	*Cymodocea nodosa*	Gabes Gulf	*Present study*
Rhizomes	0.42 ± 0.02	1.13 ± 0.06	0.34 ± 0.02	64.72 ± 3.24			
Roots	1.80 ± 0.09	2.72 ± 0.14	3.35 ± 0.17	45.94 ± 2.30			
Sediment	0.39 ± 0.02	2.70 ± 0.14	4.50 ± 0.23	9.64 ± 0.48			
Water	0.37 ± 0.02	2.95 ± 0.15	0.12 ± 0.01	2.82 ± 0.13			
Leaves	0.58 ± 0.10	4.33 ± 0.25	1.27 ± 0.20	157.67 ± 15.50	*Posidonia oceanica*		El Zrelli et al. (2017)
Rhizomes	0.17 ± 0.04	0.96 ± 0.08	0.23 ± 0.05	17.00 ± 2.00			
Roots	0.33 ± 0.05	3.29 ± 0.23	2.50 ± 0.16	48.33 ± 8.50			
Sediments	0.31 ± 0.02	3.20 ± 0.03	4.47 ± 0.07	10.51 ± 0.09			
Leaves	0.23	2.37	0.85	15.93	*Cymodocea nodosa*	Marina Cap Monastir (Tunisia)	Zakhama-Sraieb et al. (2019)
Rhizomes	0.14	1.09	0.39	17.97			
Leaves	0.41	3.55	4.76	39.22		Ghar El Melh lagoon (Tunisia)	
Rhizomes	0.20	1.04	1.30	22.04			
Leaves	0.58	6.77	2.69	74.70		Bizerte lagoon (Tunisia)	
Rhizomes	0.28	4.35	0.41	21.48			
Leaves	0.58 ± 0.05	12.7 ± 1.3	156 ± 14.8	175 ± 49.5	*Cymodocea nodosa*	Thermaikos Gulf (Greece)	Malea and Haritonidis (1999)
Stems	0.26 ± 0.03	7.7 ± 0.9	164 ± 12.1	82.4 ± 44.3			
Roots	0.56 ± 0.05	12.2 ± 2.1	157 ± 15.1	48.1 ± 4.9			
Sediment	0.15 ± 0.03	14.8 ± 0.6	–	42.7 ± 6.5			
Water	0.31 ± 0.03	2.45 ± 0.17	1.2 ± 0.06	0.5 ± 0.1			
Leaves	0.26 ± 0.03	11.0 ± 2.08	2.38 ± 0.45	55.0 ± 7.52	*Cymodocea nodosa*	Sicily (Italy)	Bonanno and Di Martino (2016)
Rhizomes	0.07 ± 0.01	9.33 ± 1.35	0.69 ± 0.08	23.7 ± 4.15			
Roots	0.30 ± 0.04	10.3 ± 2.35	5.31 ± 0.93	40.0 ± 6.78			
Sediment	0.23 ± 0.03	4.22 ± 0.68	6.04 ± 0.81	17.8 ± 3.02			
Water	0.83 ± 0.01	71.9 ± 10.2	0.72 ± 0.10	12.0 ± 1.66			

4. Conclusion

Compared to the seawater, sediments represent the main source of trace metals bioaccumulated in the seagrass species *C. nodosa*, occurring in the central part of the Gulf of Gabes. Metal bioaccumulation in this plant species was found to depend on the environmental properties of its occurrence area, type of element accumulated and accumulating organ. The results of the present work pointed out that *C. nodosa* has developed two different physiological strategies to adapt to the high levels of trace metals in the central part of the Gabes Gulf. While the first adaptive strategy consists in metal trapping in the seagrass roots, the second involves the transfer of pollutants from permanent organs (roots) to temporary organs (leaves). These findings showed the usefulness of *C. nodosa* seagrass as a monitoring tool of metallic pollution in marine sediments as well its potential use as an effective, cheap, and sustainable bioremediation tool of contaminated marine sediments. In spite of its environmental and ecological benefits, *C. nodosa* is in a continuous decline in the Gulf of Gabes. Thus, it is very important to adopt strict measures to protect the seagrass species (including *C. nodosa* and *P. oceanica*) occurring in this region and to decrease the anthropogenic effluents and stop the coastal dumping of the various industrial wastes (in particular the phosphogypsum wastes discharged from Gabes GCT factories) which are continuously contaminating the marine environment.

CRediT authorship contribution statement

Radhouan Belgacem El Zrelli: Conceptualization, Supervision, Data curation, Formal analysis, Methodology, Resources, Writing – original draft. **Lamia Yacoubi:** Data curation, Formal analysis, Methodology, Writing – review & editing. **Sylvie Castet:** Resources, Writing – review & editing. **Michel Grégoire:** Conceptualization, Resources, Supervision, Writing – review & editing. **Yu-Jia Lin:** Data curation, Methodology, Writing – review & editing. **Faouzi Attia:** Methodology, Writing – review & editing. **Korhan Ayranci:** Writing – review & editing. **Zaher Abdel Baki:** Writing – review & editing. **Pierre Courjault-Radé:** Conceptualization, Methodology, Supervision, Writing – review & editing. **Lotfi Jilani Rabaoui:** Conceptualization, Formal analysis, Methodology, Supervision, Writing – review & editing.

Declaration of competing interest

The authors declare that they have no known competing financial interests or personal relationships that could have appeared to influence the work reported in this paper.

Data availability

Data will be made available on request

Acknowledgments

The authors are grateful to the editor reviewer who helped to improve the quality of the manuscript through their constructive comments and suggestions. The authors also thank all those who helped in the collection of samples and laboratory analyses. This publication is dedicated to the memory of Saber Romdhan (10.12.1979/10.05.2018) from the maritime oasis of Chatt Sidi Abd Essalam.

Appendix A. Supplementary data

Supplementary material related to this article can be found online at https://doi.org/10.1016/j.rsma.2023.103056.

References

Aksoy, A., Duman, F., Sezen, G., 2005. Heavy metal accumulation and distribution in narrow-leaved cattail (*Typha angustifolia*) and common reed (*Phragmites australis*). J. Freshw. Ecol. 20, 783–785.

Auguy, F., Fahr, M., Moulin, P., Brugel, A., Laplaze, L., El Mzibri, M., Filali-Maltouf, A., Doumas, P., Smouni, A., 2013. Lead tolerance and accumulation in *Hirschfeldia incana*, a Mediterranean *Brassicaceae* from metalliferous mine spoils. PLoS One 8, e61932.

Barwick, M., Maher, W., 2003. Biotransference and biomagnification of selenium, copper, cadmium, zinc, arsenic and lead in a temperate seagrass ecosystem from lake Macquarie estuary, NSW, Australia. Mar. Environ. Res. 56, 471–502.

Bat, L., Arici, E., Öztekin, A., 2021. Threats to quality in the coasts of the Black sea: heavy metal pollution of seawater, sediment, macro-algae and seagrass. In: Shit, P.K., Adhikary, P.P., Sengupta, D. (Eds.), Spatial Modeling and Assessment of Environmental Contaminants. Environmental Challenges and Solutions. Springer, Cham, http://dx.doi.org/10.1007/978-3-030-63422-3_18.

Bonanno, G., Borg, J.A., 2018. Comparative analysis of trace element accumulation in seagrass *Posidonia oceanica* and *Cymodocea nodosa*: Biomonitoring applications and legislative issues. Mar. Pollut. Bull. 128, 24–31.

Bonanno, G., Di Martino, V., 2016. Seagrass *Cymodocea nodosa* as a trace element biomonitor: Bioaccumulation patterns and biomonitoring uses. J. Geochem. Explor. 169, 43–49.

Bonanno, G., Raccuia, S.A., 2018. Seagrass *Halophila stipulacea*: Capacity of accumulation and biomonitoring of trace elements. Sci. Total Environ. 633, 257–263.

Bonanno, G., Veneziano, V., Piccione, V., 2020. The alga Ulva lactuca (*Ulvaceae, Chlorophyta*) as a bioindicator of trace element contamination along the coast of Sicily, Italy. Sci. Total Environ. 699, 134329.

Brunet, J., Repellin, A., Varrault, G., Terryn, N., Zuily-Fodil, Y., 2008. Lead accumulation in the roots of grass pea (*Lathyrussativus L.*): a novel plant for phytoremediation systems? C. R. Biol. 331, 859–864.

Bustamante, P., Cherel, Y., Caurant, F., Miramand, P., 1998. Cadmium, copper and zinc in octopuses from Kerguelen islands, southern Indian ocean. Polar Biol. 19, 264–271.

Calmano, W., Hong, J., Förstner, U., 1993. Binding and mobilization of heavy metals in contaminated sediments affected by pH and redox potential. Water Sci. Technol. 28, 223–235.

Campanella, L., Conti, M.E., Cubadda, F., Sucapane, C., 2001. Trace metals in seagrass, algae and molluscs from an uncontaminated area in the Mediterranean. Environ. Pollut. 111, 117–126.

Cancemi, G., Buia, M.C., Mazzella, L., 2002. Structure and growth dynamics of cymodocea nodosa meadows. Sci. Mar. 66 (4), 365–373.

Catsiki, V.A., Panayotidis, P., 1993. Copper, chromium and nickel in tissues of the mediterranean seagrasses *Posidonia oceanica* and *Cymodocea nodosa* (Potamogetonaceae) from Greek coastal areas. Chemosphere 26, 963–978.

Conti, M.E., Cecchetti, G., 2003. A biomonitoring study: trace metals in algae and molluscs from Tyrrhenian coastal areas. Environ. Res. 93, 99–112.

Cunha, S.C., Ferreira, R., Marmelo, I., Vieira, L.R., Anacleto, P., Maulvault, A., Marques, A., Guilhermino, L., José O. Fernandes, J.O., 2022. Occurrence and seasonal variation of several endocrine disruptor compounds (pesticides, bisphenols, musks and UV-filters) in water and sediments from the estuaries of Tagus and Douro rivers (NE Atlantic ocean coast). Sci. Total Environ. 838 (2), 155814.

Darmoul, B., 1988. Pollution dans le Golfe de Gabès (Tunisie): bilan de six années de surveillance. Bull. Inst. Nat. Sci. Technol. Mer. Salammbô 15, 61–83.

Darmoul, B., Hadj Ali Salem, M., Vitiello, P., 1980. Effets des rejets industriels de la région de gabès (tunisie) sur le milieu récepteur. Bull. Inst. Nat. Sci. Technol. Mer. Salammbô 7, 5–61.

Darmoul, B., Vitiello, P., 1980. Recherches expérimentales sur la toxicité aiguë des rejets de phosphogypse sur quelques organismes benthiques marins. Bull. Inst. Nat. Sci. Technol. Mer. Salammbô 7, 63–89.

Deng, H., Yea, Z.H., Wong, M.H., 2004. Accumulation of lead, zinc, copper and cadmium by 12 wetland plant species thriving in metal-contaminated sites in China. Environ. Pollut. 132, 29–40.

El Kateb, A., Stalder, C., Neururer, C., Pisapia, C., Spezzaferri, S., 2016. Correlation between pollution and decline of Scleractinian *Cladocora caespitosa* (Linnaeus. 1758) in the gulf of Gabes. Heliyon 2, e00195.

El Zrelli, R, 2017. Metallic Trace Element Transfer Modalities in the Central Part of Gabes Gulf, Tunisia: A Geochemical, Mineralogical, Sedimentological and Biological Approach (PhD dissertation). Université Toulouse III-Paul Sabatier, France.

El Zrelli, R., Baliteau, J.Y., Yacoubi, L., Castet, S., Grégoire, M., Fabre, S., Sarazin, V., Daconceicao, L., Courjault-Radé, P., L. Rabaoui, L., 2021. Rare earth elements characterization associated to the phosphate fertilizer plants of Gabes (Tunisia, central Mediterranean sea) : Geochemical properties and behavior, related economic losses, and potential hazards. Sci. Total Environ. 791, 148268.

El Zrelli, R., Courjault-Radé, P., Rabaoui, L., Castet, S., Michel, S., Bejaoui, N., 2015. Heavy metal contamination and ecological risk assessment in the surface sediments of the coastal area surrounding the industrial complex of gabes city gulf of gabes, SE Tunisia. Mar. Pollut. Bull. 101, 922–929.

El Zrelli, R., Courjault-Radé, P., Rabaoui, L., Daghbouj, N., Mansour, L., Balti, R., Castet, S., Attia, F., Michel, S., Bejaoui, N., 2017. Biomonitoring of coastal pollution in the gulf of gabes (se. Tunisia): use of *Posidonia oceanica* seagrass as a bioindicator and its mat as an archive of coastal metallic contamination. Environ. Sci. Pollut. Res. 24, 22214–22225.

El Zrelli, R., Hcine, A., Yacoubi, L., Roa-Ureta, R.H., Gallai, N., Castet, S., Grégoire, M., Courjault-Radé, P., Rabaoui, L., 2023b. Economic losses related to the reduction of Posidonia ecosystem services in the gulf of Gabes (southern Mediterranean sea). Mar. Pollut. Bull. 186, 114418.

El Zrelli, R., Rabaoui, L., Abda, H., Daghbouj, N., Pérez-López, R., Castet, S., Aigouy, T., Bejaoui, N., Courjault-Radé, P., 2019b. Characterization of the role of phosphogypsum foam in the transport of metals and radionuclides in the southern Mediterranean sea. J. Hard Mater. 363, 258–267.

El Zrelli, R., Rabaoui, L., Ben Alaya, M., Castet, S., Zouiten, C., Bejaoui, N., Courjault-Radé, P., 2019a. Decadal effects of solid industrial wastes on the coast: Gulf of Gabes (Tunisia, southern Mediterranean sea) as an example. Estuar. Coast. Shelf Sci. 224, 281–288.

El Zrelli, R., Rabaoui, L., Ben Alaya, M., Daghbouj, N., Castet, S., Besson, P., Michel, S., Bejaoui, N., Courjault-Radé, P., 2018a. Seawater quality assessment and identification of pollution sources along the central coastal area of gabes gulf (SE Tunisia): Evidence of industrial impact and implications for marine environment protection. Mar. Pollut. Bull. 127, 445–452.

El Zrelli, R., Rabaoui, L., Daghbouj, N., Abda, H., Castet, S., Josse, C., van Beek, P., Souhaut, M., Michel, S., Bejaoui, N., Courjault-Radé, P., 2018b. Characterization of phosphate rock and phosphogypsum from gabes phosphate fertilizer factories (SE Tunisia): high mining potential and implications for environmental protection. Environ. Sci. Pollut. Res. 25, 14690–14702.

El Zrelli, R., Rabaoui, L., Roa-Ureta, R.H., Gallai, N., Castet, S., Grégoire, M., Bejaoui, N., Courjault-Radé, P., 2020. Economic impact of human-induced shrinkage of *Posidonia oceanica* meadows on coastal fisheries in the Gabes gulf (Tunisia, southern Mediterranean sea). Mar. Pollut. Bull. 155, 111124.

El Zrelli, R., Rabaoui, L., Van Beek, P., Castet, S., Souhaut, M., Grégoire, M., Courjault-Radé, P., 2019c. Natural radioactivity and radiation hazard assessment of industrial wastes from the coastal phosphate treatment plants of gabes (Tunisia, southern Mediterranean sea). Mar. Pollut. Bull. 146, 454–461.

El Zrelli, R., Yacoubi, L., Castet, S., Grégoire, M., Josse, C., Olive, J.-F., Courjault-Radé, P., van Beek, P., Zambardi, T., Souhaut, M., Sonke, J.E., Rabaoui, L., 2023a. PET plastics as a trojan horse for radionuclides. J. Hazards Mater. 441, 129886.

Feng, H., Jiang, H., Gao, W., Weinstein, M.P., Zhang, Q., Zhang, W., Yu, L., Yuan, D., Tao, J., 2011. Metal contamination in sediments of the western Bohai bay and adjacent estuaries, China. J. Environ. Manag. 92, 1185–1197.

Fritioff, A., Kautsky, L., Greger, M., 2005. Influence of temperature and salinity on heavy metal uptake by submerged plants. Environ. Pollut. 133, 265–274.

Gao, X., Chen, C.T.A., 2012. Heavy metal pollution status in surface sediments of the coastal Bohai bay. Water Res. 46, 1901–1911.

Garcia-Vazquez, E., Geslin, V., Turrero, P., Rodriguez, N., Machado-Schiaffino, G., Ardura, A., 2021. Oceanic karma? Eco-ethical gaps in African EEE metal cycle may hit back through seafood contamination. Sci. Total Environ. 762, 143098.

Gaur, V.K., Gupta, S.K., Pandey, S.D., Gopal, K., Misra, V., 2005. Distribution of heavy metals in sediment and water of river Gomti. Environ. Monit. Assess. 102, 419–433.

Green, E.P., Short, F.T., 2003. World Atlas of Seagrasses. Prepared by the UNEP World Conservation Monitoring Centre and University of California Press, Berkeley. USA.

Greger, M., 2004. Metal availability, uptake, transport and accumulation in plants. In: Prasad, M.N.V. (Ed.), Heavy Metal Stress in Plants – from Biomolecules to Ecosystems, second ed. Springer Verlag, Heidelberg, Berlin, Germany, pp. 1–27.

Gupta, D.K., Nicoloso, F.T., Rossato, L.V., Castro, G.Y., Schetinger, M.R.C., Pereira, L.B., Srivastava, S., Tripathi, R.D., 2009. Antioxidant defense mechanism in hydroponically grown zea mays seedlings under moderate lead stress. J. Hazards Mater. 172, 479–484.

Håkanson, L., 1980. An ecological risk index aquatic pollution control. A sedimentological approach. Water Res. 14, 975–1001.

Halpern, B.S., Walbridge, S., Selkoe, K.A., et al., 2008. A global map of human impact on marine ecosystems. Science 319, 948–952.

Hu, C., Yang, X., Gao, L., Zhang, P., Li, W., Dong, J., Li, C., Zhang, X., 2019. Comparative analysis of heavy metal accumulation and bioindication in three seagrasses: Which species is more suitable as a bioindicator? Sci. Total Environ. 669, 41–48.

Kaldy, J.E., 2006. Carbon, nitrogen, phosphorus and heavy metal budgets: how large is the eelgrass (*Zostera marina* L.) sink in a temperate estuary? Mar. Pollut. Bull. 52, 332–356.

Kumar, B., Smita, K., Cumbal, L., 2013. Plant mediated detoxification of mercury and lead. Arab. J. Chem. http://dx.doi.org/10.1016/j.arabjc.2013.08.010.

Lafabrie, C., Major, K.M., Major, C.S., Cebrián, J., 2013. Trace metal contamination of the aquatic plant *Hydrilla verticillata* and associated sediment in a coastal Albama creek (gulf of Mexico-USA). Mar. Poll. Bull. 68, 147–151.

Lahaye, V., Bustamante, P., Spitz, J., Dabin, W., Das, K., Pierce, G.J., Caurant, F., 2005. Long-term dietary segregation of common dolphins *Delphinus delphis* in the bay of Biscay, determined using cadmium as an ecological tracer. Mar. Ecol. Prog. Ser. 305, 275–285.

Liu, S., Lou, S., Kuang, C., Huang, W., Chen, W., Zhang, J., Zhong, G., 2011. Water quality assessment by pollution-index method in the coastal waters of Hebei province in western Bohai sea, China. Mar. Pollut. Bull. 62, 2220–2229.

Liu, B., Lv, L., An, M., Wang, T., Li, M., Yu, Y., 2022. Heavy metals in marine food web from Laizhou bay, China: Levels, trophic magnification, and health risk assessment. Sci. Total Environ. 841, 156818.
Llagostera, I., Pérez, M., Romero, J., 2011. Trace metal content in the seagrass *Cymodocea nodosa*: Differential accumulation in plant organs. Aquat. Bot. 95, 124–128.
Long, E.R., MacDonald, D.D., Severn, C.G., Hong, B.C., 2000. Classifying probabilities of acute toxicity in marine sediments with empirically derived sediment quality guidelines. Environ. Toxicol. 19, 2598–2601.
Long, E.R., Macdonald, D.D., Smith, S.L., Calder, F.D., 1995. Incidence of adverse biological effects within ranges of chemical concentrations in marine and estuarine sediments. Environ. Manag. 19, 81–97.
Long, E.R., Morgan, L.G., 1991. The Potential for Biological Effects of Sediment-Sorbed Contaminants Tested in the National Status and Trends Program. NOAA Technical Memorandum NOS OMA 52, National Oceanic and Atmospheric Administration, Seattle. WA, p. 175.
Luo, M., Zhou, C., Ma, T., Guo, W., Percival, L., Baeyens, W., Gao, Y., 2022. Anthropogenic activities influence the mobilization of trace metals and oxyanions in coastal sediment porewaters. Sci. Total Environ. 839, 156353.
Malea, P., Haritonidis, S., 1999. Cymodocea nodosa (Ucria) Aschers as a bioindicator of metals in Thermaikos gulf Greece, during monthly samplings. Bot. Mar. 42, 419–430.
Malea, P., Kevrekidis, T., 2013. Trace element (Al, As, B, Ba, Cr, Mo, Ni, Se, Sr, Tl, U and V) distribution and seasonality in compartments of the seagrass Cymodocea nodosa. Sci. Total Environ. 463–464, 611–623.
Martínez-Crego, B., Vergés, A., Alcoverro, T., Romero, J., 2008. Selection of multiple seagrass indicators for environmental biomonitoring. Mar. Ecol. Prog. Ser. 361, 93–109.
MEA (Millennium Ecosystem Assessment), 2005. Ecosystem and Human Well-Being: General Synthesis. Island Press, Washington D.C.
Menicagli, V., Castiglione, M.R., Balestri, E., Giorgetti, L., Bottega, S., Sorce, C., Spanò, C., Lardicci, C., 2022. Early evidence of the impacts of microplastic and nanoplastic pollution on the growth and physiology of the seagrass *Cymodocea nodosa*. Sci. Total Environ. 838 (3), 156514.
Müller, G., 1969. Index of geoaccumulation in the sediments of the Rhine river. Geo J. 2, 108–118.
NOAA (Oceanic and Atmospheric Administration), 2012. Screening quick reference tables. National. Available from: http://archive.orr.noaa.gov/book_shelf/122_NEW-SQuiRTs.pdf.
Orlando-Bonaca, M., France, J., Mavric, B., Grego, M., Lipej, L., Flander-Putrle, V., Sisko, M., Falace, A., 2015. A new index (MediSkew) for the assessment of the *Cymodocea nodosa* (Ucria) Ascherson meadow's status. Mar. Environ. Res. 110, 132–141.
OSPAR Commission, 2010. Background Document for Cymodocea Meadows. OSPAR Commission, London, p. 30, (487/2010).
Pérez-López, R., Macías, F., Cánovas, C.R., Sarmiento, A.M., Silvia María Pérez-Moreno, S.M., 2016. Pollutant flows from a phosphogypsum disposal area to an estuarine environment: An insight from geochemical signatures. Sci. Total Environ. 553, 42–51.
R Core Team, 2022. R: A Language and Environment for Statistical Computing. R Foundation for Statistical Computing, Vienna, Austria, https://www.R-project.org/.
Rabaoui, L., Balti, R., El Zrelli, R., Tlig-Zouari, S., 2014. Assessment of heavy metals pollution in the gulf of gabes (Tunisia) using four mollusk species. Mediterr. Mar. Sci. 15, 45–58.
Rabaoui, L., Cusack, M., Saderne, V., Krishnakumar, P.K., Lin, Y.J., Shemsi, A.M., El Zrelli, R., Arias-Ortiz, A., Masqué, P., Duarte, C.M., Qurban, M.A., 2020. Anthropogenic-induced acceleration of elemental burial rates in blue carbon repositories of the Arabian gulf. Sci. Total Environ. 719, 135177.
Rabaoui, L., El Zrelli, R., Balti, R., Mansour, L., Courjault-Radé, P., Daghbouj, N., Tlig-Zouari, S., 2017. Metal bioaccumulation in two edible cephalopods in the gulf of Gabes, south-eastern Tunisia: environmental and human health risk assessment. Environ. Sci. Pollut. Res. 24, 1686–1699.
Rabaoui, L., El Zrelli, R., Ben Mansour, M., Balti, R., Mansour, L., Tlig-Zouari, S., Guerfel, M., 2015. On the relationship between the diversity and structure of benthic macroinvertebrate communities and sediment enrichment with heavy metals in gabes gulf Tunisia. J. Mar. Biol. Assoc. UK 95, 233–245.
Rainbow, P.S., 2007. Trace bioaccumulation: models, metabolic availability and toxicity. Environ. Int. 33, 576–582.
Reizopoulou, S., Nicolaidou, A., 2004. Benthic diversity of coastal brackish-water lagoons in western Greece. Aquat. Conserv. Mar. Freshw. Ecosyst. 14, S93–S102.
Reyes, J., Sansón, M., 1994. Morfología y anatomía de *Cymodocea nodosa* (Cymodoceaceae: Magnoliophyta) en praderas de El Médano (s tenerife. islas canarias). Vieraea 23, 43–64.
Richir, J., Gobert, S., 2016. Trace elements in marine environments: occurrence, threats and monitoring with special focus on the coastal Mediterranean. J. Environ. Anal. Toxicol. 6 (1), 1–19.
Roberts, D.A., Johnston, E.L., Poore, A.G.B., 2008. Contamination of marine biogenic habitats and effects upon associated epifauna. Mar. Pollut. Bull. 56, 1057–1065.
Romero, J., Lee, K.-S., Pérez, M., Mateo, M.A., Alcoverro, T., 2006. Nutrient dynamics in seagrass ecoystems. In: Lrakum, A.W.D., Orth, R.J., Duarte, C. (Eds.), Seagrasses: Biology, Ecology and Conservation. Springer.
Sánchez-Quiles, D., Marbà, N., Tovar-Sánchez, A., 2017. Trace metal accumulation in marine macrophytes: hotspots of coastal contamination worldwide. Sci. Total Environ. 576, 520–527.
Solaun, O., Rodríguez, J.G., Menchaca, I., López-García, E., Martínez, E., Zonja, B., Postigo, Cristina, López de Alda, M., Barceló, D., Borja, Á., Manzanos, A., Larreta, J., 2021. Contaminants of emerging concern in the basque coast (n Spain): Occurrence and risk assessment for a better monitoring and management decisions. Sci. Total Environ. 765, 142765.
Tomlinson, D.C., Wilson, J.G., Harris, C.R., Jeffery, D.W., 1980. Problems in the assessment of heavy metals levels in estuaries and the formation of a pollution index. Helgol. Wiss. Meeresunters. 33, 566–575.
Tovar-Sánchez, A., Serón, J., Marbà, N., Arrieta, J.M., Duarte, C.M., 2010. Long-term records of trace metal content of western Mediterranean seagrass (*Posidonia oceanica*) meadows: natural and anthropogenic contributions. J. Geophys. Res. 115, G02006.
USEPA (U.S. Environmental Protection Agency), 1999. SW-846 reference methodology: method 3050B. Standard operating procedure for the digestion of. Soil/sediment samples using a hotplate/beaker digestion technique, Chicago, Illinois.
USEPA (U.S. Environmental Protection Agency), 2007. Framework for Metal Risk Assessment. Office of the Science Advisor, Washington D.C.
Wang, Y., Yang, L., Kong, L., Liuc, E., Wang, L., Zhu, J., 2015b. Spatial distribution, ecological risk assessment and source identification for heavy metals in surface sediments from Dongping lake. Shandong. East China. Catena 125, 200–205.
Yabanli, M., Yozukmaz, A., Sel, F., 2014. Heavy metal accumulation in the leaves, stem and root of the invasive submerged macrophyte *Myriophyllum spicatum L.* (Haloragaceae): an example of Kadın Creek (Mugla, Turkey). Braz. Arch. Biol. Technol. 57, 434–440.
Yu, R., Yuan, X., Zhao, Y., Hu, G., Tu, X., 2008. Heavy metal pollution in intertidal sediments from Quanzhou bay. China J. Environ. Sci. 20, 664–669.
Zakhama-Sraieb, R., Zribi, I., Mnasri, F., 2019. A comparative study of trace elements in *Cymodocea nodosa* from three semi-enclosed coastal areas in Tunisia. Environ. Sci. Pollut. Res. 26, 10000–10012.
Zaouali, J., 1993. Little syrte benthic communities, gulf of gabès, Tunisia. Results of the survey campaign of 1990. Preliminary study; biocenosis and recent thanatocenosis. Mar. Life 3, 47–60.
Zorba, M.A., Jacob, P.G., Al-Bloushi, A., Reem Al-Nafisi, R., 1992. Clams as pollution bioindicators in Kuwait's marine environment: metal accumulation and depuration. Sci. Total Environ. 120 (3), 185–204.

fishes

MDPI

Article

Stomach Content Analysis for Juvenile Great Hammerhead Sharks *Sphyrna mokarran* (Rüppell, 1837) from the Arabian Gulf

Hua Hsun Hsu [1,2,*], Zahid Nazeer [1], Premlal Panickan [1], Yu-Jia Lin [1,3], Ali Qasem [4], Lotfi Jilani Rabaoui [5] and Mohammad Ali Qurban [5]

[1] Center for Environment and Marine Studies, Research Institute, King Fahd University of Petroleum and Minerals, Dhahran 31261, Saudi Arabia
[2] Coastal and Offshore Resources Research Center, Fisheries Research Institute, Council of Agriculture, Kaohsiung 80672, Taiwan
[3] Institute of Marine Ecology and Conservation, National Sun Yat-sen University, Kaohsiung 80424, Taiwan
[4] Environmental Protection Department, Saudi Aramco, Dhahran 31311, Saudi Arabia
[5] National Center for Wildlife, Riyadh 12746, Saudi Arabia
* Correspondence: hsuhuahsun@yahoo.com.tw or hhhsu@mail.tfrin.gov.tw; Tel.: +886-933622027

Abstract: The stomach contents of 30 male and 43 female (age < 3 years; 74–236 cm total length) juvenile great hammerhead sharks (*Sphyrna mokarran* (Rüppell, 1837)) obtained from commercial fisheries operating in Saudi Arabian waters of the Arabian Gulf were analyzed for the first time. After exclusion of parasites and abiotics, a total of 31 prey items, including the remains of cephalopods, fish, crustaceans, and bivalve mollusks, were identified in the stomachs of 59 great hammerheads. Based on the index of relative importance, teleosts were their main prey, and *Platycephalus indicus* (Linnaeus, 1758) was the most important prey at the species level. Significant age-related dietary differences were noted (F = 1.57, p = 0.026), indicating that the prey of the hammerheads aged 0–3 years shifted from Platycephalidae to Myliobatidae. Levin's niche overlap index was low (0.05–0.21), indicating that <3-year-old juvenile great hammerheads are specialized predators. The estimated trophic level was 4.40–5.01 (mean ± SD, 4.66 ± 0.45), indicating that the great hammerhead is a tertiary consumer.

Keywords: elasmobranch; feeding habit; top predator; trophic level

Citation: Hsu, H.H.; Nazeer, Z.; Panickan, P.; Lin, Y.-J.; Qasem, A.; Rabaoui, L.J.; Qurban, M.A. Stomach Content Analysis for Juvenile Great Hammerhead Sharks *Sphyrna mokarran* (Rüppell, 1837) from the Arabian Gulf. *Fishes* **2022**, *7*, 359. https://doi.org/10.3390/fishes7060359

Academic Editor: Fabio Fiorentino

Received: 17 October 2022
Accepted: 28 November 2022
Published: 29 November 2022

1. Introduction

The great hammerhead *Sphyrna mokarran* (Rüppell, 1837), which is the largest hammerhead species belonging to the family Sphyrnidae, can grow over 6.1 m in length and inhabits circumtropical coastal reefs, lagoons, continental shelves, and deep waters throughout the world [1–6]. Because the great hammerhead is caught by various fisheries operating from the coastal to pelagic zones, its populations have drastically declined in the past three decades [1,5,7–9]. This species has thus been addressed in Appendix II of the Convention on International Trade in Endangered Species of Wild Flora and Fauna (2012), listed in Appendix II of the Convention on the Conservation of Migratory Species of Wild Animals (2014), and registered as Critically Endangered on the International Union for Conservation of Nature Red List of Threatened Species (2019) [10–12].

This species has been suspected to have declined by at least 50% over the past 75 years in the Arabian Sea region, and this decline is expected to worsen further [9]. Life history parameters are crucial for assessing the population status and helping to establish relevant management policies; however, only limited biological information is available for this critically endangered species in the northwestern Indian Ocean, particularly the Arabian Gulf.

Age- and growth-related parameters such as growth function have been estimated for the northwestern Atlantic, Pacific, Arabian Gulf and Australian great hammerhead populations [7,13–16]. Their asymptotic lengths were estimated to be 264.2 (males) and

307.8 (females) cm fork length in the northwestern Atlantic, and 402.7 (sexes combined) cm stretched total length in eastern Australian waters, respectively [7,15]. Moreover, the reproduction process of this species was studied using samples from the northern and eastern Australian and eastern South African waters [2,15,17]. Size at maturity of Australian populations was estimated to be 210–225 cm total length (TL), and 217–237 cm precaudal length for the South African population [2,15,17]. Litter size was found to be 3–42 individuals with 2-year reproductive cycle, and a size-at-birth of 50–70 cm TL [1,12,15,17]. More recently, the "Sustaining Project-Shark Study" was conducted to assess great hammerheads in the Saudi Arabian waters of the Arabian Gulf between April 2016 and January 2020; only juveniles (aged < 3 years) occurred in this region, and their early growth and reproduction processes were assessed [13]. In particular, the great hammerheads in the Arabian Gulf had larger size at birth and size at maturity than elsewhere, and the growth rates from after birth to the age of 2.9 years were estimated as 83.3 and 22.7 cm year^{-1}, respectively [13]. Studies on the great hammerheads' diet have reported that these sharks feed on a variety of prey, favoring stingrays and other batoids, groupers, and ariid catfishes [1]. A study found that elasmobranchs were the most commonly found items in the stomachs of eight great hammerheads [18]. Teleosts and elasmobranchs were the main items found in the stomachs of 347 great hammerheads sampled from northern Australia [17]. Great hammerheads preying on stingrays have been observed in the Bahama waters [19]. In addition, through stable isotope analysis, eastern Australian great hammerheads were found to prey on members of the coastal, pelagic, and benthic food webs [20].

Feeding studies will help better define their ecological role in marine communities of the Arabian Gulf [21]. Therefore, the aims of the present study were to investigate diet compositions and to estimate trophic levels for the great hammerheads in the Arabian Gulf based on stomach content analysis. The results of this study provide knowledge on the first feeding habits of great hammerheads in their early life stages sampled from the Saudi Arabian waters of the Arabian Gulf.

2. Materials and Methods

2.1. Study Site and Sampling

Most of the analyzed stomachs derived from specimens (69 sharks) used in our previous paper dealing with maturity and growth of the species, collected between April 2016 and November 2019 [13]. Four further specimens were sampled in January 2020. The sharks (30 males, TL: 75–211 cm; 43 females, TL: 74–236 cm) were caught by several types of gear (trawls, drift and set gill nets, drift and set longlines, trolls, and handlines) and landed at Qatif fishing port and Jubail landing auction fish market (Figure 1). Sexual maturity stage was assigned by macroscopic inspection of claspers and uteruses. Age was estimated by readings of a thin section of vertebra. A more detailed description of the methods is reported in [13].

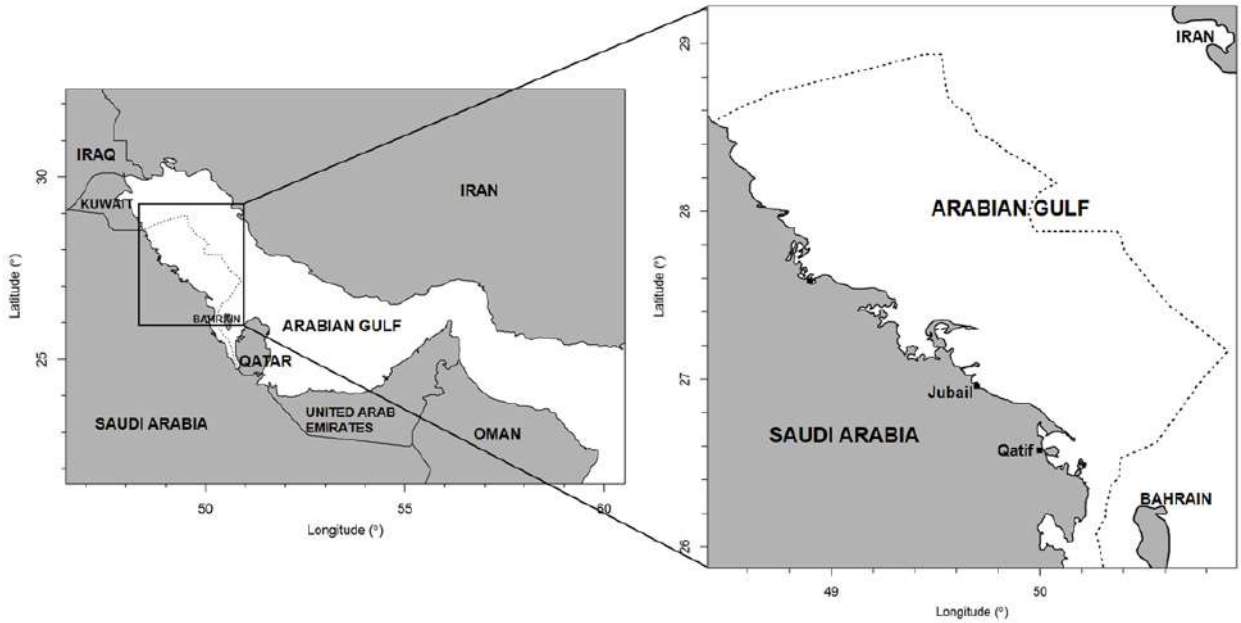

Figure 1. Study area showing the sampling sites of great hammerheads caught in the Saudi Arabian waters of the Arabian Gulf. The dotted lines show the exclusive economic zone boundary of Saudi Arabia.

2.2. Stomach Fullness

Four stomach fullness ranks were considered: Empty, small, big, and full stomach. Empty referred to no or only liquid contents in the stomach; small referred to contents of <50% of the stomach volume; big referred to contents of 50–100% of the stomach volume; and full referred to a full stomach of contents, with even the shape of the contents visible on the stomach. The vacuity index was calculated as the percentage of the number of empty stomachs with respect to the total number of stomachs [22].

Comparisons between sexes, fishing gear (nets vs. hook and line), and stomach fullness ranks (empty and small vs. big and full) were distinguished using the chi-squared test [17].

2.3. Stomach Content Analysis

The stomachs of the samples were weighed, and the contents were recovered through dissection in the laboratory. All of the stomach contents were segregated, identified to the lowest possible taxon, counted, and weighed. To avoid overestimating the occurrence of a particular item, the number of individuals of each content type was determined as the minimum number that these fragments could have originated from [22].

To assess the importance of each prey to the diet, the index of relative importance (IRI) was calculated using the following formula: IRI = (%N + %W) × (%O), where %O is the percentage of prey taxa occurrence in each stomach and %N and %W are the individual numbers of each content type and the total weight as a percentage of each prey taxon, respectively. The IRI values were standardized to percentages (%IRI) according to the protocol mentioned in a previous study [23]. The trophic niche breadth was estimated using Levin's index (Bi):

$$B_i = (\Sigma\ P_{ij}{}^2)^{-1}$$

where P_{ij} is the fraction of N represented by each prey j in the diet [23]. The B_i values were standardized using B_A, which ranged from 0 to 1:

$$B_A = (B_i - 1) \times (N - 1)^{-1}$$

where N is the number of prey categories [24]. Lower B_A values indicate more specialized diets. A species is classified as specialist feeder when $B_A < 0.40$, as intermediate feeder when the B_A value is between 0.40 and 0.60, or as generalist feeder when $B_A > 0.60$ [25].

To assess the trophic overlap in diet between sexes and age groups, the Morisita–Horn index (C_λ) [26] was calculated as follows:

$$C_\lambda = \frac{2\sum_{i=1}^{n}(P_{xi} \times P_{yi})}{\sum_{i=1}^{n} P_{xi}^2 + \sum_{i=1}^{n} P_{yi}^2}$$

where P_{xi} is the proportion of prey i of the total prey hunt by predator x; P_{yi} is the proportion of prey i of the total prey hunt by predator y; and n is the total number of prey species. The Morisita–Horn index ranges from 0 to 1, with values closer to 1 indicating higher similarities in the prey consumed [24]. A nonparametric permutational multivariate analysis of variance (PERMANOVA) was used to test the shifts in diet across years, seasons, sexes, and age groups [23]. This method allows the analysis of multivariate data, with *p* values obtained using 999 permutations by applying the R package (R Development Core Team; www.r-project.org (accessed on 22 June 2022)). The seasons were defined as follows: spring (March–May), summer (June–August), autumn (September–November), and winter (December–February) [27]. The samples were grouped into three classes based on age, from 0^+ to 2^+ years [13].

2.4. Trophic Level

The standardized trophic level was calculated using the trophic index (TrL) [21]:

$$TrL = 1 + \left(\sum_{j=1}^{n} P_j \times \ TrL_j\right)$$

where P_j is the proportion of each prey category j in the predator's diet based on the number of analyzed stomachs [21]. The trophic levels of the prey were obtained using FishBase for fishes [28]; SeaLifeBase for cephalopods and *Penaeus semisulcatus* De Haan, 1844 [29]; and the sources stated in previous studies for *Marsupenaeus japonicus* (Spence Bate, 1888) [30] and for bivalve mollusks [21].

3. Results

3.1. Gear and Stomach Fullness

The sex ratio (male:female) did not differ significantly from 1 ($X^2 = 1.11$, $p = 0.29$) for the 73 great hammerhead sharks. One (1.4%) shark was caught using a trawl, 47 (64.4%) using gill nets, 22 (30.1%) using longlines, and 3 (4.1%) using other hook and line gears; thus, 65.8% sharks were caught using net gear, which is significantly higher than the 34.2% caught using the other hook and line gear ($X^2 = 7.25$, $p = 0.007$).

Of the 73 great hammerhead stomachs, five from male sharks and nine from female sharks were empty. The vacuity index was 16.7% for the males and 20.9% for the females (overall: 19.2%). The sex ratio in terms of stomach fullness ranks did not differ significantly from 1 ($X^2 = 0.98$, $p = 0.807$). In addition to the 14 (19.2%) empty stomachs, 35 (47.9%) small stomachs, 17 (23.3%) big stomachs, and seven (9.6%) full stomachs were noted. The percentage of stomachs with empty or small status was 67.1%, significantly higher than those with big or full status ($X^2 = 8.56$, $p = 0.003$).

3.2. Stomach Content Analysis

The stomach contents were identified and categorized into nine groups: cephalopods, elasmobranchs, teleosts, crustaceans, bivalve mollusks, plants (seagrass), insects (cockroaches), parasites (Nematode and Cestoda), and abiotics (hooks and lines). Excluding parasites and abiotics, a total of 31 prey items were identified, including remains of cephalopods, fish, crustaceans, and bivalve mollusk (Table 1).

Table 1. Stomach contents of juvenile great hammerheads caught from Saudi Arabian waters of the Arabian Gulf between April 2016 and January 2020.

Content Items	%N	%W	%O	IRI	%IRI
Cephalopods	**2.60**	**1.48**	**5.08**	**22.25**	**0.18**
Octopus cyaneus Gray, 1849	0.65	0.23	1.82	1.59	0.06
Fam. Sepiidae	1.30	1.24	1.82	4.62	0.18
Cephalopod remains	0.65	0.02	1.82	1.21	0.05
Elasmobranchs	**5.19**	**21.92**	**11.86**	**345.07**	**2.84**
Maculabatis randalli (Last, Manjaji-Matsumoto & Moore, 2012)	0.65	11.02	1.82	21.22	0.84
Fam. Dasyatidae	0.65	4.82	1.82	9.95	0.39
Fam. Myliobatidae	3.25	5.93	7.27	66.74	2.64
Ord. Myliobatiformes	0.65	0.14	1.82	1.44	0.06
Teleosts	**54.55**	**73.32**	**83.05**	**13,948.84**	**93.81**
Saurida tumbil (Bloch, 1795)	1.30	5.77	3.64	25.70	1.02
Saurida spp.	1.95	4.81	3.64	24.56	0.97
Grammoplites suppositus (Troschel, 1840)	1.95	4.63	3.64	23.93	0.95
Platycephalus indicus (Linnaeus, 1758)	4.55	14.81	10.91	211.15	8.34
Epinephelus coioides (Hamilton, 1822)	0.65	7.26	1.82	14.37	0.57
Epinephelus spp.	1.30	9.23	1.82	19.15	0.76
Sillago sihama (Forsskål, 1775)	1.30	0.26	1.82	2.83	0.11
Megalaspis cordyla (Linnaeus, 1758)	0.65	1.51	1.82	3.92	0.15
Lutjanus ehrenbergii (Peters, 1869)	0.65	2.47	1.82	5.68	0.22
Gerres spp.	0.65	0.24	1.82	1.61	0.06
Acanthopagrus bifasciatus (Forsskål, 1775)	1.30	1.21	3.64	9.12	0.36
Lethrinus nebulosus (Forsskål, 1775)	0.65	0.42	1.82	1.94	0.08
Nemipterus japonicus (Bloch, 1791)	0.65	1.22	1.82	3.41	0.13
Otolithes ruber (Bloch & Schneider, 1801)	1.30	0.38	1.82	3.05	0.12
Siganus canaliculatus (Park, 1797)	0.65	4.71	1.82	9.75	0.39
Pseudorhombus spp.	1.30	0.66	1.82	3.56	0.14
Fam. Platycephalidae	3.90	4.14	10.91	87.69	3.46
Fam. Serranidae	0.65	1.98	1.82	4.78	0.19
Fam. Scombridae	0.65	0.57	1.82	2.22	0.09
Fish remains	28.57	7.04	49.09	1748.29	69.06
Crustaceans	**5.84**	**3.10**	**11.86**	**113.80**	**0.94**
Marsupenaeus japonicus (Spence Bate, 1888)	0.65	1.13	1.82	3.24	0.13
Penaeus semisulcatus De Haan, 1844	1.30	0.57	1.82	3.39	0.13
Fam. Penaeidae	3.25	1.39	7.27	33.75	1.33
Crustacean remains	0.65	0.01	1.82	1.19	0.05
Bivalves	**0.65**	**<0.01**	**1.69**	**1.18**	**0.01**
Bivalve remains	0.65	<0.01	1.82	1.18	0.05
Plants	**6.49**	**0.01**	**1.69**	**23.64**	**0.10**
Sargassum angustifolium C.Agardh 1820	0.65	<0.01	1.82	1.18	0.05
Halodule uninervis (Forssk.) Boiss.	5.84	0.01	1.82	10.64	0.42
Insects	**0.65**	**<0.01**	**1.69**	**1.19**	**0.01**
Fam. Blattidae	0.65	<0.01	1.82	1.19	0.05
Parasites	**23.38**	**0.03**	**10.17**	**255.35**	**2.10**
Phylum Nematoda	20.78	0.02	7.27	151.27	5.98
Class Cestoda	2.60	0.01	3.64	9.48	0.37
Abiotic substances	**0.65**	**0.14**	**1.69**	**1.44**	**0.01**
Hook and line	0.65	0.14	1.82	1.44	0.06

%N: percent number; %W: percent weight; %O: percent frequency of occurrence; IRI: index of relative importance; %IRI: percent index of relative importance.

Their diet mainly comprised teleosts, as evidenced by the highest occurrence (83.1%), number (54.6%), and weight (73.3%), with a %IRI of 93.81%. Elasmobranchs (2.84%) were the second most significant component of the juvenile great hammerheads' diet. The %IRI indicated that *Platycephalus indicus* (Linnaeus, 1758) (8.34%) was the most important prey found in the juvenile great hammerheads' stomachs (Table 1).

Males and females did not exhibit significant dietary differences across years (F = 0.79, $p = 0.74$) or seasons (F = 1.00, $p = 0.45$) due to small sample size. However, significant dietary differences were observed across age groups (F = 1.57, $p = 0.026$), indicating that the main prey items of the sharks in the 0^+ and 2^+ years-of-age groups shifted from Platycephalidae (particularly *P. indicus*) to Myliobatidae (particularly *Maculabatis randalli* [Last, Manjaji-Matsumoto & Moore, 2012]) and from teleosts to elasmobranchs (Table 2), respectively. In addition, the diets of the males and females across age groups were also slightly different (F = 1.36, $p = 0.062$). The males aged 1^+ year preferred to prey on teleosts and favored *P. indicus* but changed to *Epinephelus* spp. fishes when they reached 2^+ years of age; the females also liked to prey on teleosts after birth, but preferred batoids rather than teleosts in their second and third years of life (Table 2).

Table 2. Stomach content spectrum by sex and age group based on %IRI.

	Male %IRI (n = 27)				Female %IRI (n = 32)				Sex-Combined %IRI (n = 59)			
Content Items	**0^+ yr**	**1^+ yr**	**2^+ yr**	**All**	**0^+ yr**	**1^+ yr**	**2^+ yr**	**All**	**0^+ yr**	**1^+ yr**	**2^+ yr**	**All**
Cephalopods	**0.18**	**0.42**	**6.83**	**0.58**	**0**	**0**	**0**	**0**	**0.04**	**0.07**	**3.88**	**0.18**
Octopus cyaneus	0.59	0	0	0.26	0	0	0	0	0.16	0	0	0.06
Fam. Sepiidae	0	0	14.83	0.73	0	0	0	0	0	0	9.97	0.18
Cephalopod remains	0	1.25	0	0.20	0	0	0	0	0	0.29	0	0.05
Elasmobranchs	**0**	**6.04**	**0**	**0.56**	**0**	**14.70**	**85.71**	**5.65**	**0**	**9.40**	**22.17**	**2.84**
Maculabatis randalli	0	0	0	0	0	0	57.98	2.99	0	0	24.51	0.84
Fam. Dasyatidae	0	7.67	0	1.47	0	0	0	0	0	2.82	0	0.39
Fam. Myliobatidae	0	0	0	0	0	33.5	17.02	9.07	0	12.56	4.0	2.64
Ord. Myliobatiformes	0	1.42	0	0.24	0	0	0	0	0	0.35	0	0.06
Teleosts	**98.93**	**87.33**	**88.61**	**96.61**	**93.17**	**76.77**	**14.29**	**90.42**	**97.02**	**83.79**	**70.97**	**93.81**
Saurida tumbil	0	0	0	0	0	6.05	25.0	3.57	0	2.14	8.0	1.02
Saurida spp.	1.76	0	0	0.62	0	6.03	0	1.12	0.15	2.24	0	0.97
Grammoplites suppositus	0	0	0	0	8.46	0	0	3.27	2.61	0	0	0.95
Platycephalus indicus	0	45.50	0	8.60	17.0	0	0	6.58	5.24	16.07	0	8.34
Epinephelus coioides	0	10.91	0	2.12	0	0	0	0	0	4.09	0	0.57
Epinephelus spp.	0	0	46.8	2.84	0	0	0	0	0	0	24.97	0.76
Sillago sihama	0	0	0	0	0	1.42	0	0.36	0	0.69	0	0.11
Megalaspis cordyla	1.68	0	0	0.60	0	0	0	0	0.43	0	0	0.15
Lutjanus ehrenbergii	0	4.53	0	0.85	0	0	0	0	0	1.58	0	0.22
Gerres spp.	0	1.55	0	0.26	0	0	0	0	0	0.40	0	0.06
Acanthopagrus bifasciatus	0	0	6.19	0.28	0	1.96	0	0.38	0	0.77	4.41	0.36
Lethrinus nebulosus	0	0	0	0	0	1.17	0	0.26	0	0.50	0	0.08
Nemipterus japonicus	1.44	0	0	0.52	0	0	0	0	0.37	0	0	0.13
Otolithes ruber	0	0	0	0	1.04	0	0	0.39	0.30	0	0	0.12
Siganus canaliculatus	4.40	0	0	1.44	0	0	0	0	1.10	0	0	0.39
Pseudorhombus spp.	1.35	0	0	0.57	0	0	0	0	0.36	0	0	0.14
Fam. Platycephalidae	2.54	2.24	0	2.84	9.13	0	0	3.51	6.34	0.68	0	3.46
Fam. Serranidae	0	0	0	0	0	3.60	0	0.66	0	1.32	0	0.19
Fam. Scombridae	0.88	0	0	0.35	0	0	0	0	0.23	0	0	0.09
Fish remains	82.56	6.24	22.28	66.09	57.07	26.80	0	59.48	78.56	27.15	16.48	69.06
Crustaceans	**0.27**	**0.47**	**0**	**0.19**	**6.45**	**0**	**0**	**1.78**	**2.47**	**0.09**	**0**	**0.94**
Marsupenaeus japonicus	0	0	0	0	1.14	0	0	0.44	0.35	0	0	0.13
Penaeus semisulcatus	0	0	0	0	1.16	0	0	0.44	0.34	0	0	0.13
Fam. Penaeidae	0.85	1.42	0	1.15	3.32	0	0	1.25	2.13	0.35	0	1.33
Crustacean remains	0	0	0	0	0.40	0	0	0.15	0.11	0	0	0.05
Bivalves	**0**	**0**	**0**	**0**	**0**	**0.22**	**0**	**0.03**	**0**	**0.07**	**0**	**0.01**
Bivalve remains	0	0	0	0	0	0.51	0	0.15	0	0.28	0	0.05
Plants	**0**	**0**	**0**	**0**	**0**	**2.25**	**0**	**0.63**	**0**	**0.71**	**0**	**0.10**
Sargassum angustifolium	0	0	0	0	0	0.51	0	0.15	0	0.28	0	0.05
Halodule uninervis	0	0	0	0	0	4.61	0	1.33	0	2.52	0	0.42
Insects	**0**	**0**	**0**	**0**	**0**	**0.23**	**0**	**0.03**	**0**	**0.07**	**0**	**0.01**
Fam. Blattidae	0	0	0	0	0	0.52	0	0.15		0.28		0.05
Parasites	**0.62**	**5.47**	**4.56**	**2.06**	**0.24**	**5.84**	**0**	**1.42**	**0.43**	**5.79**	**2.98**	**2.10**
Phylum Nematoda	1.98	17.26	0	7.56	0	13.32	0	3.83	0.56	22.63	0	5.98
Class Cestoda	0	0	9.90	0.40	0.79	0	0	0.30	0.22	0	7.66	0.37
Abiotic substances	**0**	**0**	**0**	**0**	**0.14**	**0**	**0**	**0.04**	**0.04**	**0**	**0**	**0.01**
Hook and line	0	0	0	0	0.49	0	0	0.18	0.14	0	0	0.06

3.3. Niche Breadth and Trophic Overlap

Excluding abiotics and parasites from the stomach content items, the values of the standardized Levin's niche breadth index B_A were <0.40 (0.05–0.21) for all age groups of the male, female, and combined sexes, indicating that juvenile great hammerheads aged < 3 years are specialized predators (Table 3).

Table 3. The Morisita–Horn index ($\mathbf{C_\lambda}$) for trophic overlap, trophic level (TrL), and niche breadth ($\mathbf{B_A}$) estimated in juvenile great hammerheads sampled from Saudi Arabian waters of the Arabian Gulf for different sexes and age groups (0^+ to 2^+ years).

Sex and Age Class	Male			Female			All Male	All Female	Sex Combined			TrL	B_A	
	0^+	1^+	2^+	0^+	1^+	2^+			0^+	1^+	2^+		Lower Taxa (Order to species)	Group Class
M 0^+, n = 16	-	-	-	-	-	-	-	-	-	-	-	4.76	0.05	0.03
M 1^+, n = 8	0.007	-	-	-	-	-	-	-	-	-	-	4.71	0.21	0.16
M 2^+, n = 3	0	0	-	-	-	-	-	-	-	-	-	4.40	0.08	0.16
F 0^+, n = 20	0.04	0.53	0	-	-	-	-	-	-	-	-	4.56	0.13	0.10
F 1^+ yr, n = 9	0.12	0	0.003	0	-	-	-	-	-	-	-	4.61	0.10	0.23
F, 2+ yr, n = 3	0	0	0	0	0.08	-	-	-	-	-	-	5.01	0.06	0.13
All male, n = 27	-	-	-	-	-	-	-	-	-	-	-	4.70	0.12	0.07
All female, n = 32	-	-	-	-	-	-	0.23	-	-	-	-	4.62	0.16	0.20
All 0^+, n = 36	-	-	-	-	-	-	-	-	-	-	-	4.65	0.10	0.07
All 1^+, n = 17	-	-	-	-	-	-	-	-	0.34	-	-	4.65	0.16	0.22
All 2^+, n = 6	-	-	-	-	-	-	-	-	0	0.04	-	4.70	0.15	0.21

M: male; F: female.

The Morisita–Horn index indicated that different age groups of the male and female consumed different preys; only males aged 0^+ years and females aged 1^+ year (C_λ = 0.53) exhibited a high trophic overlap (Table 3).

3.4. Trophic Level

The overall mean trophic level was 4.66 ± 0.45. The mean trophic level for the males was 4.70, whereas that for the females was 4.62. When estimated according to age group, the mean trophic level ranged from 4.76 to 4.40 for males, and from 4.56 to 5.01 for females, indicating that great hammerheads are tertiary consumers (Table 3) [21].

4. Discussion

Although *S. mokarran* is distributed globally, owing to difficulty in sampling, only a few studies are available on the feeding habits of great hammerheads. This species is not abundant in the Arabian Gulf, and only 2.7% elasmobranch landings have been reported from the Saudi Arabian Gulf [31]. This study examined the specimens obtained from landings in Saudi Arabia. To the best of our knowledge, this study is the first providing stomach content information for this critically endangered shark species sampled from the northwestern Indian Ocean.

The vacuity index of 19.2% for the *S. mokarran* from the Arabian Gulf was close to a vacuity index of 18.5% for those sampled from eastern South Africa and higher than that for those sampled from northern Australia (12.4%) [2,17]. Compared with other large hammerhead (>2 m TL) species, the vacuity index of *S. mokarran* was close to that of the scalloped hammerhead *Sphyrna lewini* (Griffith & Smith, 1834) found in the southern Gulf of California and northern Australia (19.2%–21.5%); moreover, the vacuity index of *S. mokarran* was higher than that of the winghead shark *Eusphyra blochii* (Cuvier, 1816) found in northern Australia (14.3%) and the smooth hammerhead *Sphyrna zygaena* (Linnaeus, 1758) found in Ecuadorean waters (8.1%); however, the vacuity index of *S. mokarran* was obviously lower than that of the scalloped (67.9–73.2%) and smooth (48.5%) hammerheads found in Taiwan's waters [17,23,32,33]. Most great hammerheads used in this study were caught using gill nets [31], similarly to that reported for the hammerheads (winghead, smooth and scalloped hammerheads) in a previous study [17]; by contrast, the hammerheads obtained from the southern Gulf of California and Taiwan waters were caught using

longlines [32–34]. The southern Gulf of California's longline fishery is operated in coastal and inshore shallow waters (<90 m) using traditional fleets; by contrast, the Taiwan longline fishery is operated 20–200 m deep in offshore waters with a much longer main line and hundreds of hooks [32–34]. Therefore, the hammerheads caught from the Taiwan waters were soaked much longer and struggled more than those caught from elsewhere, resulting in a higher vacuity index.

In general, teleosts were the main prey of *E. blochii*, *S. mokarran*, and *S. lewini* found in northern Australia [17] and of *S. mokarran* found in the Arabian Gulf (Table 1). However, the scalloped hammerheads in the Pacific were found to mainly feed on not only teleosts but also cephalopods for their diet [33–35]. For *S. zygaena*, cephalopods were always the dominant prey item [24,34,36]. However, small-sized (<2 m TL) hammerhead shark species preferred shrimps [35].

In addition to teleosts and cephalopods, elasmobranchs were a part of the hammerhead sharks' diets, particularly of *S. mokarran*. Several studies have reported that great hammerheads feed on other elasmobranchs [1,17–19]. Compagno reported that great hammerheads seemed to especially favor stingrays and other batoids [1]. *Hypanus americanus* (Hildebrand & Schroeder, 1928), the southern stingray, is reportedly preyed on by a 3-m-TL great hammerhead in the Bahama waters, the western North Atlantic [19]. An adult female great hammerhead was observed to attack a school of approximately 100 gray reef sharks (*Carcharhinus amblyrhynchos* [Bleeker, 1856]) and prey on one of them in French Polynesian waters [4]. In northern Australia, elasmobranchs were found in 30.6% of 304 *S. mokarran* stomachs [17], higher than the 11.9% rate observed in the present study on the same species sampled from the Arabian Gulf (Table 1). In eastern South Africa, elasmobranchs were found in 83.2% of *S. mokarran* stomachs, batoids being their predominant prey [2]. In eastern Australia, large great hammerheads mainly feed on other sharks and rays, with a preference for benthic species [20]. In the present study, neonatal great hammerheads seemed to be unable to prey on other elasmobranchs; however, this ability increased with age in females, such that at ≥2 years, the females reached the highest trophic level (TrL = 5.0) (Tables 2 and 3). Other large and more pelagic hammerhead sharks, such as the scalloped, smooth hammerheads and the winghead shark, did not feed on elasmobranchs as frequently as *S. mokarran* did. Elasmobranchs were found neither in the scalloped hammerhead from the southern Gulf of California nor in the smooth hammerhead from the Ecuadorean and northeastern Taiwan waters [24,32,34]. Elasmobranchs barely contributed to the dietary composition of the scalloped hammerhead and winghead shark in northern Australia (0.3%–0.8%) and the scalloped hammerhead in the northeastern Taiwan waters (0.8%–1.3%) [17,33,34].

The juvenile great hammerheads were determined to be specialized predators in this study (Table 3). In eastern Australia, through stable isotope analysis, adult great hammerheads were found to be specialists that fed primarily on elasmobranchs [20]. Other large hammerheads, such as *S. lewini* (B_A: 0.32–0.39) and *S. zygaena* (B_A: 0.07–0.23), were mostly determined to be specialized predators [24,33,34], although *S. lewini* from the Mexican Pacific coastal waters was considered an opportunistic predator [37]. Unlike large-sized hammerhead species, small-sized demersal sharks, such as several Scyliorhinidae spp. (e.g., *Galeus melastomus* Rafineque 1810), opportunistic generalist predators that adapt their diet to the available prey in various environments, seem to be better able to resist heavy exploitation [25,38]. Hence, the impact of target and bycatch fishing for large hammerhead species needs more concern.

Ontogenetic shifts in resource use were detected for several large hammerheads, including *S. mokarran*. The diets of the Arabian Gulf *S. mokarran* shifted from teleosts to elasmobranchs within 3 years after birth. Smaller *S. mokarran* may feed more on teleosts; when they grow, they shift to apex predator roles [20]. Smaller *S. zygaena* (<150 cm TL) from Ecuador consumed prey of coastal origin, whereas larger individuals fed in oceanic waters and near the continental shelf [24]. Using both stomach content and stable isotope

analyses, resource-use shifts relating to size increase were also detected for *S. lewini* from the Taiwan waters [33,34].

The trophic level estimate for *S. mokarran* was scanty. The mean trophic level of the juvenile great hammerheads in this study was 4.66, slightly higher than the 4.3 reported in another study of *S. mokarran* [21]. This value was close to that of the large hammerhead species, such as the smooth hammerhead in the east (4.7) and northwest Pacific (4.82) [24,34] and the scalloped hammerhead in the east (4.22–4.95) and northwest Pacific (4.89) [34,37]. Conversely, small-sized hammerhead species, such as *Sphyrna corona* Springer, 1940, *Sphyrna media* Springer, 1940, and *Sphyrna tiburo* (Linnaeus, 1758), seemed to occupy lower trophic positions and had a maximum TL of 0.92–1.5 m and a lower trophic level of 3.95–4.26 [35].

Among all Sphyrnidae species, *S. tiburo* had the lowest trophic level (3.2–3.95; always <4) [21,35]. The main reason for this is that seagrass commonly occurs in the diets of *S. tiburo* [39]. Subsequent studies confirmed that *S. tiburo* is an omnivore that can digest and assimilate seagrass nutrients [40]. The great hammerhead is mostly a carnivore; however, two seagrass species were found in one great hammerhead stomach in the present study (Table 1). Seagrass might have been incidentally ingested and may not be a common food of great hammerheads. Not only seagrass but also terrestrial cockroach ingestion was found in another stomach; therefore, it can be inferred that some individuals frequented shallower and more coastal waters as their habitat. In other regions, great hammerheads were also found to use inshore, flat shallow water environments (<1.5 m), and young-of-the-year *S. mokarran* used nearshore, even highly human-impacted marine habitats as its nursery ground [41–44].

Classical stomach content analysis and the more recently introduced stable isotope analysis have their limitations [45]. Using stomach content analysis with stable isotope analysis on various tissues (e.g., muscles, the liver, and the vertebra) provides insights into the trophic niches at different time scales (from days to years); however, to realize the latest feeding behaviors and food composition patterns, stomach content analysis remains important and difficult to replace. Studies are necessary on the biology and ecology of the great hammerhead, as the second largest predatory shark after the tiger shark *Galeocerdo cuvier* (Péron & Lesueur, 1822) in the Arabian Gulf and the largest predatory shark in Saudi Arabian waters [9,13,27,32]. Cooperation among the countries in the Arabian Gulf is required for large-scale investigations and beyond, in order to gain a better understanding of the life history of this critically endangered species and devise appropriate management policies and strategies.

Author Contributions: Conceptualization, H.H.H. and M.A.Q.; Data curation, H.H.H.; Formal analysis, H.H.H.; Funding acquisition, A.Q., L.J.R. and M.A.Q.; Investigation, H.H.H., Z.N., P.P. and Y.-J.L.; Methodology, H.H.H.; Project administration, A.Q. and L.J.R.; Resources, H.H.H. and Y.-J.L.; Software, H.H.H.; Supervision, L.J.R. and M.A.Q.; Validation, Y.-J.L.; Visualization, HHH; Writing—original draft, H.H.H.; Writing—review and editing, all authors. All authors have read and agreed to the published version of the manuscript.

Funding: This research was funded by Saudi Aramco Oil Co. (Dhahran, Saudi Arabia), grant number: CEW02428.

Institutional Review Board Statement: Samples of specimens for this study were obtained from the catches of licensed fishermen as per the Law of Fisheries and Aquaculture Resources Investment and Protection in KSA Territorial Waters. This study complied with all ethical requirements in Saudi Arabian animal welfare laws and guidelines. No experiments were conducted on live animals.

Data Availability Statement: The data presented in this study are available on request from the corresponding author.

Acknowledgments: We acknowledge the Center for Environment and Marine Studies, Research Institute, King Fahd University of Petroleum and Minerals, Dhahran, Saudi Arabia, for providing manpower resources and research facilities, and we also thank Saudi Aramco Oil Co. (Dhahran, Saudi Arabia) for funding and for continued support.

Conflicts of Interest: The authors declare that there are no conflict of interest.

References

1. Compagno, L.J.V. *Sharks of the World: An Annotated and Illustrated Catalogue of Shark Species Known to Date*; FAO Fisheries Synopsis; FAO Species Catalogue; Food and Agriculture Organization of the United Nations: Rome, Italy, 1984; Volume 4, pp. 251–655.
2. Cliff, G. Sharks caught in the protective gill nets off KwaZulu-Natal, South Africa. 8. The Great hammerhead shark *Sphyrna mokarran* (Rüppell). *S. Afr. J. Mar. Sci.* **1995**, *15*, 105–114. [CrossRef]
3. Ebert, D.A.; Fowler, S.; Compagno, L. *Sharks of the World—A Fully Illustrated Guide*; Wild Nature Press: Plymouth, UK, 2013; p. 528.
4. Mourier, J.; Planes, S.; Buray, N. Trophic interactions at the top of the coral reef food chain. *Coral Reefs* **2013**, *32*, 285. [CrossRef]
5. Guttridge, T.L.; Van Zinnicq Bergmann, M.P.M.; Bolte, C.; Howey, L.A.; Finger, J.S.; Kessel, S.T.; Brooks, J.L.; Winram, W.; Bond, M.E.; Jordan, L.K.B.; et al. Philopatry and regional connectivity of the great hammerhead shark, *Sphyrna mokarran* in the U.S. and the Bahamas. *Front. Mar. Sci.* **2017**, *4*, 3. [CrossRef]
6. Gallagher, A.J.; Klimley, A.P. The biology and conservation status of the large hammerhead shark complex: The great, scalloped, and smooth hammerheads. *Rev. Fish Biol. Fish.* **2018**, *28*, 777–794. [CrossRef]
7. Piercy, A.N.; Carlson, J.K.; Passerotti, M.S. Age and growth of the great hammerhead shark, *Sphyrna mokarran*, in the north-western Atlantic Ocean and Gulf of Mexico. *Mar. Freshw. Res.* **2010**, *61*, 992–998. [CrossRef]
8. Gulak, S.J.B.; de Ron Santiago, A.J.; Carlson, J.K. Hooking mortality of scalloped hammerhead *Sphyrna lewini* and great hammerhead *Sphyrna mokarran* sharks caught on bottom longlines. *Afr. J. Mar. Sci.* **2015**, *37*, 267–273. [CrossRef]
9. Jabado, R.W.; Kyne, P.M.; Pollom, R.A.; Ebert, D.A.; Simpfendorfer, C.A.; Ralph, G.M.; Dulvy, N.K. *The Conservation Status of Sharks, Rays, and Chimaeras in the Arabian Sea and Adjacent Waters*; Environment Agency—Abu Dhabi and IUCN Species Survival Commission Shark Specialist Group: Abu Dhabi, United Arab Emirates, 2017; p. 230.
10. Checklist of CITES Species. Available online: http://checklist.cites.org/#/en (accessed on 21 June 2022).
11. Appendices I and II of the Convention on the Conservation of Migratory Species of Wild Animals (CMS). Available online: https://goo.gl/Ta4agj (accessed on 21 June 2022).
12. Rigby, C.L.; Barreto, R.; Carlson, J.; Fernando, D.; Fordham, S.; Francis, M.P.; Herman, K.; Jabado, R.W.; Liu, K.M.; Marshall, A.; et al. *Sphyrna mokarran*; The IUCN Red List of Threatened Species 2019: e.T39386A2920499; International Union for Conservation of Nature and Natural Resources: Gland, Switzerland, 2019. Available online: https://dx.doi.org/10.2305/IUCN.UK.2019-3.RLTS.T39386A2920499.en (accessed on 27 November 2022).
13. Hsu, H.H.; Nazeer, Z.M.; Lin, Y.J.; Panickan, P.; Al-Abdulkader, K.; Loughland, R.; Qurban, M.A. Biological aspects of juvenile great hammerhead sharks *Sphyrna mokarran* from the Arabian Gulf. *Mar. Freshw. Res.* **2021**, *72*, 110–117. [CrossRef]
14. Passerotti, M.S.; Carlson, J.K.; Piercy, A.N.; Campana, S.E. Age validation of great hammerhead shark (*Sphyrna mokarran*), determined by bomb radiocarbon analysis. *Fish. Bull.* **2010**, *108*, 346–351.
15. Harry, A.V.; Macbeth, W.G.; Gutteridge, A.N.; Simpfendorfer, C.A. The life histories of endangered hammerhead sharks (Carcharhiniformes, Sphyrnidae) from the east coast of Australia. *J. Fish Biol.* **2011**, *78*, 2026–2051. [CrossRef]
16. Tovar-Ávila, J.; Gallegos-Camacho, R. Oldest estimated age for *Sphyrna mokarran* (Carcharhiniformes: Sphyrnidae) in the Mexican Pacific. *Hidrobiológica* **2014**, *24*, 163–165.
17. Stevens, J.D.; Lyle, J.M. Biology of three hammerhead sharks (*Eusphyra blochii*, *Sphyrna mokarran* and *S. lewini*) from Northern Australia. *Mar. Freshw. Res.* **1989**, *40*, 129–146. [CrossRef]
18. Bass, A.J.; D'Aubrey, J.D.; Kistnasamy, N. Sharks of the east coast of Southern Africa. III. In *The Families Carcharhinidae (Excluding Mustelus and Carcharhinus) and Sphyrnidae*; Oceanography Research Institute: Durban, South Africa, 1975; Volume 38, pp. 44–45.
19. Strong, W.R., Jr.; Snelson, F.F., Jr.; Gruber, S.H. Hammerhead shark predation on stingrays: An observation of prey handling by *Sphyrna mokarran*. *Copeia* **1990**, *1990*, 836–840. [CrossRef]
20. Raoult, V.; Broadhurst, M.K.; Peddemors, M.; Williamson, M.E.; Gaston, M.F. Resource use of great hammerhead sharks *Sphyrna mokarran* off eastern Australia. *J. Fish Biol.* **2019**, *95*, 1430–1440. [CrossRef]
21. Cortés, E. Standardized diet compositions and trophic levels of sharks. *ICES J. Mar. Sci.* **1999**, *56*, 707–717. [CrossRef]
22. Rastgoo, A.R.; Navarro, J.; Valinassab, T. Comparative diets of sympatric batoid elasmobranchs in the Gulf of Oman. *Aquat. Biol.* **2018**, *27*, 35–41. [CrossRef]
23. Cortés, E. A critical review of methods of studying fish feeding based on analysis of stomach contents: Application to elasmobranch fishes. *Can. J. Fish. Aquat. Sci.* **1997**, *54*, 726–738. [CrossRef]
24. Estupiñán-Montaño, C.; Cedeño-Figueroa, L.; Estupiñán-Ortiz, J.F.; Galván-Magaña, F.; Sandoval-Londoño, A.; Castañeda-Suarez, D.; Polo-Silva, V.J. Feeding habits and trophic level of the smooth hammerhead shark, *Sphyrna zygaena* (Carcharhiniformes: Sphyrnidae), off Ecuador. *J. Mar. Biol. Assoc. U. K.* **2019**, *99*, 673–680. [CrossRef]
25. D'Iglio, C.; Albano, M.; Tiralongo, F.; Famulari, S.; Rinelli, P.; Savoca, S.; Spanò, N.; Capillo, G. Biological and ecological aspects of the blackmouth catshark (*Galeus melastomus* Rafinesque, 1810) in the southern Tyrrhenian Sea. *J. Mar. Sci. Eng.* **2021**, *9*, 967. [CrossRef]
26. Smith, E.P.; Zaret, T.M. Bias in estimating niche overlap. *Ecology* **1982**, *63*, 1248–1253. [CrossRef]
27. Jabado, R.W.; Al-Ghais, S.M.; Hamza, W.; Shivji, M.S.; Henderson, A.C. Shark diversity in the Arabian/Persian Gulf higher than previously thought: Insights based on species composition of shark landings in the United Arab Emirates. *Mar. Biodivers.* **2015**, *45*, 719–731. [CrossRef]

28. Froese, R.; Pauly, D. FishBase. World Wide Web Electronic Publication, Version (12/2019). Available online: www.fishbase.org (accessed on 5 September 2022).
29. Palomares, M.L.D.; Pauly, D. SeaLifeBase. World Wide Web Electronic Publication, Version (07/2020). 2020. Available online: www.sealifebase.org (accessed on 5 September 2022).
30. Guo, K.; Zhao, W.; Wang, S.; Liu, B.; Zhang, P. Food web structure and trophic levels in a saltwater pond sea cucumber and prawn polyculture system. *Acta Oceanol. Sin.* **2016**, *35*, 58–62. [CrossRef]
31. Hsu, H.H.; Yacoubi, L.; Lin, Y.-J.; Le Loc'h, F.; Katsanevakis, S.; Giovos, I.; Qurban, M.A.; Nazeer, Z.; Panickan, P.; Maneja, R.H.; et al. Elasmobranchs of the western Arabian Gulf: Diversity, status, and implications for conservation. *Reg. Stud. Mar. Sci.* **2022**, *56*, 102637. [CrossRef]
32. Torres-Rojas, Y.E.; Hernandez-Herrera, A.; Galván-Magaña, F. Feeding habits of the scalloped hammerhead shark, *Sphyrna lewini*, in Mazatlán waters, southern Gulf of California, Mexico. *Cybium* **2007**, *30*, 85–90.
33. Lai, W. Analyzes of Stomach Contents of Four Large Shark Species in the Waters of Northeastern Taiwan. Master Thesis, National Taiwan Ocean University, Keelung, Taiwan, June 2011. (In Chinese with English Abstract)
34. Yeh, S.Y. Feeding Ecology of Two Hammerhead Shark Species from Northeastern Taiwan Waters. Master Thesis, National Taiwan Ocean University, Keelung, Taiwan, July 2017. (In Chinese with English Abstract)
35. Galindo, E.; Giraldo, A.; Navia, A.F. Feeding habits and trophic interactions of four sympatric hammerhead shark species reveal trophic niche partitioning. *Mar. Ecol. Prog. Ser.* **2021**, *665*, 159–175. [CrossRef]
36. Smale, M.J. Occurrence and feeding of three shark species, *Carcharhinus brachyurus*, *C. obscurus* and *Sphyrna zygaena*, on the Eastern Cape coast of South Africa. *S. Afr. J. Mar. Sci.* **1991**, *11*, 31–42. [CrossRef]
37. Torres-Rojas, Y.E.; Páez Osuna, F.; Camalich, J.; Galván-Magaña, F. Diet and trophic level of scalloped hammerhead shark (*Sphyrna lewini*) from the Gulf of California and Gulf of Tehuantepec, Mexico. *Iran. J. Fish. Sci.* **2015**, *14*, 767–785.
38. D'Iglio, C.; Savoca, S.; Rinelli, P.; Spanò, N.; Capillo, G. Diet of the deep-Sea shark *Galeus melastomus* Rafinesque, 1810, in the Mediterranean Sea: What we know and what we should know. *Sustainability* **2021**, *13*, 3962. [CrossRef]
39. Cortés, E.; Manire, C.A.; Hueter, R.E. Diet, feeding habits, and diel feeding chronology of the bonnethead shark, *Sphyrna tiburo*, in southwest Florida. *Bull. Mar. Sci.* **1996**, *58*, 353–367.
40. Leigh, S.C.; Papastamatiou, Y.P.; German, D.P. Seagrass digestion by a notorious 'carnivore'. *Proc. R. Soc. B Biol. Sci.* **2018**, *285*, 20181583. [CrossRef]
41. Hueter, R.E.; Tyminski, J.P. Species-specific distribution and habitat characteristics of shark nurseries in Gulf of Mexico waters off peninsular Florida and Texas. *Am. Fish. Soc. Symp.* **2007**, *50*, 193–223.
42. Roemer, R.P.; Gallagher, A.J.; Hammerschlag, N. Shallow water tidal flat use and associated specialized foraging behavior of the great hammerhead shark (*Sphyrna mokarran*). *Mar. Freshw. Behav. Physiol.* **2016**, *49*, 235–249. [CrossRef]
43. Barker, A.M.; Frazier, B.S.; Bethea, D.M.; Gold, J.R.; Portnoy, D.S. Identification of young-of-the-year great hammerhead shark *Sphyrna mokarran* in northern Florida and South Carolina. *J. Fish Biol.* **2017**, *91*, 664–668. [CrossRef]
44. Macdonald, C.; Jerome, J.; Pankow, C.; Perni, N.; Black, K.; Shiffman, D.; Wester, J. First identification of probable nursery habitat for critically endangered great hammerhead *Sphyrna mokarran* on the Atlantic Coast of the United States. *Conserv. Sci. Pract.* **2021**, *3*, e418. [CrossRef]
45. Hammerschlag, N. Quantifying shark predation effects on prey: Dietary data limitations and study approaches. *Endanger. Species Res.* **2019**, *38*, 147–151. [CrossRef]

Regional Studies in Marine Science 56 (2022) 102637

Contents lists available at ScienceDirect

Regional Studies in Marine Science

journal homepage: www.elsevier.com/locate/rsma

Elasmobranchs of the western Arabian Gulf: Diversity, status, and implications for conservation

Hua Hsun Hsu [a,b], Lamia Yacoubi [c], Yu-Jia Lin [a,d], François Le Loc'h [e], Stelios Katsanevakis [f], Ioannis Giovos [g,h], Mohammad A. Qurban [a,i], Zahid Nazeer [a], Premlal Panickan [a] Rommel H. Maneja [a], Perdana K. Prihartato [j], Ronald A. Loughland [j], Lotfi Jilani Rabaoui [c,i,*]

[a] Center for Environment & Marine Studies, Research Institute, King Fahd University of Petroleum & Minerals, Dhahran, Saudi Arabia
[b] Coastal and Offshore Resources Research Center, Fisheries Research Institute, Council of Agriculture, Taiwan
[c] University of Tunis El Manar, Faculty of Science of Tunis, Laboratory of Biodiversity and Parasitology of Aquatic Ecosystems (LR18ES05), 2092 Tunis, Tunisia
[d] Institute of Marine Ecology and Conservation, National Sun Yat-sen University, Kaohsiung, Taiwan
[e] University of Brest, CNRS, IRD, Ifremer, LEMAR, F-29280 Plouzane, France
[f] Department of Marine Sciences, University of the Aegean, University Hill, Mytilene, Greece
[g] iSea, Environmental Organization for the Preservation of the Aquatic Ecosystems, Thessaloniki, Greece
[h] Marine and Environmental Research (MAR) Lab Ltd, Limassol, Cyprus
[i] National Center for Wildlife, Riyadh, Saudi Arabia
[j] Environmental Protection Department, Saudi Aramco, Dhahran, Saudi Arabia

ARTICLE INFO

Article history:
Received 17 March 2022
Received in revised form 16 July 2022
Accepted 14 August 2022
Available online 18 August 2022

Keywords:
Batoid
Sharks
Diversity
Conservation
Fishery
Management

ABSTRACT

In spite of the ecological services provided by elasmobranchs, their diversity and populations are significantly declining even before appropriate assessments are conducted. This paper presents information on elasmobranch diversity in the Saudi waters of the Arabian Gulf based on fishery-independent and dependent surveys. A total of 369 individual sharks and batoids were collected from 119 out of 228 trawl stations surveyed between 2013 and 2016. *Gymnura poecilura* and *Carcharhinus dussumieri* were the most dominant batoid and shark species, respectively. The catch per unit area indicated the waters around Jana Island as a hotspot of elasmobranchs. A total of 135 surveys at the landing sites and fish markets from 2016 to 2020 showed that 88% of elasmobranchs (out of 4,055 individuals recorded) were caught by gill nets. Sharks were the most abundant (> 80 %) with three dominant species: *Carcharhinus sorrah*, *C. humani*, and *C. limbatus*. In total, 47 species of elasmobranchs (24 sharks and 23 batoids) belonging to 16 families and 5 orders were recorded from a possible 58 total species predicted by species richness extrapolators (Chao 1). High values of Margalef richness (> 2) and Shannon–Wiener index (3–4) suggested rich diversity of elasmobranchs in the study area with homogeneous distribution over the years and seasons as shown by cluster and similarity profile analysis. Of the 47 species recorded, six species were Critically Endangered regionally, six Endangered, and seven species Vulnerable according to the IUCN Red List of Threatened Species, necessitating proper management and conservation measures.

1. Introduction

Sharks and batoids are members of the class Elasmobranchii, which is distributed worldwide in the tropical, subtropical, temperate, and cold waters. They are found from the coastal to offshore waters except in the freshwater habitats (Gemaque et al., 2017). Their fundamental role as top predators is crucial for the health of marine ecosystems through their regulatory role on the structure and function of marine communities (Chapman et al., 2006; Heithaus et al., 2008; Bornatowski et al., 2014). However, elasmobranchs are one of the most threatened groups of marine wildlife because of their reproductive traits and long-life span (Stevens et al., 2000; Lucifora et al., 2011; Gemaque et al., 2017). An estimated 71% reduction in biomass of elasmobranchs globally has been estimated since the 1970s with around 75% of the species threatened with extinction (Pacoureau et al., 2021).

The Arabian Gulf (also known as the Persian Gulf, hereinafter referred to as the 'Gulf') is known for its fossil fuel reserves. It witnesses a flurry of activities associated with the expansion of oil exploration and production. In addition, the Gulf is considered an extreme environment due to high evaporation rate, high salinity, low rainfall, and extreme temperatures (Reynolds, 1993; Almazroui et al., 2013; Naser, 2014; Pal and Eltahir, 2015;

* Corresponding author at: National Center for Wildlife, Riyadh, Saudi Arabia.
E-mail addresses: lrabaoui@kfupm.edu.sa, lrabaoui@gmail.com (L.J. Rabaoui).

https://doi.org/10.1016/j.rsma.2022.102637
2352-4855/

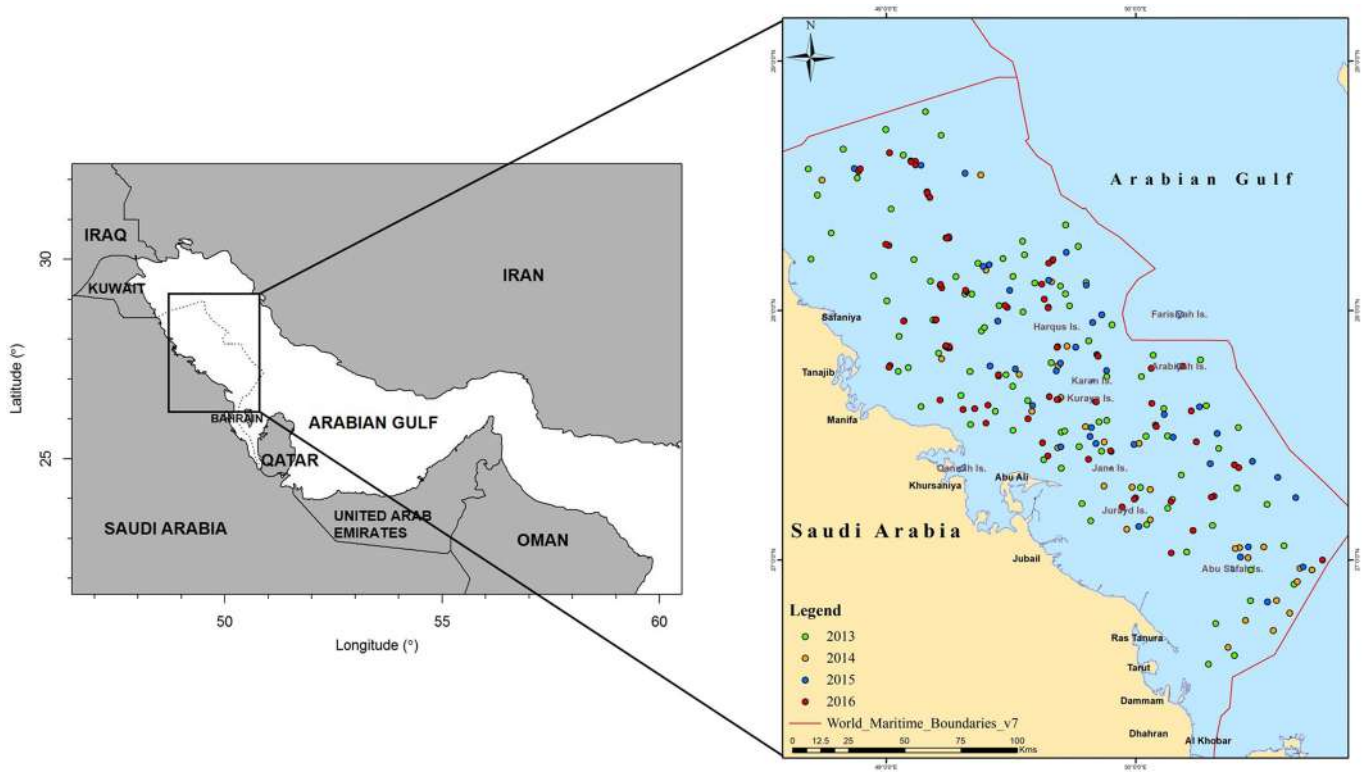

Fig. 1. Study area showing the location of the trawled stations in the Saudi waters of the Arabian Gulf, within the fishery-independent surveys conducted between 2013 and 2016. Dot lines show Saudi exclusive economic zone boundary.

Hasanean and Almazroui, 2015). Therefore, the marine environment of the Gulf is reported to be under increased pressure (Sheppard et al., 2010; Jabado et al., 2015b; Rabaoui et al., 2015; Vaughan et al., 2019). In spite of the extreme environmental conditions and the increasing anthropogenic pressures in this region, the Gulf still hosts various habitats such as coral reefs, seagrass meadows and mangroves, and rich fish and shellfish biodiversity (Rabaoui et al., 2015, 2017, 2019, 2021a,b; Lin et al., 2021a,b,c).

Among the different zoological groups living in the Gulf, elasmobranchs are still very poorly known, and their biodiversity is not yet fully documented, in particular in the Saudi waters. Given the anthropogenic pressures posing on the Gulf environment, the protection of elasmobranchs and sustainability of their fisheries is challenging without strong information on their biodiversity and distribution. Compared to the Red Sea where elasmobranchs have been already assessed as overexploited (Sheppard et al., 2010; Qurban et al., 2012; Naser, 2014; Spaet and Berumen, 2015), knowledge on the status of elasmobranchs in the Gulf are still limited and patchy. An interview-based survey conducted in the United Arab Emirates (UAE) showed that sharks have been overexploited in the southern Gulf (Jabado et al., 2015a) and that elasmobranchs are facing the risk of regional extinction in the Gulf (Jabado et al., 2017a; Moore, 2017; Jabado, 2018). The present work was conducted with this concern, and it aims at (*i*) characterizing the elasmobranch community in the Saudi waters of the Gulf based on fishery-independent and dependent surveys, (*ii*) reviewing the conservation status of these taxa, and (*iii*) making recommendations for strengthening management plans for these natural resources.

2. Materials and methods

2.1. Fishery-independent surveys

Four trawling surveys were conducted between 2013 and 2016 using a chartered commercial outrigger. To adequately cover the entire territorial waters of Saudi Arabia in the Gulf, sampling was done in 228 stations (Fig. 1). The trawl surveys were conducted on a commercial outrigger *Afrah* in 2013 and 2016 (Rabaoui et al., 2015) and on a research vessel *RV Bahith II* in 2014 and 2015. We compared the length distributions of the fish from both fleets to assess the catchability of elasmobranchs. The differences were observed only on extremely small-sized fish (total length <30 mm), which was greatly smaller than the observed elasmobranch (>300 mm). Therefore, we assumed that the catchability of elasmobranchs was similar between the two fleets.

All the trawling operations were conducted following a standard operation protocol. Trawling was done during the daytime with the speed of three knots for 30 min. At each station, the total catch consisting of fishes, invertebrates, and sea snakes was weighed. The total number of individuals and total weight of all elasmobranchs were recorded species-wise after photographing and identification. Specimens collected were identified following the identification keys of Carpenter et al. (1997), Ebert et al. (2013), Almojil et al. (2015), Jabado and Ebert (2015), and Last et al. (2016).

In addition, data on the occurrence of the blotched fantail ray, *Taeniurops meyeni,* and the whale shark, *Rhincodon typus*, were collected through a series of boat-based observational surveys conducted between 2014 and 2020. These surveys were conducted as part of another study on the migration patterns of *R. typus*. (Table 1; Hsu et al. *unpublished data*). The scientists were on a commercial boat and navigated to areas where *R. typus* was previously observed. The team patrolled around this area and assessed the occurrence of *R. typus* by visual observation.

2.2. Fishery-dependent surveys

2.2.1. Landing surveys

Elasmobranch landings from the commercial fisheries were surveyed over the 135 visits to fishing ports and fish auction

Table 1
Taxonomic list of elasmobranch species in the Arabian Gulf based on literature, fisherman's reports, and social media, with specimens encountered after 1998. IUCN Red List Status is also included (CR: Critically Endangered; EN: Endangered; NT: Near Threatened; VU: Vulnerable; LC: Least Concern; DD: Data Deficient; NE: Not Evaluated). X: species present.

Family/Species	IUCN global status	IUCN Arabian Sea status	Kuwait	Saudi Arabia	Bahrain	Qatar	Gulf Iran waters	Gulf UAE waters
Hemiscylliidae								
Chiloscyllium arabicum	NT	NE	X	X[a,b]	X	X	X	X
Chiloscyllium griseum	NT	NT						X
Chiloscyllium punctatum	NT	NE					X	
Ginglymostomatidae								
Nebrius ferrugineus	VU	NT						X
Stegostomatidae								
Stegostoma fasciatum	EN	VU		X[a]				X
Rhincodontidae								
Rhincodon typus	EN	EN		X	X	X	X	X
Odontaspididae								
Carcharias taurus	VU	CR						X
Triakidae								
Mustelus mosis	NT	LC	X	X[b]	X	X		X
Hemigaleidae								
Chaenogaleus macrostoma	VU	VU	X	X[b]	X	X	X	X
Hemipristis elongata	VU	VU	X	X[b]	X	X		X
Paragaleus randalli	NT	VU	X	X[b]	X	X		X
Carcharhinidae								
Carcharhinus amblyrhynchoides	NT	VU	X	X[b]				X
Carcharhinus amblyrhynchos	NT	EN						X
Carcharhinus amboinensis	DD	VU	X	X[b]	X	X		X
Carcharhinus brevipinna	NT	VU		X[b]	X			X
Carcharhinus dussumieri	EN	EN	X	X[a,b]	X	X	X	X
Carcharhinus falciformis	VU	NT						X
Carcharhinus humani	DD	DD		X[a,b]				X
Carcharhinus leiodon	EN	NE	X	X[b]				X
Carcharhinus leucas	NT	EN	X	X[b]		X	X	X
Carcharhinus limbatus	NT	VU	X	X[b]	X	X		X
Carcharhinus macloti	NT	NT	X	X[a,b]	X		X	X
Carcharhinus melanopterus	NT	VU		X[b]				X
Carcharhinus plumbeus	VU	EN						X
Carcharhinus sorrah	NT	VU	X	X[a,b]	X	X		X
Galeocerdo cuvier	NT	VU						X
Loxodon macrorhinus	LC	NT		X[b]	X	X	X	X
Negaprion acutidens	VU	EN		X[b]				X
Rhizoprionodon acutus	LC	NT	X	X[a,b]	X	X	X	X
Rhizoprionodon oligolinx	LC	NT	X	X[b]	X			X
Sphyrnidae								
Sphyrna lewini	CR	EN		X[b]				X
Sphyrna mokarran	CR	EN	X	X[b]	X	X		X
Pristidae								
Anoxypristis cuspidata	EN	CR					X	
Pristis zijsron	CR	CR			X			X
Rhina ancylostoma	CR	VU		X[a]				X
Rhynchobatidae								
Rhynchobatus australiae	CR	EN		X[a,b]				
Rhynchobatus djiddensis	CR	EN	X		X	X	X	
Rhynchobatus laevis	CR	EN		X[a,b]				X
Rhinobatidae								
Acroteriobatus omanensis	DD	NE						X
Acroteriobatus salalah	NT	NE						X
Glaucostegus granulatus	CR	EN	X				X	X
Glaucostegus halavi	CR	NE		X[a,b]	X			X
Rhinobatos annandalei	DD	NT					X	X
Rhinobatos punctifer	NT	NE		X[a,b]	X	X	X	X
Rhinobatos schlegelii	DD	NE					X	
Torpedinidae								
Torpedo sinuspersici	DD	DD		X[a]			X	
Dasyatidae								
Bathytoshia lata	LC	DD		X[a]				
Brevitrygon walga	NT	NE	X	X[a]		X	X	
Himantura leoparda	VU	VU		X[a,b]				X
Himantura uarnak	VU	VU	X	X[a]	X	X	X	X
Maculabatis gerrardi	VU	EN					X	

(*continued on next page*)

markets at Manifa, Jubail and Qatif between March 2016 and February 2020 (Fig. 1). The team identified the elasmobranchs species and recorded species-specific landing in numbers and weights every month. The gears used to catch elasmobranchs,

Table 1 (*continued*).

Family/Species	IUCN global status	IUCN Arabian Sea status	Kuwait	Saudi Arabia	Bahrain	Qatar	Gulf Iran waters	Gulf UAE waters
Maculabatis randalli	LC	NE	X	X[a,b]	X		X	X
Pateobatis fai	VU	NT						X
Pastinachus ater	LC	NT		X[a,b]				
Pastinachus sephen	NT	NE	X	X[a]	X	X	X	
Taeniurops meyeni	VU	NT		X				X
Gymnuridae								
Gymnura poecilura	NT	NT	X	X[a,b]	X	X	X	X
Myliobatidae								
Aetobatus flagellum	EN	EN	X	X[b]			X	
Aetobatus ocellatus	VU	VU	X	X[a,b]		X	X	X
Aetomylaeus milvus	EN	NE	X	X[b]	X	X	X	
Aetomylaeus nichofii	VU	VU	X	X[a,b]	X	X	X	
Rhinopteridae								
Rhinoptera javanica	VU	EN	X				X	
Rhinoptera jayakari	NE	EN	X	X[a,b]		X		
Mobulidae								
Mobula eregoodootenkee	NT	NT				X		
Mobula kuhlii	DD	NT		X[b]				
References	Jabado et al. (2017b); IUCN (2020)		Vossoughi and Vosoughi (1999); Moore et al. (2010); Moore et al. (2012); Moore and Peirce (2013); Robinson et al. (2013); Ghotbeddin et al. (2014); Jabado et al. (2015b); Bishop et al. (2016); Rastgoo et al. (2016); Raeisi et al. (2017); Rastgoo and Navarro (2017); YouTube (2017); Jabado (2018); Jabado et al. (2018); UAE (2018); *Present Study*					

[a]Species documented from fishery-independent surveys.
[b]Species documented from landing surveys.

such as trawl and gill nets, longlines, traps, trolling and handlines, were also recorded.

2.2.2. Data analysis

The catch per unit area (CPUA, ind./km^2) and biomass per unit area (BPUA, kg/km^2) were calculated as the abundance and biomass index for the fishery-independent surveys (Ghotbeddin et al., 2014; Scanlon, 2018):

CPUA = catch in numbers × [trawling speed × trawling time × net-width)]$^{-1}$

BPUA = catch in biomass × [trawling speed × trawling time × net-width)]$^{-1}$

As the elasmobranch CPUA and BPUA did not meet the normality assumptions according to the Shapiro–Wilk test (Abundance: $n = 119$, $W = 0.609$, $P < 0.001$; Biomass: $n = 119$, $W = 0.665$, $P < 0.001$), the nonparametric Wilcoxon test was performed to compare the CPUA and BPUA of stations close to oil and gas facilities with that of stations far from such facilities.

A one-way non-parametric permutational multivariate analysis of variance (PERMANOVA) was used to test for shifts in elasmobranch community in relation to years, latitude (26.5–29.0°N by 0.5 degree), longitude (48.5–51.0°E by 0.5 degree), and CPUA ranges (0–>500 ind./km^2 by 100 ind./km^2) on fishery-independent surveys. Species compositions between the landings and fishery-independent surveys were also compared by PERMANOVA. This analysis was conducted in package *vegan* (Oksanen et al., 2019) in R (R Core Team, 2021) with 999 permutations (Anderson, 2001).

In landing surveys, weighing all specimens was not always feasible. On such occasions, we randomly selected sub-samples of more than 10 individuals for each species from the landings and calculated their average weights to estimate the total biomass of each species. In the case of species with a single individual records such as *Chiloscyllium arabicum* and *Himantura leopard* and with which it was not possible to take measurements, we used the average weights from the trawl surveys where they were collected. Seasons were defined as spring (March–May), summer (June–August), autumn (September–November), and winter (December–February) following Jabado et al. (2015b). Assemblage of elasmobranchs during the various years, seasons, and gears (gill net, longline, trawl, trap, other hook and line gears, and unknown gears) was compared employing Similarity Profile Analysis over Bray–Curtis similarity matrix using PRIMER 7 (Version 7.0.13).

The diversity of elasmobranchs was assessed through various ecological parameters such as Shannon–Wiener diversity index ($H'\log_2$), Margalef richness index (d), Pielou's evenness index (J'), and Simpson dominance index (λ'). Chao 1 estimator was used to estimate the lower limit of the species richness.

To estimate the actual number of elasmobranch species in the region, a species accumulation curve was drawn using a variety of estimators, such as Chao 1, Chao 2, Jackknife 1, Jackknife 2, Bootstrap, and Michaelis Menton (MM) employing PRIMER 7.

The number of species listed in the literature for the Gulf countries since 1999 combined with fishermen's and social media reports with images sufficient to identify the species was used to determine the presence–absence of the species in six Gulf countries (Saudi Arabia, Bahrain, Kuwait, Qatar, UAE, and Iran). Hierarchical cluster analysis was applied to assess the degree of elasmobranch community similarity among these countries based on Jaccard's similarity index and Ward's algorithm (ward. D2) using R.

3. Results

3.1. Fishery-independent surveys

A total of 369 elasmobranch specimens were collected from 119 out of 228 trawled stations. Among these, 324 individuals were weighed with a total weight of 1,178 kg. The estimated total weight of all 369 individuals was 1386 kg (Table S1). Elasmobranchs formed 12.9% of the total catch in biomass. When the stations with no elasmobranch catches were excluded, the elasmobranch biomass was in the range of 0.1–80.6% of the total biomass with an average of 19.7% (± SD 20.5%) of the total catch.

During these surveys, a total of 24 elasmobranch species (7 sharks and 17 batoids) were identified in addition to two batoid species of doubtful identification (Table 1, Table S1, Fig. S1). In terms of abundance, the total catch was dominated by the single gymnurid species, *Gymnura poecilura*, which constituted 37.7% of the total number of individuals, followed by dasyatids (20.6%) and carcharhinids (15.2%). Species such as *G. poecilura*, *Carcharhinus*

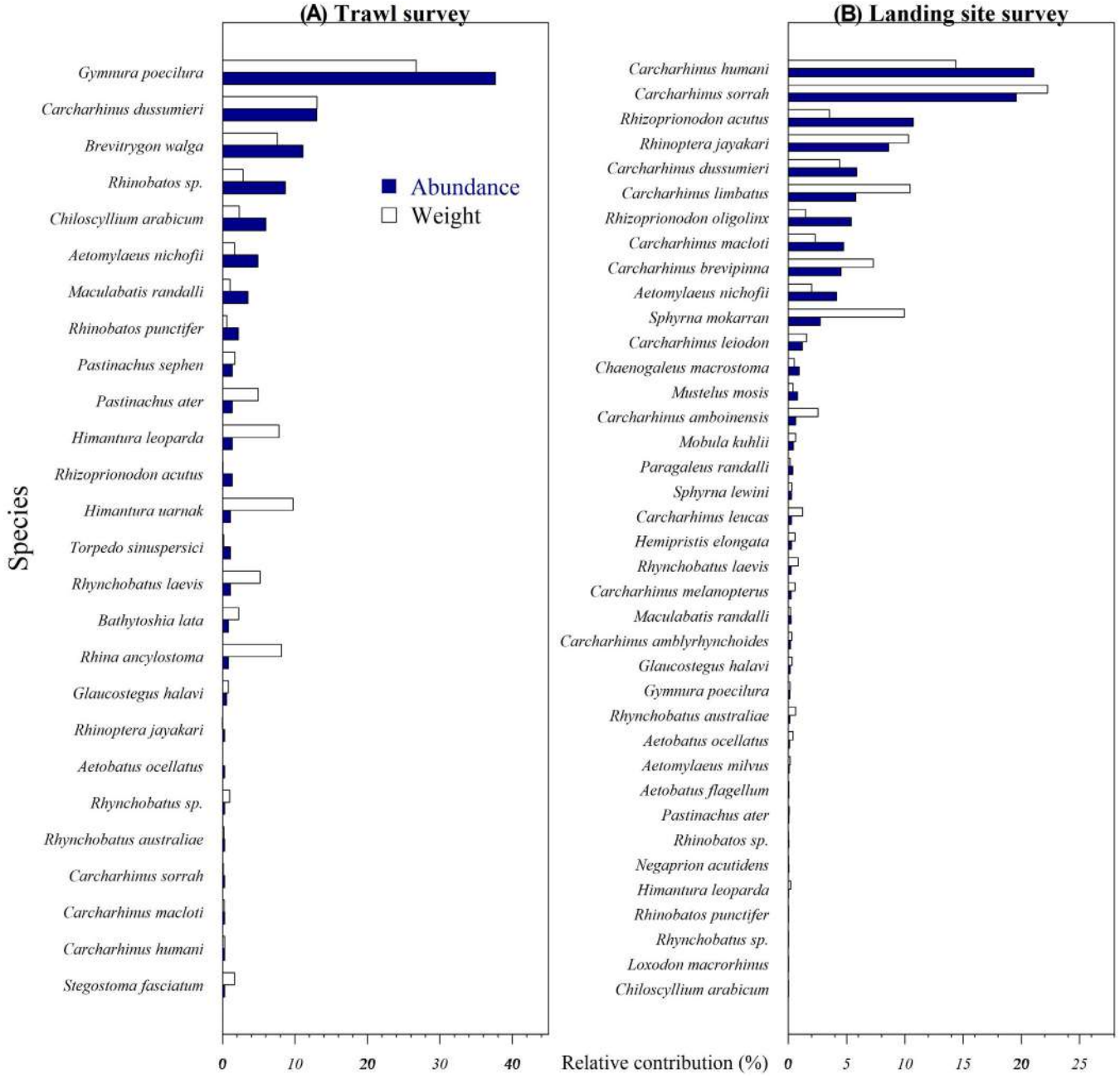

Fig. 2. Pie-charts showing the contribution of various species of elasmobranchs to the total catch in terms of numbers and weights for (A) fishery-independent surveys and (B) landing surveys. The species are ranked according to their contribution from high to low.

dussumieri, and *Brevitrygon walga* constituted respectively 37.7%, 13.0%, and 11.1% of the total number of individuals. In terms of biomass, dasyatids (38.0%), gymnurids (25.1%), and carcharhinids (12.7%) contributed more than 75% of the total weight. The dominant species were *G. poecilura* (25.1%), *C. dussumieri* (12.1%), and *H. leoparda* (11.1%) (Fig. 2A & B; Table S1). In the Saudi waters of the Gulf, the most commonly distributed species were *G. poecilura* and *C. dussumieri* (Table S1). Elasmobranch community structure did not vary significantly with respect to latitude, longitude, and year among 0.5 × 0.5-degree cells (Table 2).

In general, high values of CPUA (> 800 ind./km^2) were observed around the offshore island of Jana (Fig. 3A). Low CPUA values were recorded along the coastal and offshore waters of Ras Tanura with an average (±SD) of 149.4 ± 209.9 ind./km^2 (Fig. 3A). The high BPUA values (>1,500 kg/km^2) were found in three areas: Jana Island waters, Manifa-Safaniya offshore waters, and the southeastern waters close to the border between Saudi Arabia and Bahrain with an average of 550.8 ± 834.3 kg/km^2 (Fig. 3B). Our results suggested that the habitats around Jana Island act as a hotspot for elasmobranch abundance. Large-sized elasmobranchs

Table 2
Permutational multivariate analysis of variance (PERMANOVA) of elasmobranch community data based on fishery-independent surveys. Lat.: latitude range; Lon.: longitude range; CPUA: catch per unit area range; df: degree of freedom; *F*: *F*-value; *P*: *P*-value.

Factor	Year × Lat.	Year × Lon.	Year × CPUA	CPUA × Lat.	CPUA × Lon.	Lat. × Lon.
df	11	7	10	7	3	3
F	0.796	0.725	0.793	0.742	0.854	0.896
P	0.923	0.952	0.927	0.934	0.674	0.595

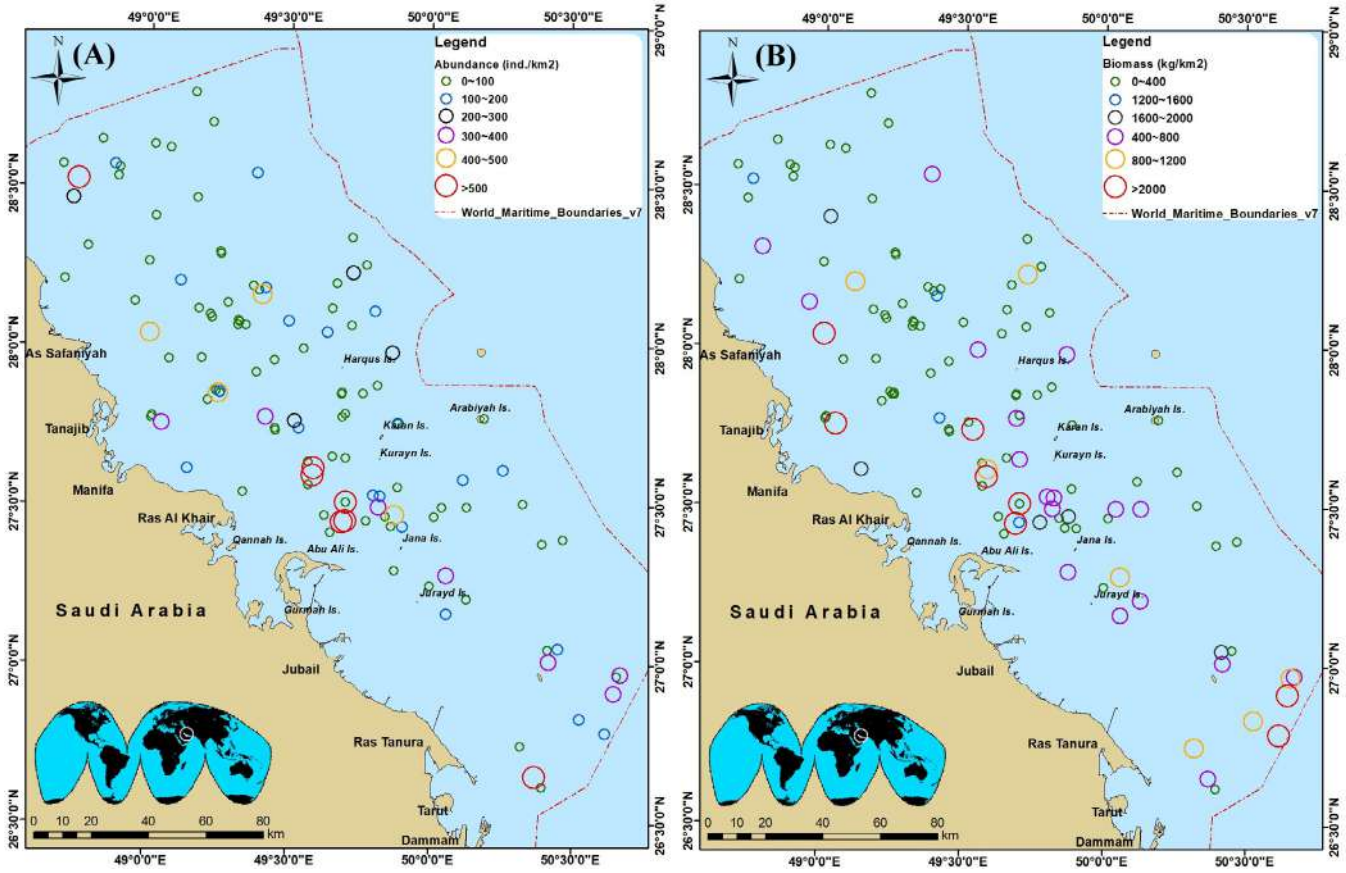

Fig. 3. Distribution of elasmobranch catch per unit area in terms of abundance (A) and biomass (B) data collected during the fishery-independent surveys conducted between 2013 and 2016.

occurred mainly in the areas off Manifa to Safaniya, and in the southeastern waters.

No significant differences were observed in CPUAs between the areas with and without marine facilities for both perimeters of 5 and 10 km (Wilcoxon test, 5 km: $W_{119} = 2106.5$, $P = 0.37$; 10 km: $W_{119} = 2368$, $P = 0.40$). Similarly, no significant differences were found in BPUA at an α level = 0.05 (5 km: $W_{119} = 2181.5$, $P = 0.08$; 10 km: $W_{119} = 2215.5$, $P = 0.09$).

3.2. Landing surveys

In total, 4,055 elasmobranchs were recorded during the 135 monthly visits conducted between March 2016 and February 2020 to fish landings sites and fish auction markets. Out of these, 3,554 specimens (87.6%) were caught by gill nets, 323 (8.0%) by hook and line, 151 (3.7%) by trawl net, and two specimens (0.1%) by traps. The remaining 25 individuals (0.6%) were caught by unknown gears. A total of 38 species of elasmobranchs was recorded, including 22 sharks, 14 batoids, and 2 un-identified species (Table 1; Table S2; Fig. S1). Sharks contributed the majority of the landings in both abundance (85.6%) and biomass (84.1%) (Table S2). In terms of abundance, carcharhinids were dominant and contributed 80.2%, followed by rhinopterids (8.6%) and myliobatids (4.4%). In terms of biomass, carcharhinids also prevailed the total landings (72.2%), followed by rhinopterids (10.3%) and sphyrnids (10.2%). In terms of spatial occurrence, carcharhinids were the most common group followed by sphyrnids (Table S2). At species level, highest abundance values were recorded with *C. humani* and *C. sorrah* (21.1% and 19.6% of the total number of landed elasmobranchs, respectively). The contributions of *Rhizoprionodon acutus* (10.7%) and *Rhinoptera jayakari* (8.6%) were comparatively lower. In terms of biomass, *C. sorrah* contributed the most with 22.3% of the total landings, followed by *C. humani* (14.4%) and *C. limbatus* (10.4%) (Fig. 2B; Table S2). Significant difference in the structure of elasmobranch community was found between fishery-independent surveys and landing surveys (PERMANOVA: $F = 37.819$, $P < 0.001$).

3.3. Diversity indices

In total, 45 elasmobranch species (24 shark species + 21 batoid species + 2 un-identified species) belonging to 16 families and 5 orders were recorded during this study (considering all survey types conducted in the Saudi waters of the Gulf).

The number of species in the fisheries-independent surveys conducted during 2013–2016 ranged between 10 (in 2015) and 15 (in both 2013 and 2016). Overall, Chao 1 predicted the occurrence of 58 species. While the highest values of Margalef richness (4.29), Shannon–Wiener diversity (3.73), and Pielou's evenness (0.95) were recorded in 2016, the lowest records were found in 2015. An opposite trend was observed with the Simpson dominance index (λ'), with the highest record (0.117) in 2015 and the lowest (0.049) in 2016 (Table S3). Species assemblage did not differ significantly among the years (Similarity Profile Analysis, $\pi = 0.99$, $P = 0.896$).

Table 3
Permutational multivariate analysis of variance (PERMANOVA) of elasmobranch communities among fishing gears, seasons, and trawling/non-trawling periods based on landing surveys. df: degree of freedom; *F*: *F*-value; *P*: *P*-value.

Factor	Trawl included		Trawl excluded	
	Gear × Period	Gear × Season	Gear × Period	Gear × Season
df	3	10	3	6
F	1.361	1.311	1.205	1.395
P	0.033	0.003	0.15	0.01

The number of species varied among seasons with 21 in autumn and 32 in winter in the fishery-dependent surveys. Similar seasonal variations were observed with elasmobranch abundance, with the lowest (545 individuals) and highest (1435 individuals) values recorded in incidences in autumn and winter, respectively. The diversity indices taken into consideration also followed the same seasonal patterns showing the lowest records in autumn and the highest in winter or spring (Table S4). However, the elasmobranch assemblage did not differ significantly among the seasons (Similarity Profile Analysis, $\pi = 1.78$, $P = 0.088$). Some shark species caught in winter, such as *C. arabicum*, *Mustelus mosis*, *Paragaleus randalli*, *Loxodon macrorhinus*, *C. melanopterus*, and *Sphyrna lewini* as well as the batoids *Rhynchobatus australiae*, *Glaucostegus halavi*, *Rhinobatos* sp., *Pastinachus ater*, *G. poecilura*, *Aetobatus flagellum*, and *Aetomylaeus milvus* were conspicuous by their absence during autumn. Similarly, species such as *Hemipristis elongate* and *A. ocellatus* caught during autumn were never found during winter.

Gear-wise analysis of data collected during the years 2016–2020 showed that the lowest and highest number of species and individuals were collected in traps (2 species, 2 specimens) and gill nets (35 species, 3565 specimens), respectively (Table S5; Fig. S2). Similarly, minimum and maximum values of Margalef richness and Shannon diversity were also recorded with catches of these fishing gears. In the case of Shannon's diversity index, the highest value was recorded with the catches of longline. While the highest records of Pielou's evenness and dominance index were found with the catches of traps and hook and line, respectively, the lowest records were noted with gill nets and traps, respectively (Table S5). The species compositions were significantly different among fishing gears ($\pi = 8.29$, $P = 0.001$; Fig. 4A), except between the trawl and longline ($\pi = 0$, $P = > 0.9$, Fig. 4A).

Taking into consideration the gear-wise data, the elasmobranch community structure was found to vary significantly among seasons and trawling/non-trawling periods (Table 3). However, when the trawl landings data were excluded, no significant changes were revealed among the trawling and non-trawling periods. The significant seasonal changes in the elasmobranch community structure indicate that elasmobranch landings varied among seasons (Table 3). Although carcharhinids prevailed in the catches throughout the year, they showed low percentages in the gillnet and longline catches during spring and summer. It is also worth noting that no guitarfishes (rhynchobatids and rhinobatids) were recorded in summer, and that myliobatids were mainly caught by trawls and longlines. In addition, hammerhead sharks (sphyrnids) were mainly caught by hook and line (Figs. S2 and S3).

3.4. Similarity in the elasmobranch communities among the gulf countries

Historical data showed the occurrence of 45 species of elasmobranchs in the Saudi waters, 29 species in Kuwait, 26 species in Bahrain, 25 species in Qatar, 27 species in Iran, and 47 species in UAE, totaling 70 species in the Gulf (Table 1). The Jaccard's similarity index among the Gulf countries showed higher similarity in the elasmobranch community between Bahrain and Qatar (0.65; Table 4). Lower similarity was found between the communities occurring in Iran and UAE (0.25; Table 4). The dendrogram showed two groups in different intra-similarity levels: one group with high similarity formed by the elasmobranch communities occurring in the waters of Kuwait, Saudi Arabia, and Bahrain (Western Arabian Gulf countries), and the other with less similarity formed by the communities occurring in the Qatari, Iranian, and Emirati waters (Fig. 4B).

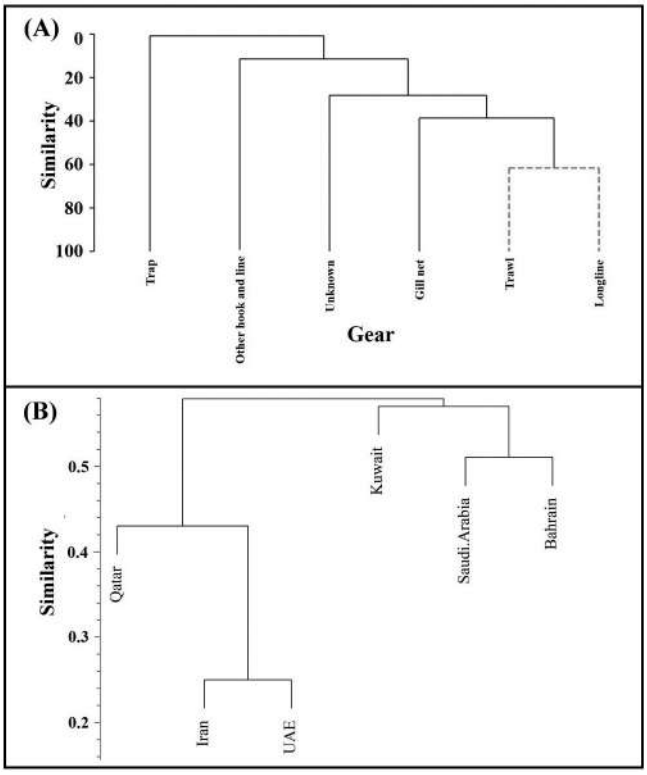

Fig. 4. (A) Gear-wise similarity of elasmobranch diversity based on the data collected during the 135 landing sites visits conducted between March 2016 and February 2020. (B) Hierarchical cluster analysis of the elasmobranch assemblages recorded in the six Gulf countries based on the presence–absence of elasmobranch taxa and Jaccard's similarity index.

Table 4
Jaccard's similarity index values illustrating the degree of similarity in the species composition among countries in the Arabian Gulf.

Number of species	Kuwait 29	Saudi Arabia 45	Bahrain 26	Qatar 25	Iran 27	UAE 47
Kuwait	*	0.54	0.57	0.64	0.47	0.38
Saudi Arabia	*	*	0.51	0.49	0.36	0.59
Bahrain	*	*	*	0.65	0.39	0.43
Qatar	*	*	*	*	0.44	0.33
Iran	*	*	*	*	*	0.25
UAE	*	*	*	*	*	*

4. Discussion

Knowledge on elasmobranch diversity remained fragmentary in the Gulf region despite several studies conducted in various countries (Vossoughi and Vosoughi, 1999; Moore et al., 2012; Moore and Peirce, 2013; Niamaimandi et al., 2014; Jabado et al., 2015b; Bishop et al., 2016). The present study attempted to fill this knowledge gap. Employing both fisheries-independent

and dependent data, the occurrence of 47 elasmobranch species in the Saudi waters of the Gulf is reported (Table 1, S1, S2). Jabado et al. (2015b) found in UAE higher species richness of elasmobranchs based on fisheries data than what was previously thought. Landing survey data showed higher records of species richness, diversity, and evenness index compared to those of fisheries-independent surveys conducted using a single fishing gear. Margalef species richness (2.71–6.18) and Shannon–Wiener diversity (3.01–4.4) values recorded in this study were on the higher side. Higher Margalef richness value of above 2.05 and Shannon diversity in the range of 3–4 indicated that the elasmobranch diversity and community structure occurring in the Saudi waters of the Gulf are in good status, as per the Water Framework Directive of the European Union (Borja et al., 2004).

It is crucial to integrate multiple surveys like a long-term and continuous monitoring of landings and various fishery-independent surveys to reveal the full picture of the elasmobranchs in the Saudi waters of the Arabian Gulf. The occurrence of only one shark and five batoid species in the fishery-independent trawl surveys lend support to the fisheries-dependent landing site surveys as species like *C. arabicum* and *Stegostoma fasciatum* are always discarded offshore due to low market value, as well as covered a large part of uncommon fishing areas. In the fishery independent surveys, batoids formed 78.6% in terms of abundance. However, in the fishery dependent surveys, batoids formed only 14.4%. On the contrary, the fishery-independent survey using trawl net might also miss specimens due to gear selectivity as 16 shark and three batoid species documented in the landing surveys were never encountered in the fishery-independent surveys (Table 1). Moreover, we documented *R. typus* and *T. meyeni* in boat surveys, further widening the spatial coverage of this study.

The species recorded in the study area included six regionally Critically Endangered (CR), six Endangered (EN), and seven Vulnerable (VU) species as per the IUCN (International Union for Conservation of Nature) Red List of Threatened Species (Table 1; Jabado et al., 2017b; IUCN, 2020). Due to poor knowledge on the ecology, biology, and population status of these species, ecological risk assessment could not be done besides adopting appropriate management plans (Moore, 2012; Rastgoo et al., 2016; Raeisi et al., 2017; Rastgoo et al., 2018). *C. limbatus*, *C. sorrah*, *R. acutus*, and *S. lewini* are the four heavily exploited species in the Arabian Peninsula (Spaet and Berumen, 2015) and were found to be dominant in the commercial catches (except *S. lewini*). *C. sorrah* contributed more in terms of biomass and ranked second in terms of abundance. *C. limbatus* was the second most dominant species in terms of biomass. *R. acutus* ranked third in terms of abundance (Fig. 2B, Table S2). The biology and population status of these species besides the two endemic species of the Gulf, *C. humani* and *R. jayakari*, which were recorded for the first time in this study, should also be studied to know their stock structure and to draw management plans (Fig. 2B, Table S2). Due to the secluded nature of the Western Gulf region, conservation of elasmobranch diversity and resources has to be prioritized (Lucifora et al., 2011).

Higher similarity in elasmobranch assemblages between the Kuwaiti, Saudi, and Bahraini waters (Jaccard's index; 0.49–0.65, average 0.57) revealed homogenous distribution of shark species in this contiguous waterbody (Table 2, Fig. 4B). The higher turnover of species in Iran and UAE waters is attributed to proximity with the Strait of Hormuz that connects the Gulf to the Arabian Sea. These facts suggest the need for regional collaboration and cooperation between these countries to protect and conserve the elasmobranch resources. Moreover, the recent capture of the longcomb sawfish (*Pristis sijsron*) from Fasht al Jārim, north off Bahrain (March 2018; Fig. S4) confirmed that this Critically Endangered species is still present in the Arabian Gulf, in particular in the Saudi-Bahraini waters. This necessitates appropriate management plan for protecting this species.

The waters around Jana Island were found to be an elasmobranch hotspot in the Saudi Gulf waters, showing the ecological importance of this island. It is the second largest coral Island in the Saudi waters of the Arabian Gulf (after Karan Island; Miller et al., 2019), which hosts a great biodiversity of fish and shellfish that might attract elasmobranchs (Lin et al., 2021a,b,c). Al Merghani et al. (2000) also reported that the waters of Jana Island constitute an important habitat for marine turtles. Because of its closeness to the coast and as it hosts various megafauna species in its waters, Jana Island has been exposed to various human activities such as sport fishing and tourist diving, impacting the local fauna, including elasmobranchs as observed during our field observations. In view of these facts, establishment of a marine protected area must be considered to protect the biodiversity of the ecologically important Jana Island. In the same sense, Manifa-Safaniya complex was also found to host an important biodiversity of elasmobranchs, most likely because this region hosts important seagrass meadows and a great shellfish and fish associated community (Rabaoui et al., 2015, 2017, 2021a). These faunistic assemblages are likely to attract megafauna species such as marine mammals and elasmobranchs (Rabaoui et al., 2021b).

As per the findings of the present study, the Saudi waters were found to host the second richest elasmobranch diversity in the Gulf region (Tables 1 and 4). The elasmobranch biomass was also found to be higher than that of the Iranian waters (Ghotbeddin et al., 2014; Niamaimandi et al., 2014). The average depth of the Gulf is around 35 m, with a high range of variation in sea surface temperature between winter and summer (15–36 °C), and salinity exceeding 43 psu (Naser, 2014). In such an extreme environment, Saudi Arabia has a relatively high elasmobranch diversity, species richness, and biomass in the Gulf. One of the important reasons for this may be the presence of higher number of oil platforms which restrict fishing operations in their vicinity and thus, serve as the biggest "de facto MPA" (marine protected area) in the Gulf (Rabaoui et al., 2015). The elasmobranchs occurring in these areas seem to feed on the fish and shellfish assemblages associated with these marine structures. In other areas of the Gulf, tuna also gather under or close to marine platforms, probably to spawn in these locations. This suggests the role of marine platforms as fish aggregating devices, which indirectly attract megafauna such as *R. typus* for feeding (Robinson et al., 2013).

Saudi Arabia has banned shark fishing in the Red Sea and the Gulf since 2008 and requires fishermen to release all the sharks alive when caught (Jabado et al., 2017b). Also closed season for trawl fishing has been implemented for years (Jabado et al., 2017b). However, gill net happens to be the main gear for the capture of elasmobranchs in the Gulf based on the present data. A similar study conducted in the Mediterranean Sea showed that illegal fishing of elasmobranchs is a reality (Giovos et al., 2020). Moreover, small sized pregnant specimens of many species of elasmobranch were caught through gill nets (H. H. Hsu *pers. comm.*). Therefore, bringing additional limitations on the gear design (like mesh size) and fishing ban for gill net (fishing season) in addition to the creation of MPAs (covering Jana Island) are recommended to protect elasmobranch diversity in the Saudi Arabian waters of the Gulf.

5. Conclusion

The set of information provided in this manuscript shows the diversity and community structure of elasmobranchs occurring in the Saudi waters of the Gulf. The important ecological roles played by the offshore island of Jana and the northern offshore marine structures are also highlighted. This study also showed that many threatened species are being caught by the

local fisheries, necessitating adoption of an adequate and urgent management and conservation plan. Further detailed studies are still needed to better understand the ecological importance of elasmobranch community and its interactions with the other components of the Gulf ecosystem.

CRediT authorship contribution statement

Hua Hsun Hsu: Conceptualization, Data curation, Formal analysis, Methodology, Writing - original draft. **Lamia Yacoubi:** Formal analysis, Methodology, Validation, Writing - review & editing. **Yu-Jia Lin:** Data curation, Formal analysis, Writing - review & editing. **François Le Loc'h:** Writing - review & editing. **Stelios Katsanevakis:** Writing - review & editing. **Ioannis Giovos:** Writing - review & editing. **Mohammad A. Qurban:** Writing - review & editing. **Zahid Nazeer:** Data Curation, Writing - review & editing. **Premlal Panickan:** Data Curation, Writing - review & editing. **Rommel H. Maneja:** Writing - review & editing. **Perdana K. Prihartato:** Funding acquisition, Writing - review & editing. **Ronald A. Loughland:** Funding acquisition, Writing - review & editing. **Lotfi Jilani Rabaoui:** Conceptualization, Data curation, Funding acquisition, Investigation, Methodology, Project administration, Resources, Supervision, Validation, Writing - review & editing.

Declaration of competing interest

The authors declare that they have no known competing financial interests or personal relationships that could have appeared to influence the work reported in this paper.

Data availability

Data will be made available on request.

Acknowledgments

The authors are grateful to the four anonymous reviewers who helped to improve the quality of the manuscript through their constructive comments and suggestions. We thank Syed Azher Hussain for the GIS assistance, and Barrett Brookshire for providing elasmobranch documentary.

Appendix A. Supplementary data

Supplementary material related to this article can be found online at https://doi.org/10.1016/j.rsma.2022.102637.

References

Al Merghani, M., Miller, J.D., Pilcher, N.J., Al Mansi, A., 2000. The green and hawksbill turtles in the Kingdom of Saudi Arabia: Synopsis of nesting studies 1986–1997. Fauna Arab. 18, 369–384.

Almazroui, M., Abid, M.A., Athar, H., Islam, M.N., Ehsan, M.A., 2013. Interannual variability of rainfall over the Arabian Peninsula using the IPCC AR4 Global Climate Models. Int. J. Climatol. 33, 2328–2340.

Almojil, D.K., Moore, A.B.M., White, W.T., 2015. Sharks & Rays of the Arabian/Persian Gulf. MBG (INT) Ltd, London, UK.

Anderson, M.J., 2001. Permutation tests for univariate or multivariate analysis of variance and regression. Can. J. Fish. Aquat. Sci. 58, 626–639.

Bishop, J.M., Moore, A.B.M., Alsaffar, A.H., Abdul Ghaffa, A.R., 2016. The distribution, diversity and abundance of elasmobranch fishes in a modified subtropical estuarine system in Kuwait. J. Appl. Ichthyol. 32, 75–82.

Borja, Á., Aguirrezabalaga, F., Martínez, J., Sola, J.C., García-Arberas, L., Gorostiaga, J.M., 2004. Benthic communities, biogeography and resources management. In: Borja, A., Collins, M. (Eds.), In: Oceanography and Marine Environment of the Basque Country, Elsevier Oceanography Series, vol. 70, Elsevier, Amsterdam, Nederland, pp. 455–492.

Bornatowski, H., Navia, A.F., Braga, R.R., Abilhoa, V., Corrêa, M.F.M., 2014. Ecological importance of sharks and rays in a structural foodweb analysis in southern Brazil. ICES J. Mar. Sci. 71, 1586–1592.

Carpenter, K.E., Krupp, F., Jones, D.A., Zajonz, U., 1997. FAO Species Identification Field Guide for Fishery Purposes- Living Marine Resources of Kuwait, Eastern Saudi Arabia, Bahrain, Qatar, and the United Arab Emirates. FAO, Rome, Italy.

Chapman, D.D.F., Pikitch, E.K., Babcock, E.A., 2006. Marine parks need sharks? Science 312, 526–527.

Ebert, D.A., Fowler, S., Compagno, L.J.V., 2013. Sharks of the World: A Fully Illustrated Guide. Wild Nature Press, Plymouth, UK.

Gemaque, R., Monteiro, I.L.P., Gomes, F., Sodré, D., Sampaio, I., de Luna Sales, J.B., da Silva Rodrigues Filho, L.F., 2017. Why implement measures to conserve the diversity of elasmobranchs? The case of the northern coast of Brazil. Rev. Biol. 17, 1–7.

Ghotbeddin, N., Javadzadeh, N., Azhir, M.T., 2014. Catch per unit area of batoid fishes in the Northern Oman Sea. Iran. J. Fish. Sci. 13, 47–57.

Giovos, I., Arclueo, M., Doumpas, N., Katsada, D., Maximadi, M., Mitsou, E., Paravas, V., Aga-Spyridopoulou, R.N., Stoilas, V.-O., Tiralongo, F., Tsamadias, I.E., Vecchioni, L., Moutopoulos, D.K., 2020. Assessing multiple sources of data to detect illegal fishing, trade and mislabelling of elasmobranchs in Greek markets. Mar. Policy 112, 103730.

Hasanean, H., Almazroui, M., 2015. Rainfall: Features and variations over Saudi Arabia, a review. Climate 3, 578–626. http://dx.doi.org/10.3390/cli3030578.

Heithaus, M.R., Frid, A., Wirsing, A.J., Worm, B., 2008. Predicting ecological consequences of marine top predator declines. Trends. Ecol. Evol. 23, 202–210.

IUCN, 2020. The IUCN red list of threatened species. Available at https://www.iucnredlist.org/. (Last accessed 30 August 2020).

Jabado, R.W., 2018. The fate of the most threatened order of elasmobranchs: Shark-like batoids (Rhinopristiformes) in the Arabian Sea and adjacent waters. Fish. Res. 204, 448–457.

Jabado, R.W., Al Baharna, R.A., Al Ali, S.R., Al Suwaidi, K.O., Al Blooshi, A.Y., Al Dhaheri, S.S., 2017a. Is this the last stand of the Critically Endangered green sawfish *Pristis zijsron* in the Arabian Gulf? Endanger Species Res. 32, 265–275.

Jabado, R.W., Al Ghais, S.M., Hamza, W., Henderson, A.C., 2015a. The shark fishery in the United Arab Emirates: an interview based approach to assess the status of sharks. Aquat. Conserv. 25, 800–816.

Jabado, R.W., Al-Ghais, S.M., Hamza, W., Shivji, M.S., Henderson, A.C., 2015b. Shark diversity in the Arabian/Persian Gulf higher than previously thought: insights based on species composition of shark landings in the United Arab Emirates. Mar. Biodivers. 45, 719–731.

Jabado, R.W., Al Hameli, S.M., Grandcourt, E.M., Al Dhaheri, S.S., 2018. Low abundance of sharks and rays in baited remote underwater video surveys in the arabian gulf. Sci. Rep. 8, 15597.

Jabado, R.W., Ebert, D.A., 2015. Sharks of the Arabian Seas: An Identification Guide. The International Fund for Animal Welfare, Dubai, UAE.

Jabado, R.W., Kyne, P.M., Pollom, R.A., Ebert, D.A., Simpfendorfer, C.A., Ralph, G.M., Dulvy, N.K., 2017b. The Conservation Status of Sharks, Rays, and Chimaeras in the Arabian Sea and Adjacent Waters. Environment Agency - Abu Dhabi and IUCN Species Survival Commission Shark Specialist Group, Abu Dhabi, UAE.

Last, P.R., White, W.T., de Carvalho, M.R., Séret, B., Stehmann, M.F.W., Naylor, G.J.P., 2016. Rays of the World. Cornell University Press, NY, USA.

Lin, Y.-J., Rabaoui, L., Basali, A.U., Lopez, M., Lindo, R., Krishnakumar, P.K., Qurban, M.A., Prihartato, P.K., Cortes, D.L., Qasem, A., et al., 2021a. Long-term ecological changes in fishes and macroinvertebrates in the world's warmest coral reefs. Sci. Total Environ. 750, 142254.

Lin, Y.-J., Roa-Ureta, R.H., Basali, A.U., Alcaria, J.F.A., Lindo, R., Qurban, M.A., Prihartato, P.K., Qasem, A., Rabaoui, L., 2021b. Coarser taxonomic resolutions are informative in revealing the fish community abundance trends for the world's warmest coral reefs. Coral Reefs 40, 1741–1756.

Lin, Y.-J., Roa-Ureta, R.H., Pulikkoden, A.R.K., Premlal, P., Nazeer, Z., Qurban, M.A., Rabaoui, L., 2021c. Essential fish habitats of demersal fish in the western Arabian Gulf. Mar. Pollut. Bull. 173, 113013.

Lucifora, L.O., García, V.B., Worm, B., 2011. Global diversity hotspots and conservation priorities for sharks. PLoS One 6, e19356.

Miller, J., Hayes, M.O., Michel, J., Krishnakumar, P.K., Loughland, R., 2019. Coastal beach and island ecosystems. In: Al Abdulkader, K., Loughland, R., Qurban, M.A. (Eds.), Ecosystems and Biodiversity of the Arabian Gulf. Saudi Aramco, King Fahd University of Petroleum & Minerals, Dhahran, Saudi Arabia, pp. 68–99.

Moore, A.B.M., 2012. Elasmobranchs of the Persian (Arabian) Gulf: ecology, human aspects and research priorities for their improved management. Rev. Fish. Biol. Fish. 22, 35–61.

Moore, A.B.M., 2017. Are guitarfishes the next sawfishes? Extinction risk and an urgent call for conservation action. Endanger. Species Res. 34, 75–88.

Moore, A.B.M., McCarthy, I.D., Carvalho, G.R., Peirce, R., 2012. Species, sex, size and male maturity composition of previously unreported elasmobranch landings in Kuwait, Qatar and Abu Dhabi Emirate. J. Fish. Biol. 80, 1619–1642.

Moore, A.B.M., Peirce, R., 2013. Composition of elasmobranch landings in Bahrain. Afr. J. Mar. Sci. 35, 593–596.

Moore, A.B.M., White, W.T., Peirce, R., 2010. Additions to the shark fauna of the Persian (Arabian) Gulf (Carcharhiniformes: Hemigaleidae and Carcharhinidae). Zool. Middle East 50, 83–88.

Naser, H.A., 2014. Marine ecosystem diversity in the Arabian Gulf: Threats and conservation. In: Grillo, O. (Ed.), Biodiversity - The Dynamic Balance of the Planet. IntechOpen, London, UK, pp. 297–328.

Niamaimandi, N., Valinassab, T., Zarshenas, G.A., 2014. Stock assessment of sharks in the northern part (Iranian waters) of the Persian Gulf. Agric. Fish. 3, 397–400.

Oksanen, J., Blanchet, F.G., Friendly, M., Kindt, R., Legendre, P., McGlinn, D., Minchin, P.R., O'Hara, R.B., Simpson, G.L., Solymos, P., Stevens, M.H.H., Szoecs, E., Wagner, H., 2019. vegan: Community Ecology Package. R Package Version 2.5-6. https://CRAN.R-project.org/package=vegan.

Pacoureau, N., Rigby, C.L., Kyne, P.M., Sherley, R.B., Winker, H., Carlson, J.K., Fordham, S.V., Barreto, R., Fernando, D., Francis, M.P., Jabado, R.W., Herman, K.B., Liu, K.M., Marshall, A.D., Pollom, R.A., Romanov, E.V., Simpfendorfer, C.A., Yin, J.S., Kindsvater, H.K., Dulvy, N.K., 2021. Half a century of global decline in oceanic sharks and rays. Nature 589, 567–571. http://dx.doi.org/10.1038/s41586-020-03173-9.

Pal, J.S., Eltahir, E.A.B., 2015. Future temperature in southwest Asia projected to exceed a threshold for human adaptability. Nature Clim. Change 6, 197–200. http://dx.doi.org/10.1038/NCLIMATE2833.

Qurban, M.A., Krishnakumar, P.K., Joydas, T.V., Mohamed Ashraf, T.T., Manikandan, K.P., Al-Abdulkader, K., Loughland, R.A., 2012. Overview of the Gulf marine ecosystem. In: Loughand, R.A., Al-Abdulkader, K. (Eds.), Marine Atlas of the Western Arabian Gulf. Saudi Aramco, Dhahran, Saudi Arabia, pp. 23–37.

Rabaoui, L., Lin, Y.-J., Maneja, R.H., Qurban, M.A., Abdurahiman, P., Premlal, P., Al-Abdulkader, K., Roa-Ureta, R.H., 2017. Nursery habitats and life history traits of the green tiger shrimp *Penaeus semisulcatus* (De Haan, 1844) in the Saudi waters of the Arabian Gulf. Fish. Res. 195, 1–11.

Rabaoui, L., Lin, Y.J., Qurban, M.A., Maneja, R.H., Franco, J., Joydas, T.V., Panickan, P., Al-Abdulkader, K., Roa-Ureta, R.H., 2015. Patchwork of oil and gas facilities in Saudi waters of the Arabian Gulf has the potential to enhance local fisheries production. ICES J. Mar. Sci. 72, 2398–2408.

Rabaoui, L., Roa-Ureta, R.H., Yacoubi, L., Lin, Y.-J., Maneja, R., Joydas, T.V., Panickan, P., Gopalan, J., Loughland, R., Prihartato, P.K., et al., 2021a. Diversity, distribution, and density of marine mammals along the Saudi waters of the Arabian Gulf: update from a multi-method approach. Front. Mar. Sci. 8, 687445.

Rabaoui, L., Yacoubi, L., Lin, Y.-J., Joydas, T.V., Maneja, R.H., Dagoy, J., Qurban, M.A., Roa-Ureta, R.H., 2021b. Distribution, abundance, and life history traits of the blue swimming crab *Portunus segnis* (Forskål, 1775) in the Saudi waters of the Arabian Gulf. Reg. Stud. Mar. Sci. 46, 101895.

Rabaoui, L., Yacoubi, L., Sanna, D., Casu, M., Scarpa, F., Lin, Y.-J., Shen, K.-N., Clardy, T.R., Arculeo, M., Qurban, M.A., 2019. DNA barcoding of marine fishes from Saudi Arabian waters of the Gulf. J. Fish Biol. 95, 1286–1297.

Raeisi, H., Kamrani, E., Walter, C., Patimar, R., Sourinejad, I., 2017. Growth and maturity of *Carcharhinus dussumieri* (Muller and Hellen, 1839) in the Persian Gulf and Oman Sea. Turk. J. Fish. Aquat. Sci. 17, 353–361.

Rastgoo, A.R., Fatemi, M.R., Valinassab, T., Mortazavi, M.S., 2016. Length-weight relationships for 10 elasmobranch species from the Oman Sea. J. Appl. Ichthyol. 32, 734–736.

Rastgoo, A.R., Navarro, J., 2017. Trophic levels of teleost and elasmobranch species in the Persian Gulf and Oman Sea. J. Appl. Ichthyol. 33, 403–408.

Rastgoo, A.R., Navarro, J., Valinassab, T., 2018. Comparative diets of sympatric batoid elasmobranchs in the Gulf of Oman. Aquat. Biol. 27, 35–41.

Reynolds, R.M., 1993. Physical oceanography of the Gulf, Strait of Hormuz, and the Gulf of Oman – Results from the Mt. Mitchell Expedition. Mar. Pollut. Bull. 27, 35–59.

Robinson, D.P., Jaidah, M.Y., Jabado, R.W., Lee-Brooks, K., El-Din, N.M.N., Al Malki, A.A., Elmeer, K., McCormick, P.A., Henderson, A.C., Pierce, S.J., Ormond, R.F.G., 2013. Whale sharks, *Rhincodon typus*, aggregate around offshore platforms in Qatari waters of the Arabian Gulf to feed on fish spawn. PLoS One 8, e58255.

Scanlon, M.M., 2018. Evaluating Elasmobranch Bycatch and Shark Depredation in the Georgia Shrimp Fishery (Electronic Theses and Dissertations. 1801). https://digitalcommons.georgiasouthern.edu/etd/1801.

Sheppard, C., Al-Husiani, M., Al-Jamali, F., Al-Yamani, F., Baldwin, R., Bishop, J., Benzoni, F., Dutrieux, E., Dulvy, N.K., Durvasula, S.R.V., Jones, D.A., Loughland, R., Medio, D., Nithyanandan, M., Pillingm, G.M., Polikarpov, I., Price, A.R.G., Purkis, S., Riegl, B., Saburova, M., Namin, K.S., Taylor, O., Wilson, S., Zainal, K., 2010. The Gulf: a young sea in decline. Mar. Pollut. Bull. 60, 13–38.

Spaet, J.L.Y., Berumen, M.L., 2015. Fish market surveys indicate unsustainable elasmobranch fisheries in the Saudi Arabian Red Sea. Fish. Res. 161, 356–364.

Stevens, J.D., Bonfil, R., Dulvy, N.K., Walker, P.A., 2000. The effects of fishing on sharks, rays, and chimaeras (chondrichthyans), and the implications for marine ecosystems. ICES J. Mar. Sci. 57, 476–494.

UAE, 2018. UAE Shark Assessment Report 2018. Ministry of Climate Change and Environment, Abu Dhabi, UAE.

Vaughan, G.O., Al-Mansoori, N., Burt, J.A., 2019. The Arabian Gulf. In: Sheppard, C. (Ed.), World Seas: An Environmental Evaluation-Volume II: The Indian Ocean To the Pacific, second ed. Academic Press, London, UK, pp. 1–23.

Vossoughi, G.H., Vosoughi, A.R., 1999. Study of batoid fishes in northern part of Hormoz Strait, with emphasis on some species new to the Persian Gulf and Sea of Oman. Indian J. Fish. 46, 301–306.

YouTube, 2017. Iranian Fisherman Sparks Outrage By Surfing Atop Whale Shark. Available at https://www.youtube.com/watch?v=jusmMVhZ1FU. (Last accessed 17 January 2019).

selcrs.nsysu.edu.tw/menu1/qrycrsfrm.asp?HIS=2&eng=0

※課程學年期 111上 一、查詢依開課系所 *全部 年級 班級 組別 查詢項目 課程時間

二、依授課教師 林裕 (可部份查詢)　四、依課程名稱 (可部份查詢) 英語授課課程

三、依課別代號 六、選課名額尚未額滿課程

五、查詢時間 星期 節次

驗證碼：7372 重新產生驗證碼 7372 開始查詢 重設條件

國立中山大學歷年課程查詢

學年	學期	系所別	課號	年級	班別	科目名稱	學分	學年期	必選修	修課人數	授課教師	教室	上課時間 一	二	三	四	五	六	日	備註
111	1	跨院選修(海)	GEAI1559	0	不分班	基礎海洋學 FUNDAMENTALS OF OCEANOGRAPHY	3	學期	選修	58	林玉詩,林裕嘉,陳冠宇,簡國童	海MA 3021					234			《講授類》跨院通識與海科院（學）MRSC102課程併班上課環境教育學程 熱帶海洋微學程
111	1	海科院（學）	MRSC102	0	不分班	基礎海洋學 FUNDAMENTALS OF OCEANOGRAPHY	3	學期	選修	4	林玉詩,林裕嘉,陳冠宇,簡國童	海MA 3021					234			《講授類》限海工系及海科系以外學生選修。 環境教育學程 熱帶海洋微學程
111	1	海生保育碩	MEC501	1	不分班	海洋生物專題討論（一） SEMINAR IN MARINE BIOLOGY （I）	1	學期	必修	10	林裕嘉	海MA 3020			6					《研討類》※英語授課
111	1	海生保育碩	MEC503	2	不分班	海洋生態與保育專題研究（一） INDEPENDENT STUDIES IN MARINE ECOLOGY AND CONSERVATION （I）	3	學期	必修	9	陳孟仙,布蓮思,林裕嘉,洪慶章,張揚祺,陳慶能,熊寶兒,劉莉蓮	海MA 3020	CDE							《獨立研究》
111	1	海生保育碩	MEC514	1	不分班	海洋保育個案研析 CASE STUDIES IN MARINE CONSERVATION	3	學期	必修	9	陳孟仙,布蓮思,林裕嘉	海MA 3020					567			《研討類》※英語授課
111	1	海生保育碩	MEC517	1	不分班	水產資源 FISHERIES RESOURCE MANAGEMENT	2	學期	選修	4	林裕嘉	海MA 2037			34					《講授類》※英語授課

第一頁First Page 1 這是最後一頁!!This is Last Page!!

第 1 / 1 頁 Showing page 1 of 1 pages 第 1 筆　到　第 6 筆　　共 6 筆Showing 1 of 6 results 6 results found

※課程學年期 111下 一、查詢依開課系所 *全部 年級 班級 組別 查詢項目 課程時間

二、依授課教師 林裕 (可部份查詢)

四、依課程名稱 (可部份查詢) 英語授課課程

三、依課別代號 六、選課名額尚未額滿課程

五、查詢時間 星期 節次

驗證碼： 7478 重新產生驗證碼 7478 開始查詢 重設條件

國立中山大學 111 學年度 第 2 學期 學期課程查詢

異動說明	多門必修	系所別	課號	年級	班別	科目名稱	學分	學年期	必選修	限修	點選	選上	餘額	授課教師	教室	上課時間 一	二	三	四	五	六	日	備註
		博雅向度六	GEAE2604	0	不分班	環境變遷與生態保育 ENVIRONMENTAL CHANGE AND ECOLOGICAL CONSERVATION	2	期	必	80	11	94	-14	陳孟仙,劉莉蓮,林梅芳,林裕嘉	海MA 3021				89				《講授類》 限大2以上修習。環境教育學程 永續管理微學程 實踐環境教育微學程 熱帶海洋微學程 生態旅遊解說學程 氣候變遷與調適學分學程 地方創生與永續發展整合學程 印象海味微學程 企業社會責任學程 生物多樣性學程
		海生保育碩	MEC502	1	不分班	海洋生物專題討論（二） SEMINAR IN MARINE BIOLOGY （II）	1	期	必	50	0	8	42	林裕嘉	海MA 2032			6					《研討類》 ※英語授課
		海生保育碩	MEC504	2	不分班	海洋生態與保育專題研究（二） INDEPENDENT STUDIES IN MARINE ECOLOGY AND CONSERVATION （II）	3	期	必	50	0	9	41	陳孟仙,劉莉蓮,布蓮思,張揚祺,林裕嘉,洪慶章,陳慶能	海MA 3020	CDE							《獨立研究》 ※英語授課
新增	1/17	海生保育碩	MEC520	0	不分班	生物統計 BIOSTATISTICS	3	期	選	50	0	18	32	林裕嘉	海MA 3020				234				《講授類》 ※英語授課
		海生保育碩	MEC502	1		海洋生物專題討論（二） SEMINAR IN MARINE BIOLOGY （II）	1	期	必	50	0	8	42	林裕嘉	海MA 2032			6					《研討類》 ※英語授課
		海生保育碩	MEC504	2		海洋生態與保育專題研究（二） INDEPENDENT STUDIES IN MARINE ECOLOGY AND CONSERVATION （II）	3	期	必	50	0	9	41	陳孟仙,劉莉蓮,布蓮思,張揚祺,林裕嘉,洪慶章,陳慶能	海MA 3020	CDE							《獨立研究》 ※英語授課

第一頁First Page 1 這是最後一頁!!This is Last Page!!